26. slovenski kolokvij o betonih

PROJEKTIRANJE MIKROARMIRANIH BETONSKIH KONSTRUKCIJ IN NJIHOVE APLIKACIJE

ZBORNIK

GRADIV IN REFERATOV

LJUBLJANA, 16. MAJ 2019

IRMA Inštitut za raziskavo materialov in aplikacije
Ljubljana

Založnik: IRMA inštitut za raziskavo materialov in aplikacije Ljubljana, Slovenčeva 95, 1000 Ljubljana, Slovenija

Redakcija: doc.dr. Andrej Zajc

Tisk: KOPI TIM d.o.o., Slovenčeva ulica 97, 1000 Ljubljana

Naklada: 200 izvodov
Leto izida: 2019

CIP - Kataložni zapis o publikaciji
Narodna in univerzitetna knjižnica, Ljubljana

624.012.45(082)

SLOVENSKI kolokvij o betonih (26 ; 2019 ; Ljubljana)
Projektiranje mikroarmiranih betonskih konstrukcij in njihove aplikacije: zbornik gradiv in referatov / 26. slovenski kolokvij o betonih, Ljubljana, 16. maj 2019 ; [redakcija Andrej Zajc]. - Ljubljana : IRMA, Inštitut za raziskavo materialov in aplikacije, 2019

ISBN 978-961-93671-5-5
1. Gl. stv. nasl. 2. Zajc, Andrej, 1938-
COBISS.SI-ID 299846144

Spoštovani!

Na 1. slovenskem kolokviju o betonih, leta 1994, z naslovom: »Mikroarmirane malte in betoni« smo obravnavali lastnosti malt in betonov z različnimi vrstami vlaken ter nekatere pionirske aplikacije teh kompozitov pri izdelavi konstrukcijskih elementov. Od takrat pa do danes je na osnovi rezultatov raziskav in ugotovitev opazovanj številnih novih aplikacij postal mikroarmirani beton (MAB) material, uporaben za proizvodnjo konstrukcijskih elementov ob upoštevanju pravil projektiranja, ki so na voljo v številnih državah. Pripravljen pa je že osnutek priloge L k »Eurocodu 2«.

Na letošnjem 26. kolokviju o betonih z naslovom: »Projektiranje mikroarmiranih betonskih konstrukcij in njihove aplikacije« bomo obravnavali ta pravila projektiranja, nekatere nove aplikacije, pri katerih se želi povečati predvsem trajnost konstrukcijskih elementov, nekaj pa bo govora o trajnosti MAB konstrukcij, ki so že vrsto let v uporabi.

Kot predavatelji bodo na kolokviju nastopili aktivni strokovnjaki različnih mednarodnih in nacionalnih komisij, ki obravnavajo predmetno problematiko in pripravljajo pravila projektiranja MAB konstrukcij. Ker prihajajo iz različnih držav, pa bo možno spoznati tudi različne poglede pri reševanju te problematike, kakor tudi ugotovitve raziskav in aplikacij MAB konstrukcij. Za njihov trud pri pripravi gradiv za Zbornik predavaj in njihovo prisotnost na kolokviju se jim iskreno zahvaljujem.

Ker je med udeleženci kolokvija veliko strokovnjakov, ki imajo bogate izkušnje pri razvoju, pripravi in uporabi MAB, pričakujem, da se bodo med in po kolokviju razvile plodne razprave in morda porodile nove ideje, ki jih bomo lahko uporabljali pri svojem vsakdanjem delu. S tem bi bil uresničen tudi glavni namen tega kolokvija in prepričan sem tudi vseh naslednjih.

Tako kot vedno, bi se želel še enkrat zahvaliti za prisotnost in interes vseh udeležencem, iz Slovenije in iz naše bližnje ter širše okolice. Prav tako pa se moram zahvaliti vsem našim poslovnim prijateljem, ki ste z objavami oglasov v Zborniku gradiv in referatov ali z razstavnimi paneli finančno podprli naš kolokvij in omogočili njegovo izvedbo.

Ljubljana, maj 2019

Direktor

dr.Jakob Šušteršič, univ.dipl.ing.grad.

Sponzorji

CGP, d.d., Novo mesto

DARS Družba za avtoceste Slovenije, Celje

DELTABLOC, varnostne in protihrupne ograje d.o.o., Murska Sobota

Elea iC, projektiranje in svetovanje d.o.o., Ljubljana

Form + Test Seidner + Co. GmbH, Riedlingen, ZR Nemčija

Gorenjska gradbena družba d.d., Kranj

Hidroelektrarne na Spodnji Savi, d.o.o., Brežice

HSE Invest d.o.o., Maribor

Hidrotehnik Vodnogospodarsko podjetje d.d., Ljubljana

IBE, d.d., svetovanje, projektiranje in inženiring, Ljubljana

IZS Inženirska zbornica Slovenije, Ljubljana

IRI d.d., Ljubljana

Kostak d.d., Krško

Lespatex d.o.o., Ljubljana

Map-trade d.o.o., Slovenska Bistrica

Rafael, gradbena dejavnost d.o.o., Sevnica

RGP Rudarski gradbeni programi d.o.o., Velenje

Salonit Anhovo d.d., Anhovo

Saning, sanacije in gradnja objektov d.o.o., Kranj

SGD Strdin d.o.o., Lovrenc na Pohorju

Stanovanjski sklad Republike Slovenije, javni sklad, Ljubljana

Šuštar Trans d.o.o., Kresnice

TEB Termoelektrarna Brestanica, Brestanica

TKK Proizvodnja kemičnih izdelkov Srpenica ob Soči d.d., Srpenica

Zavod za gradbeništvo Slovenije, Ljubljana

ZBS, Združenje za beton Slovenije

Vsebina

Recent developments on the design of FRC structures

Najnovejši razvoji projektiranja MAB konstrukcij

Joaquim António Oliveira de Barros

University of Minho, ISISE, Department of Civil Engineering, Portugal

Abstract

In this work, two models are presented for the design of fibre reinforced concrete (FRC) structural elements. These elements also include conventional flexural reinforcement, and are herein designated by the acronym R/FRC. The first model is dedicated to the evaluation of the flexural capacity of R/FRC elements, by considering the constitutive laws of the intervenient materials, where the post-cracking tensile capacity of the FRC is simulated by a tensile-crack width multi-branch diagram. The model accounts for the sliding between conventional flexural reinforcement and surrounding FRC. It estimates a moment-rotation relationship for the cross section, as well as the moment-crack width. The good predictive performance of this model is demonstrated by simulating experimental tests with R/FRC beams. The second model is dedicated to the evaluation of the shear capacity of R/FRC beams, and it considers the fibre distribution profile, the fibre pull-out resistance and the modified compression field theory by using a comprehensive integrated strategy. To assess the performance of the developed model, a database consisting of 122 steel fibre reinforced and prestressed concrete beams failing in shear was assembled. The model predictions are shown to correlate well with the test data, and better the ones obtained with the two approaches of fib *Model Code 2010.*

Povzetek

V tem prispevku sta predstavljena dva modela za projektiranje konstrukcijskih elementov iz mikroarmiranega betona (MAB). Ti elementi vključujejo tudi običajno upogibno armaturo in so tukaj označeni z akronimom A/MAB. Prvi model je namenjen oceni upogibne nosilnosti A/MAB elementov z upoštevanjem zakonov sestavljanja vnesenih materialov, pri katerih je natezna nosilnost MAB po razpokanju simulirana z večdelnim diagramom nateg - širina razpoke. Model upošteva drsenje med konvencionalno upogibno armaturo in obdajajočim MAB. Ocenjuje se razmerje moment-rotacija za prečni prerez, kakor tudi moment-širina razpoke. Dobra napovedna učinkovitost tega modela je prikazana s simulacijo eksperimentalnih preskusov A/MAB nosilcev. Drugi model je namenjen vrednotenju strižne nosilnosti A/MAB nosilcev, pri čemer upošteva profil porazdelitve vlaken, odpornost vlakna na izvlek in modificirano teorijo tlačnega polja z uporabo celovite integrirane strategije. Za oceno uspešnosti razvitega modela je bila sestavljena baza podatkov iz 122 prednapetih MAB nosilcev, ki so se strižno porušili. Predvidevanja modela se dobro ujemajo s testnimi podatki in boljše od tistih, ki so bili pridobljeni z dvema pristopoma fib Model Code 2010.

Keywords: Fibre reinforced concrete, flexural capacity, crack width, shear capacity
Ključne besede: mikroarmirani beton, upogibna nosilnost, širina razpoke, strižna nosilnost

1. INTRODUCTION

Fibre reinforcement has been investigated and used as an alternative and a complement to traditional steel reinforcements in several structural and non-structural applications. As an alternative reinforcement to conventional ones, discrete fibres have been used, mainly, for flooring [1,2] and tunnelling [3-5]. However, even in these applications, there are zones of high tensile strain gradients that require the use of both conventional and fibre reinforcement, which will be

hereafter designated by R/FRC. Several models have been proposed to estimate the flexural capacity of R/FRC elements [6-11]. However, few of them are capable of estimating the crack width by considering simultaneously the possibility of occurring debond between conventional reinforcement and surrounding FRC [6]. This aspect is fundamental in the objective of estimating with more rigour the crack width, flexural stiffness and capacity, and ductility at failure, which are essential features when designing for attending the requisites at serviceability and ultimate limit state (SLS, ULS) conditions. The model that are presented in this work has these potentialities and is simple of implementing in a excel data sheet of similar tool, therefore very convenient for serving as a design method.

Fibres are also being explored for the replacement of steel stirrups in reinforced concrete (RC) beams [12-17], due to the relatively high costs for the preparation and installation of this type of reinforcement, and its susceptibility to be corroded, since in general, it is the reinforcement closest to the external surface of RC elements. However, estimating the contribution of fibre reinforcement for the shear capacity of a R/FRC beam includes several challenges due to the complex phenomena it involves, such it the case of the influence of fibre orientation, the mobilized fibre pull-out resistance, and interaction between these resisting mechanisms. The model that is proposed in the present work integrates the relevant shear resisting mechanisms in an integrated framework, thereby has higher potential of providing better and more reliable predictions than the available ones.

2 – APPROACH FOR THE DESIGN OF FRC MEMBERS IN BENDING

2.1 – Formulation

In the section a model is briefly described for the evaluation of the flexural capacity and crack width of R/FRC elements submitted to bending moment. The possibility of occurring sliding between conventional reinforcement and surrounding FRC is accounted for. This model assumes that failure of the elements only occur by bending. It will be used to determine not only the flexural capacity at SLS and ULS conditions, but also the bending moment *vs* crack width relationship, and therefore verify its potential for being a design tool for crack width estimation. This capability will be assessed by simulating some available experimental results, and compared to the predictive performance assured by *fib* Model Code 2010 (MC2010) [18] and RILEM TC 162-TDF [19]. The detailed description of this model can be found in [20].

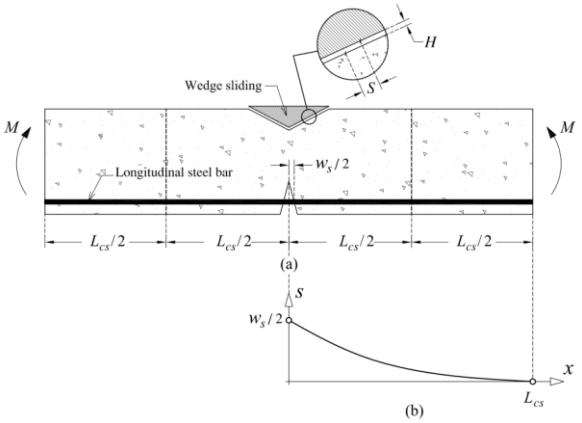

Fig 2.1: - Idealized representation of flexural deformation of R/FRC beams and crack spacing.

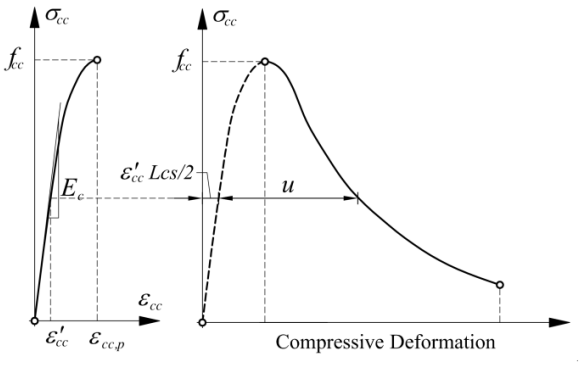

Fig. 2.2 Constitutive law for the FRC in compression: a) pre-peak stress-strain response, b) post-peak stress deformation response.

Fig. 2.1 represents a segment of a R/FRC subjected to pure bending, where is it assumed that cracks are formed at a distance L_{cs}.

Fig. 2.2 shows the constitutive law adopted for the concrete in compression. The compressive response is decomposed in two phases: a pre-peak phase characterized by a stress-strain law $(\sigma_{cc} - \varepsilon_{cc})$, as represented in Fig. 2.2a; and a post peak phase simulated by a stress-deformation relationship $(\sigma_{cc} - u)$, as shown in Fig. 2.2b.

In tension, the FRC is assumed described by the linear stress-strain diagram, $\sigma_{ct}(\varepsilon_{ct}) = E_c \varepsilon_{ct} \quad (0 \le \varepsilon_{ct} \le \varepsilon_{cr})$, Fig. 2.3a, while after crack initiation, the tensile behaviour is simulated by a stress-crack width diagram $(\sigma - w)$ that can be formed by several linear branches (Fig. 2.3b).

For simulating both the tension and compression behaviour of steel reinforcement is assumed a bilinear diagram formed by a linear elastic stress-strain branch up to yield initiation (ε_{sy}), followed by a perfectly plastic regime up to the ultimate strain (ε_{su}), above which rupture is assumed, i.e. $\sigma_{st} = E_s \varepsilon_{st} \ (\varepsilon_{st} \le \varepsilon_{sy}); \sigma_{st} = f_{sy} \ (\varepsilon_{sy} < \varepsilon_{st} \le \varepsilon_{su}); \sigma_{st} = 0 \ (\varepsilon_{st} > \varepsilon_{su})$, where E_s is the elasticity modulus of steel and f_{sy} the yield stress.

For modelling the bond behaviour between conventional reinforcement and surrounding FRC, a linear bond stress-slip relationship, $\tau(x) = k_{bs}\, s(x)$, where k_{bs} is the bond stress-slip stiffness.

The overall deformational response of the beam can be obtained by using the moment-rotation response of each prism, $M - \theta$, as depicted in Fig. 2.4. A symmetric cross section that can have a width varying along its depth (Fig. 2.4b), and a height *h*, is discretized in *n* layers in order to take into account the appropriate constitutive law for each concrete layer during the loading procedure. The width, the thickness and the depth of the i^{th} layer (with respect to the beam's top surface) is designated, respectively, by b_i, t_i, and d_i. For the concrete layer at the level of the reinforcement $(d_i = d_s)$, the total width of this layer (b_i) is decomposed in the part corresponding to the reinforcement $b_s \ (= A_s / t_i)$ and to the concrete b_c $(= b_i - b_s)$.

The equations of the constitutive laws of the intervenient materials are provided comprehensively in [20], being introduced in Table 2.1 with the flowchart shown in Fig. 2.5 for the understanding how the $M - \theta$

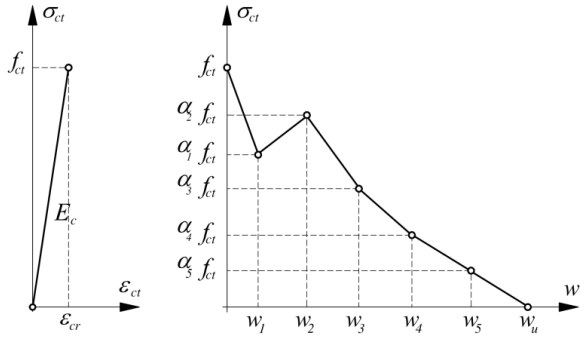

a) b)

Fig. 2.3 Tensile behaviour of FRC: a) linear stress-strain relationship before cracking, b) Post-cracking stress-crack width response.

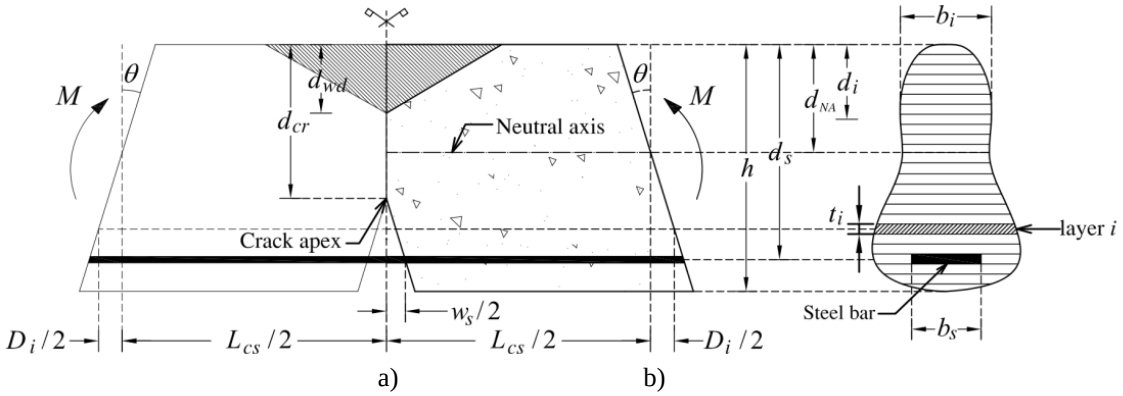

a) b)

Fig. 2.4 - a) Cracked R/FRC segment of length cs L submitted to pure bending, b) layered approach to discretize the cross section.

Table 2.1: Equations of the model (the subscript i represent a generic i[th] layer of the cross section, while the superscript k represents a generic loading step)

Main equation	Eq. n° in Fig.2.5	Dependent Eq. and physical meaning of the variables
$L_{cs} = \frac{2}{\beta_s}$	(4)	$\beta_s = \sqrt{k_{bs}\left(\frac{L_{ps}}{A_s E_s} + \frac{L_{ps}}{E_c A_{c,ef}}\right)}$; $A_{c,ef} = 2.5cb$, L_{ps} is the perimeter of the steel reinforcement, c =concrete cover; b =width of the cross section
$D_i^k = \theta_k \lvert d_i - d_{NA} \rvert$	(16)	D_i^k =axial displacement; d_{NA} = distance of the neutral axis
$\varepsilon_i^{ef} = \frac{2D_i}{L_{cs}}$ (17)		effective strain
$F_i^c = \begin{cases} \sigma_{cc}\left(\varepsilon_i^{ef}\right) b_i t_i & if\ \varepsilon_i^{ef} \le \varepsilon_{cc,p} \\ \sigma_{cc}\left(u_i\right) b_i t_i & if\ \varepsilon_i^{ef} > \varepsilon_{cc,p} \end{cases}$	(18a) (18b)	compressive force
$\begin{cases} \varepsilon_i^{ef} - \varepsilon'_{cc,i} - \left(2u_i / L_{cs}\right) = 0 \\ \sigma_{cc}\left(u_i\right) - \sigma_{cc}\left(\varepsilon'_{cc,i}\right) = 0 \end{cases}$	(19a) (19b)	$\varepsilon'_{cc,i}$ =compressive strain of the layer when subjected to the axial displacement u_i
$F_i^c = \begin{cases} \sigma_{ct}\left(\varepsilon_i^{ef}\right) b_i t_i & if\ \varepsilon_i^{ef} \le \varepsilon_{cr} \\ \sigma_{ct}\left(w_i\right) b_i t_i & if\ \varepsilon_i^{ef} > \varepsilon_{cr} \end{cases}$	(20a) (20b)	F_i^c = tensile force; ε_{cr} =strain at concrete crack initiation
$w_i = \left[2D_i - \frac{\sigma_{ct}\left(w_i\right)}{E_c} L_{cs} \right]$	(21)	Crack width
$F_i^s = b_s t_i \sigma_{st}\left(\varepsilon_i^{ef}\right)$	(22)	Force in the reinforcement when in perfect bond conditions
$F_i^s = \frac{A_s E_s \left[(w_s / 2)\beta_s E_c + 0.76\sigma_{ct}(w_s) \right]}{0.76E_c}$	(23)	Force in the reinforcement when sliding occurs.
$M_k = \sum_{i=1}^{n} F_i^c d_i + F_i^s d_s$		Bending moment of the cross section

is obtained together with the other relevant results (see also Figs. 2.1 to 2.4 for the physical meaning of the variables). The model requires the following data: h, n, t_i, b_i, d_i, A_s, $\sigma_{cc}\left(\varepsilon_{cc}\right)$, $\sigma_{cc}(u)$, $\sigma_{ct}\left(\varepsilon_{ct}\right)$, $\sigma_{ct}\left(w\right)$, $\sigma_{st}\left(\varepsilon_{st}\right)$ and k_{bs}.

2.2 – ASSESSMENT OF THE PREDICTIVE PERFORMANCE OF THE MODEL

The predictive performance of the proposed model is evaluated by simulating the experimental program formed by three series of three R/FRC beams, each beam with a cross section of a width of 150 mm and a height of 110 mm reinforced flexurally with a steel bar of 8 mm diameter. The beams were tested in four point bending configuration, as represented in Fig. 2.6. To obtain the average value of crack width formed along the central pure bending zone, the elongation of the pure bending zone of the beam, measured by LVDT1 in Fig. 2.6, was divided by the number of cracks formed at the stabilized cracking process (the elastic deformation of concrete between cracks is considered negligible for the evaluation of the average crack width).

The beams are designated by B1, B2 and B3, and their respective steel fibre reinforced self-compacting concrete (SFRSCC) was reinforced with 45, 60 and 90 kg/m^3 of hooked end steel fibres, respectively, planned to have a compressive strength at 28 days of, respectively, 15, 25, and 45 MPa, therefore the designation of C15f45, C25f60, and C45f90 was attributed to these SFRSCC.

Tables 2.2 indicates the average compressive strength (f_{cm}) obtained experimentally at 28 days according to EN 206-1 [21] recommendations, while the average tensile strength (f_{ctm}), and the average Young's modulus (E_{cm}) where determined according the equations proposed by MC2010 [18], using f_{cm}. To characterize the toughness class of the developed SFRSCCs, three-point notched beam bending tests (TPBT) were performed on representative notched beams of 600×150×150 mm, following the recommendations of MC2010 [18]. The obtained

characteristic and average values of flexural residual strengths corresponding to the crack mouth opening displacement (CMOD) of 0.5 and 2.5 mm, designated by $f_{R1,k}$ and $f_{R3,k}$, respectively, and the corresponding toughness class of the SFRSCCs are also included in Table 2.2.

The post-cracking response of the used SFRSCCs was characterized by inverse analysis applied to the force-deflection responses registered in the performed TPBT. The adopted inverse approach is detailed elsewhere [22]. The post-cracking response of the SFRSCCs is depicted in Fig. 2.7, according which the intervening parameters defining the stress-crack width constitutive law of Fig. 2.3 are summarized in Table 2.3.

The tensile stress-strain of the steel bar was obtained through direct tensile tests conducted according to the recommendations of ASTM A370 [23], according to which the mechanical properties of steel bar including, modulus of elasticity (E_s), stress and strain at yielding (σ_{sy} and ε_{sy}) and ultimate stress and strain (σ_{su} and ε_{su}) were determined: E_s =204.8GPa, $\sigma_{sy}=\sigma_{su}$ =575MPa, ε_{sy} =2.8‰, ε_{su} =32‰.

In Fig. 2.8 the average moment-crack opening relationship predicted by the proposed model is compared to the one obtained experimentally, according which it can be concluded that the proposed model has predicted with high accuracy the experimental results. In Fig. 2.8 is also included the predictions according to the formulations recommended by MC2010 [18] and RILEM TC 162-TDF [19], where it is verified that these approaches lead to moment-crack width responses noticeably lower (predicted higher crack width) than the ones measured in the tested beams.

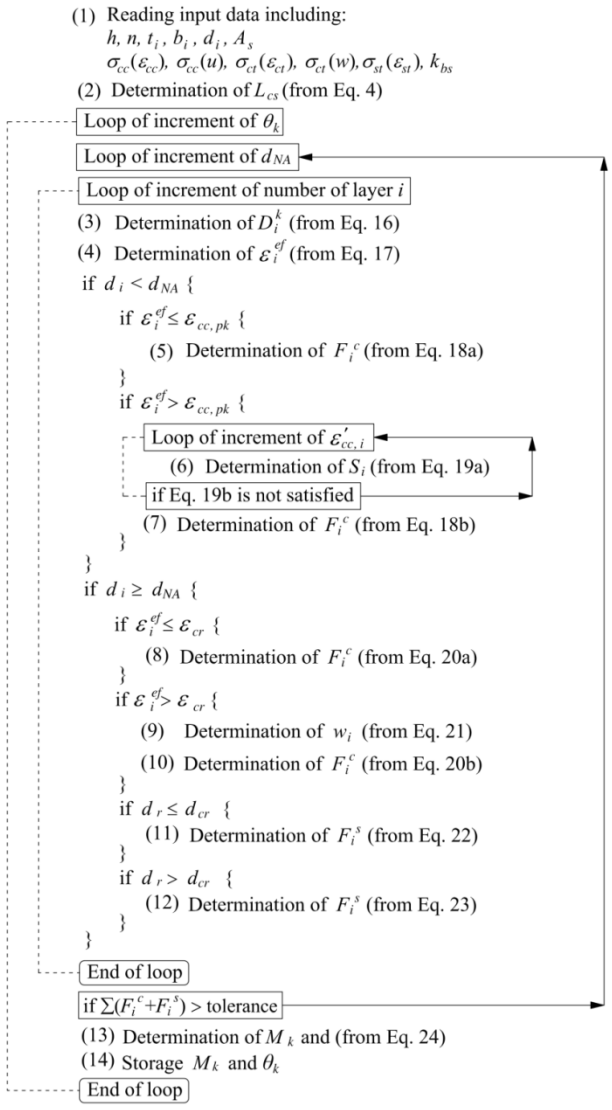

Fig. 2.5 - Flowchart of the algorithm of the model.

Table 2.2: Mechanical properties of the SFRSCCs used in the experimental program

Designation	FRC indication	f_{cm} [MPa]	f_{ctm} [MPa]	E_{cm} [GPa]	$f_{R1,k}/f_{R1,m}$ [MPa]	$f_{R3,k}/f_{R3,m}$ [MPa]	Toughness class
B1	C15f45	13.12	1.31	23.31	2.97/4.02	2.05/3.20	2*c*
B2	C25f60	23.57	1.74	28.62	4.14/7.36	3.54/6.44	4*e*
B3	C45f90	44.42	2.53	35.23	8.73/11.59	7.40/9.70	8*d*

3 – APPROACHES FOR PREDICTING THE SHEAR CAPACITY OF R/FRC BEAMS

3.1 - Introduction

In this chapter is concisely described an approach recently developed for predicting the shear capacity of R/FRC beams. This approach, which is described in detail in [24], was named as Integrated Shear Model (ISM), and is based on the following strategy: (i) evaluation of fibre distribution profile (FOP) according to the approach proposed in [25]; (ii) determination of the resisting stress assured by fibres bridging the critical diagonal crack, CDC, $f_{fuk}(w)$, by considering the fibre pull-out resistance according to the recommendations in [26, 27]; and (iii) evaluation of crack width at mid depth of the CDC, at shear failure conditions, w_u, by using the modified compression field theory (MCFT) [28].

3.2 – Formulation

3.2.1 – Main frame

The shear resistance of R/FRC beams is obtained from:

$$V_{Rd} = V_{Rd,F} + V_{Rd,s} \quad (3.1)$$

where:

$$V_{Rd,F} = k_f \left(V_{Rd,c} + V_{Rd,f} \right) \quad (3.2)$$

represents the contribution of concrete ($V_{Rd,c}$) and the one provided by fibre reinforcement ($V_{Rd,f}$):

$$V_{Rd,c} = \frac{k_p k_v}{\gamma_c} \sqrt{f_{ck}}\, z b_w \text{ with } \sqrt{f_{ck}} \le 8MPa \quad (3.3)$$

$$V_{Rd,f} = \frac{F_{fuk}\left[w_{uv}\left(w_u\right)\right]}{\gamma_F} \quad (3.4)$$

while $V_{Rd,s}$ corresponds to the contribution of steel stirrups:

$$V_{Rd,s} = \frac{A_{sw}}{s_w} z f_{ywd} \left(\cot\theta + \cot\alpha\right)\sin\alpha \quad (3.5)$$

being A_{sw}, s_w, f_{ywd} and α the, respectively, cross sectional area, spacing, yield stress and orientation of the stirrups towards the axis of the beam, $z = 0.9d$ the effective shear depth (d is replaced by d_{eq}, Eq. (3.11), when using passive and prestressed reinforcement), and θ is the inclination of the CDC in relation to the axis of the beam.

In Eq. (3.2) k_f is a parameter to take into account the extra contribution for the shear resistance the propagation of the shear failure crack through the web-flange interface in case of a I or a T cross-section RC beam (Fig. 3.1):

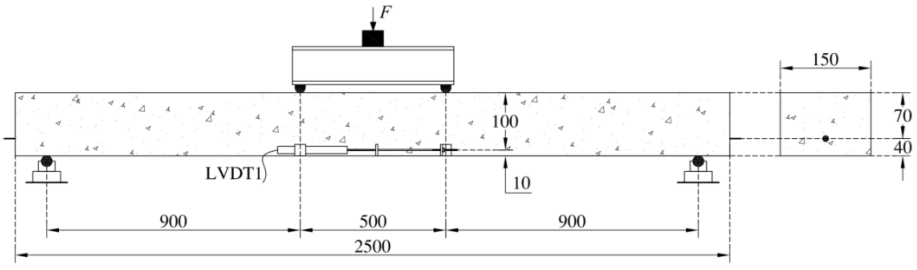

Fig. 2.6- Four point bending test setup and position of LVDT to measure the horizontal elongation in the pure bending region at the level of the reinforcement (dimensions in mm).

Table 2.3: Mechanical properties of intervening materials of the simulated beams

		C15f45	C25f60	C45f90
f_{cm}	[MPa]	13.12	23.57	44.42
f_{ctm}	[MPa]	1.31	1.74	2.39
α_1	[-]	1.22	1.15	1.21
α_2	[-]	0.95	1.32	1.55
α_3	[-]	0.88	1.15	0.67
α_4	[-]	0.42	0.34	0.38
α_5	[-]	0.19	0.29	0.29
w_1	[mm]	0.01	0.01	0.065
w_2	[mm]	0.2	0.03	0.2
w_3	[mm]	0.7	1.0	3.5
w_4	[mm]	3.0	4.6	5.1
w_5	[mm]	5.0	6.5	6.5
w_u	[mm]	9.5	9.0	9.0

$$k_f = 1 + \frac{n}{s}\left(\frac{h_{c,eq}}{b_w}\right)\left(\frac{h_{c,eq}}{d_{eq}}\right) \le 1.5 \qquad (3.6)$$

$$n = \frac{b_{c,eq} - b_w}{h_{c,eq}} \le 3 \ \wedge \ n \le 3\frac{b_w}{h_{c,eq}} \qquad (3.7)$$

$$s = \begin{cases} 2, & \text{T-section} \\ 6, & \text{I-section} \end{cases} \qquad (3.8)$$

where $b_{c,eq}$ and $h_{c,eq}$ are the equivalent of the width and height of the flange, and internal arm of the reinforcement (Fig. 3.1):

$$b_{c,eq} = \frac{b_c A_{c1} + \left(b_c + b_w\right)/2\, A_{c2}}{A_{c1} + A_{c2}} \qquad (3.9)$$

$$h_{c,eq} = \frac{h_{c1} A_{c1} + h_{c2} A_{c2}}{A_{c1} + A_{c2}} \qquad (3.10)$$

$$d_{eq} = \frac{d_l A_l + d_p A_p}{A_l + A_p} \qquad (3.11)$$

being A_l and d_l, and A_p and d_p the cross sectional area and internal arm of passive (subscript "*l*") and prestressed (subscript "*p*") reinforcements, and b_w the width of the web's cross section.

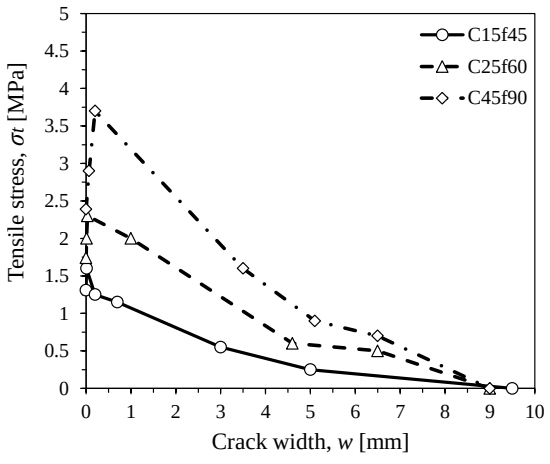

Fig. 2.7- Tensile stress-crack width relationship of the SFRSCCs).

In Eq. (3.3) k_p is a parameter that simulates the favourable effect of prestress in terms of extra shear capacity, adapted from [14]:

$$k_p = \sqrt{1+2.0\frac{\sigma_{cp}}{f_{ctk}}} \quad (3.12)$$

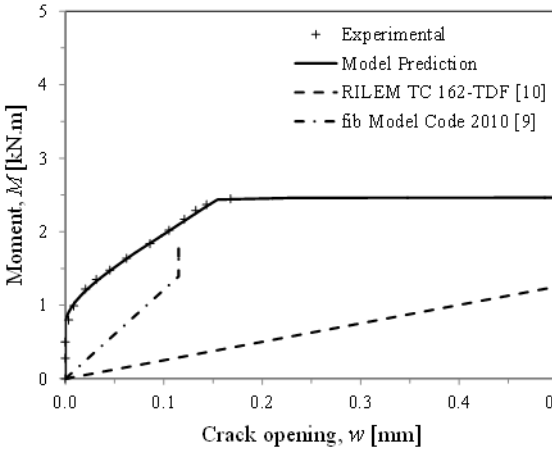

(a)

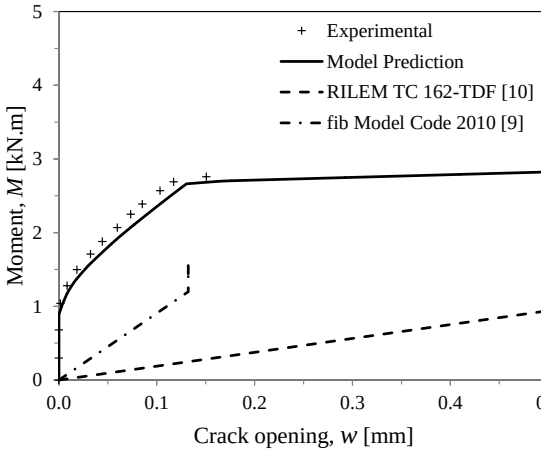

(b)

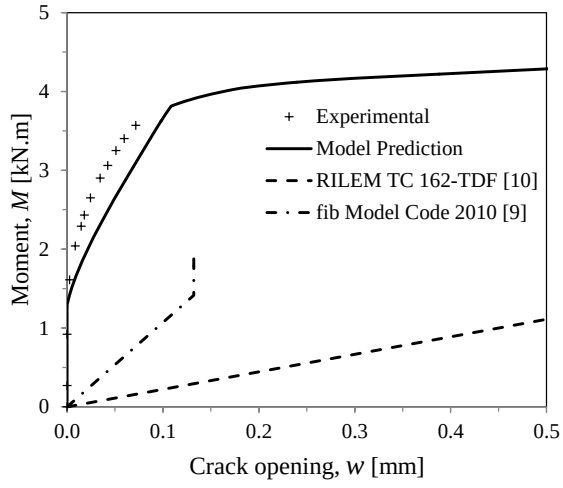

(c)

Fig. 2.8- Moment-crack width response of (a) B1, (b) B2, (c) B3 R/SFRSCC beams (in the legends [9] and [10] correspond to references [18] and [19], respectively.

where $\sigma_{cp} = N_{sd}/A_c < 0.2\, f_{ck}/\gamma_c$ is the average stress acting on the concrete cross section, A_c, for an axial force, N_{sd}, due to loading or prestressing actions ($N_{sd} > 0$ for compression).

In Eq. (3.3) k_v is a parameter aiming to simulate the influence of cross section dimension and the favourable effect of the aggregate interlock for the shear resistance:

$$k_v = \begin{cases} \dfrac{0.4}{1+1500\varepsilon_x}\dfrac{1300}{1000+zk_{dg}} & \text{... for } \rho_w < 0.08\sqrt{f_{ck}}/f_{lyk} \\ \dfrac{0.4}{1+1500\varepsilon_x} & \text{... for } \rho_w \geq 0.08\sqrt{f_{ck}}/f_{lyk} \end{cases} > 0.0 \quad (3.13)$$

where ε_x is the longitudinal strain determined at the mid-depth of the section (Fig. 3.2):

$$0 \leq \varepsilon_x \leq 0.003 = \begin{cases} \dfrac{1}{2E_lA_l}\left(\dfrac{M_{Ed}}{z}+\dfrac{V_{Ed}\cot\theta}{2}+N_{Ed}\left(\dfrac{1}{2}-\dfrac{\Delta e}{z}\right)\right) & \text{for RC beams} \\ \dfrac{\left(\dfrac{M_{Ed}}{z}+\dfrac{V_{Ed}\cot\theta}{2}+N_{Ed}\left(\dfrac{1}{2}-\dfrac{\Delta e}{z}\right)\right)}{2\left(\dfrac{z_l}{z}E_lA_l+\dfrac{z_p}{z}E_pA_p\right)} & \text{for PC beams} \end{cases} \quad (3.14)$$

In this equation, M_{Ed}, V_{Ed} and N_{Ed} are the design values of the bending moment, shear and axial forces acting on the cross section, respectively. The bending moment and shear force are taken as positive; the axial force is positive for tension and negative for compression. The eccentricity of the beam axis with respect to section mid-depth (Δe), shown in Fig. 3.2, is a positive value when positioned above the centre of gravity of the cross section. For R/SFRC hybrid flexurally reinforced beams, with passive and prestressed reinforcements, the effective shear depth, z, is evaluated from:

$$z = \frac{z_l^2A_l + z_p^2A_p}{z_lA_l + z_pA_p} \quad (3.15)$$

where $z_l = 0.9d_l$ and $z_p = 0.9d_p$ (Fig. 3.2).

In Eq. (3.13) k_{dg} parameter aims to simulate the aggregate interlock effect:

$$k_{dg} = \begin{cases} \dfrac{32}{16+d_g} \geq 0.75 & \text{... for normal-weight concrete with } f_{ck} \leq 70\,\text{MPa} \\ 2.0 & \text{... for } f_{ck} > 70\,\text{MPa and for light-weight concrete} \end{cases} \quad (3.16)$$

where d_g is maximum dimension of aggregates (in mm). In Eq. (3.13) $\rho_w = A_{sw}/\left(b_w\, s_w \sin\alpha\right)$ is the percentage of steel stirrups, and f_{lyk} is the characteristic value of the yield strength of the main longitudinal bars:

$$f_{lyk} = \frac{E_l\varepsilon_{lyk}A_l + \left(E_p\varepsilon_{pyk} - f_{po}\right)A_p}{A_l + A_p} \quad (3.17)$$

where for the case of beams reinforced with passive and prestressed longitudinal reinforcements, ε_{lyk} and ε_{pyk} are their respective characteristic value of the yield strain, while f_{po} is the applied prestress. The evaluation of the inclination of the CDC, θ, an updated version of the MCFT is adopted, by considering the recommendations of [14] for taking into account the beneficial effects of fibre reinforcement and the compressive axial load in the prestressed R/SFRC beams:

$$\theta = Min\left\{\begin{array}{l} 29^\circ + 7000\varepsilon_x \le 45^\circ \text{ for } V_f > 0 \\ 20^\circ + 10000\varepsilon_x \le 75^\circ \text{ for } V_f = 0 \end{array}, \ \text{arctg}\left(1 + 4\frac{\sigma_{cp}}{f_{ck}}\right)\right. \tag{3.18}$$

In Eq. (3.4) $F_{fuk}\left[w_{uv}(w_u)\right]$ is evaluated considering the fibre orientation profile (FOP), the fibre pull-out constitutive law (FPCL) representative of each domain adopted for the FOP, and the corresponding number of fibres crossing the CDC. The $\left[w_{uv}(w_u)\right]$ means that F_{fuk} is evaluated for the variable w_{uv} (vertical movement of the two faces composing the CDC) that depends of w_u (crack opening orthogonal to the CDC plane at shear failure conditions).

In Eq. (3.4) γ_F is the partial safety factor for the parcel corresponding to the contribution of the fibre reinforcement for the shear resistance of R/FRC beam, which according to the MC2010 should be considered equal to 1.5 [18].

The design shear resistance cannot be greater than the crushing capacity of FRC in the web:

$$V_{Rd,\max} = k_c \cdot \frac{f_{ck}}{\gamma_c} \cdot b_w \cdot z \cdot \frac{\cot\theta + \cot\alpha}{1 + \cot^2\theta} \tag{3.19}$$

where:

$$k_c = k_\varepsilon \, \eta_{fc}; \; k_\varepsilon = 0.55 \tag{3.20}$$

$$\eta_{fc} = (30/f_{ck})^{1/3} \le 1.0 \quad (f_{ck} \text{ in MPa}) \tag{3.21}$$

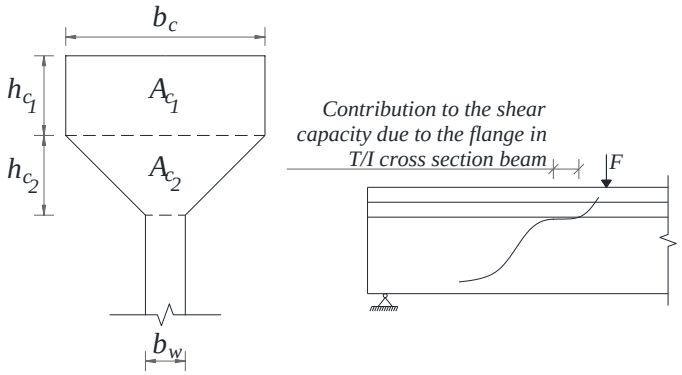

Fig. 3.1- Representation of the variables for the simulation of the contribution of the flange of T or I cross section shape beam for its shear capacity.

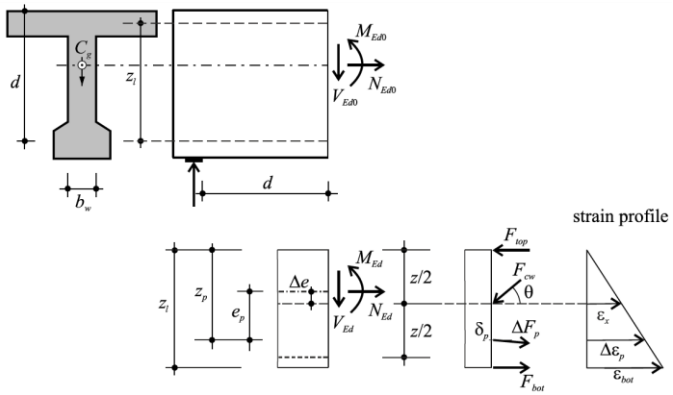

Fig. 3.2- Physical meaning of the variables of Eqs. (3.14) and (3.15) [18].

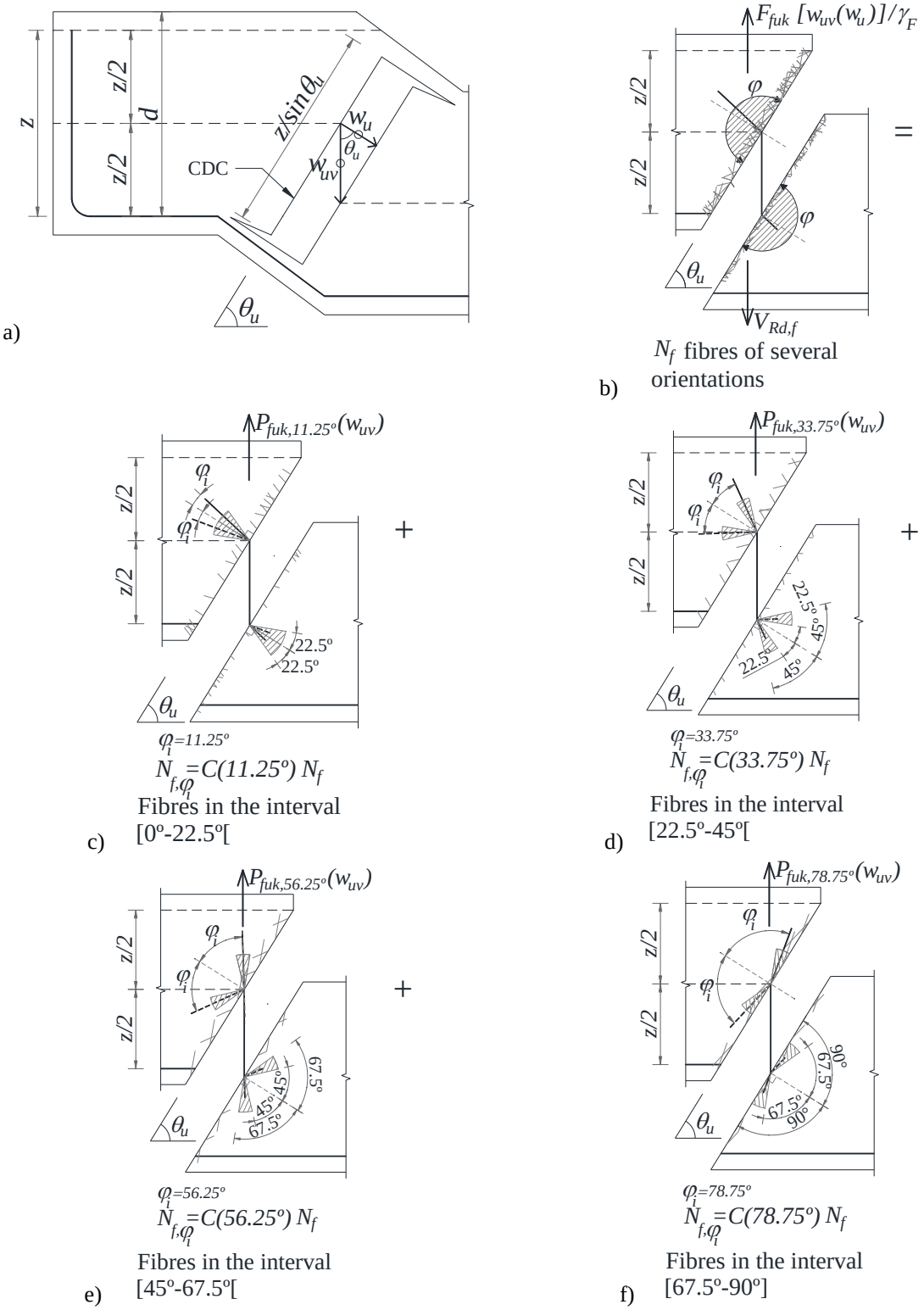

Fig. 3.3 –Schematic representation of the proposed approach for the contribution of fibres bridging the CDC: a) relevant variables and concept of $F_{fuk}[w_{uv}(w_u)]$; b) to f) example where the interval of fibre orientation domain was decomposed in four equal intervals of 25° of amplitude - contribution of fibre reinforcement with orientation in the: b) full interval ([0°-90°]), c) [0-22.5°[, d) [22.5°-45°[, e) [45°-67.5°[, and f) [67.5°-90°].

3.2.2 –Fibre orientation profile (FOP)

The contribution of fibre reinforcement crossing the CDC can be determined by:

$$F_{fuk}\left[w_{uv}\left(w_u\right)\right]=\sum_{i=1}^{n\Delta\varphi}P_{fuk,\varphi_i}\left[w_{uv}\left(w_u\right)\right] \tag{3.22}$$

where $n\Delta\varphi$ is the number of intervals in the fibre orientation range [0-90°] adopted for the evaluation of the fibre orientation profile, and $P_{fuk,\varphi_i}\left(w_u\right)$ is the force supported by the percentage of fibres with an inclination φ_i, obtained for a crack opening representative of the shear failure condition, w_u (Fig. 3.3), where φ_i is the angle between the direction of the fibres representative of the i^{th} fibre orientation interval and the orthogonal to the crack plane (Fig. 3.3b-f).

Fig. 3.3 illustrates conceptually the proposed approach. The figure shows the domain of fibre orientation decomposed in four equal intervals of 22.5° ($n\Delta\varphi$ = 4; $\Delta\varphi$ = 22.5°). The $P_{fuk,\varphi_i}\left(w_u\right)$ is evaluated in the middle of each interval by considering the number of fibres with orientation in this interval, therefore Eq. (3.22) becomes:

$$\begin{aligned}F_{fuk}\left[w_{uv}\left(w_u\right)\right]=&P_{fuk,11.25^\circ}\left[w_{uv}\left(w_u\right)\right]\\&+P_{fuk,33.75^\circ}\left[w_{uv}\left(w_u\right)\right]\\&+P_{fuk,56.25^\circ}\left[w_{uv}\left(w_u\right)\right]\\&+P_{fuk,78.75^\circ}\left[w_{uv}\left(w_u\right)\right]\end{aligned} \tag{3.23}$$

where $P_{fuk,\varphi_i}\left[w_{uv}\left(w_u\right)\right]$ (φ_i = 11.25°, 33.75°, 56.25° and 78.75°) are the forces supported by the percentage of fibres within inclination intervals [0-22.5°[, [22.5°-45°[, [45°-67.5°[and [67.5°-90°], respectively, at w_u.

The force $P_{fuk,\varphi_i}\left[w_{uv}\left(w_u\right)\right]$ is determined from:

$$P_{fuk,\varphi_i}\left[w_{uv}\left(w_u\right)\right]=P_{\varphi_i}^{FPCL}\left[w_{uv}\left(w_u\right)\right]N_{f,\varphi_i} \tag{3.24}$$

where $P_{\varphi_i}^{FPCL}\left[w_{uv}\left(w_u\right)\right]$ is the resisting pull-out force for the crack opening at w_u for a fibre at an inclination φ_i, described in the following section, and N_{f,φ_i} is the number of fibres crossing the CDC within the range of orientations $\varphi_i\pm\Delta\varphi_i/2$:

$$N_{f,\varphi_i}=C\left(\varphi_i\right)N_f \tag{3.25}$$

$$N_f=\frac{A_{sec}}{A_f}V_f\eta_\varphi \tag{3.26}$$

where A_f, V_f and η_φ are the cross sectional area of a fibre, the fibre volume percentage, and the fibre orientation factor, respectively.

In Eq. (3.26) A_{sec} is the area of CDC (Fig. 3.3a):

$$A_{sec}=\frac{z}{\sin\theta}b_w \tag{3.27}$$

while $C\left(\varphi_i\right)$ is the ratio of number of fibres crossing the CDC that lie in the range $\varphi_i\pm\Delta\varphi_i/2$ to the total number of fibres crossing the crack. A detailed description of this approach is available in [25], therefore in the present work only the relevant concepts and equations are presented, namely:

$$C\left(\varphi_i\right)=f\left(\varphi_i\right)F_{RE}\left(\eta_\varphi\right) \tag{3.28}$$

where $f\left(\varphi_i\right)$ is the frequency of fibres within $\varphi_i\pm\Delta\varphi_i/2$, and $F_{RE}\left(\eta_\varphi\right)$ accounts for the error that results from adopting discrete ranges of $\Delta\varphi_i$, compared with a continuous distribution function:

$$F_{RE}\left(\eta_\varphi\right)=\begin{cases}1.29-0.38\eta_\varphi & for\ \eta_\varphi<0.75\\ 1 & for\ \eta_\varphi\geq 0.75\end{cases} \tag{3.29}$$

which depends of the fibre orientation factor, η_φ. In the present model, η_φ, is evaluated according to an enhanced strategy of the approach proposed in 29] is adopted in order to take into account the fibre orientation during the cracking process up to shear failure stage, as well as the wall effect due to the element boundaries on fibre orientation, as detailed in [24,25].

The evaluation of $f\left(\varphi_i\right)$ is as follow:

$$f\left(\bar{\varphi}_i\right)=F\left(\varphi_i,\varphi_m,\sigma\left(\varphi_m\right)\right)-F\left(\varphi_{i-1},\varphi_m,\sigma\left(\varphi_m\right)\right) \tag{3.30}$$

where $F\left(\bar{\varphi}_i,\varphi_m,\sigma\left(\varphi_m\right)\right)$ is the cumulative distribution of the standardized Gaussian law at $\bar{\varphi}_i=\left(\varphi_i+\varphi_{i-1}\right)/2$, with:

$$\varphi_m=\arccos\left(\eta_\varphi\right)180/\pi \tag{3.31}$$

$$\sigma\left(\varphi_m\right)=90\eta_\varphi\left(1-\eta_\varphi\right) \tag{3.32}$$

3.2.3 Fibre pullout constitutive law (FPCL)

The evaluation of the pull-out force $N_{f,\bar{\varphi}_i}$ for fibres orientated at $\bar{\varphi}_i$, for a crack opening displacement (COD) *w*, $P_{\bar{\varphi}_i}^{FPCL}(w)$, is obtained according to the unified variable engagement model (UVEM) proposed in [26, 27], while for the evaluation of crack width at shear failure (w_u) at the mid-depth (z/2), the MCFT is used.

According to [30], a fibre at $N_{f,\bar{\varphi}_i}$, of orientation $\bar{\varphi}_i$, is activated when the COD (vertical direction) equals the crack width required for engagement:

$$w_{ev,i} = \frac{1}{3.5} d_f \tan^3\left(\frac{\gamma_{u,i}}{\gamma_u^{\max}}\frac{\pi}{2}\right) \tag{3.33}$$

where $\gamma_{u,i}$ is the angle between the direction of loading (*V*) and fibre orientation, as shown in Fig. 3.4, while $\gamma_u^{\max}$ is its maximum value, both cases at shear failure conditions (represented by the subscript *u*). In this figure $\bar{\varphi}_i$ represents the fibre orientation of the i^{th} interval (towards the orthogonal to the CDC plane, taken as positive in the clockwise direction), ϕ is the orientation of loading towards the normal to the CDC plane (due to the almost vertical movement of the crack opening process of the CDC, Fig. 3.4, it is assumed ϕ=θ), and *w* and *s* are the crack opening and sliding displacements, respectively.

For a pull-out failure mechanism, when a crack opens, on one side the fibre remains embedded in the matrix and on the other it slips. The average bonded length of fibre crossing the failure plane ($L_{bf,o}$), on the short embedment side, is $l_f/4$.

From the geometry described in Fig. 3.4:

$$\gamma_{u,i} = \left|\bar{\varphi}_i - \phi_u\right| \quad \text{for} \quad 0 \le \gamma_{u,i} \le \pi \tag{3.34}$$

$$\gamma_u^{\max} = \left|\phi_u\right| + \pi/2 \quad \text{for} \quad \pi/2 \le \gamma_u^{\max} \le \pi \tag{3.35}$$

According to the UVEM, $P_{\bar{\varphi}_i}^{FPCL}(w_u)$ is given by:

$$P_{\bar{\varphi}_i}^{FPCL}\left[w_{uv}(w_u)\right] = k_{u,i}\pi d_f \tau_{bu,i} L_{bf,o} \tag{3.36}$$

where

$$k_{u,i} = \begin{cases} 0 & \text{... for } \begin{cases} w_{uv} < w_{ev,i} \\ w_{uv} \ge L_{bf,o} \\ L_{bf,o} - w_{uv} \ge L_{cru,i} \end{cases} \\ \dfrac{2\left(L_{bf,o} - w_{uv}\right)}{l_f} & \text{... for } w_{ev,i} \le w_{uv} < L_{bf,o} \end{cases} \tag{3.37}$$

with (Fig. 3.4):

$$w_{uv} = \frac{w_u}{\cos(\phi_u)} \tag{3.38}$$

The fibre embedment length $L_{cru,i}$ is a critical length beyond which the force in the fibre, due to bond, is such at the fibre fractures, rather than slips [30]:

$$L_{cru,i} = \frac{d_f}{2}\frac{\bar{\sigma}_{fu}}{\tau_{bu,i}} \tag{3.39}$$

In this equation $\tau_{bu,i}$ is the average fibre bond strength and includes the relevant fibre reinforcement

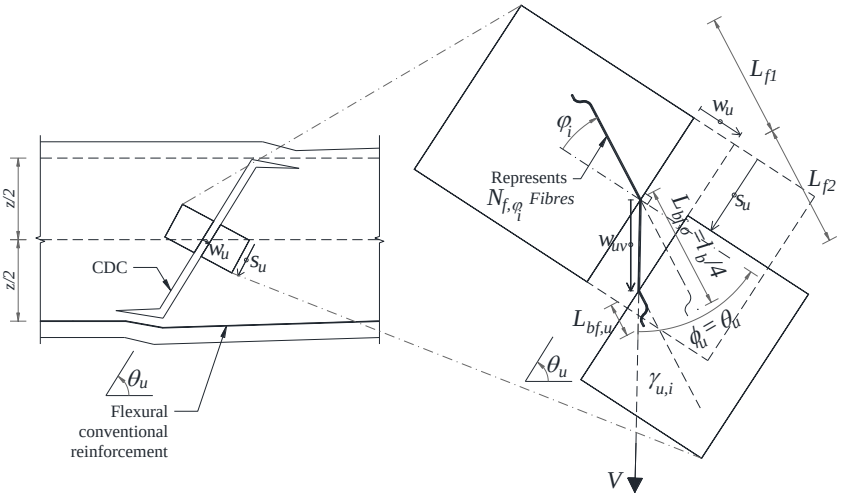

Fig. 3.4 – Kinematics of fibre pull-out according to the UVEM.

Table 3.1: Values of k_b (adapted from [26, 27]).

Matrix type	Fibre type			
	HE	HE-HS	S	C, FE and S-HS
Mortar	0.67	0.75	0.3	0.5
Concrete	0.8	1.0	0.4	0.6

Table 3.2: Interval of values of the database for the model parameters.

Model parameter	Value	
	Minimum	Maximum
Beam's geometry		
b_w (mm)	50	1000
d (mm)	112.79	1440
Concrete properties		
f_{cm} (MPa), cylinders	19.6	205.0
d_g (mm)	5	25
f_{R1m} (MPa)	1.18	40.89
f_{R2m} (MPa)	0.82	41.20
f_{R3m} (MPa)	0.62	35.74
f_{R4m} (MPa)	0.49	29.44
Steel fibres		
V_f (%)	0.25	2.0
l_f (mm)	13	60
d_f (mm)	0.16	1.12
σ_{fu} (MPa)	966	3000
Passive longitudinal reinforcement		
A_l (mm^2)	0*	3694
ρ_l (%)	0*	4.35
E_l (MPa)	200000	
ε_{lym} (‰)	2.0	2.78
Prestressed reinforcement		
A_p (mm^2)	0**	2520
ρ_p (%)	0**	6.23
E_p (MPa)	200000	
ε_{pym} (‰)	7.85	9.59

mechanisms (e.g. hooked ends, if provided) and the snubbing effect [31-33], and $\bar{\sigma}_{fu}$ is the effective tensile strength of the fibre:

$$\bar{\sigma}_{fu} = \sigma_{fu} \frac{\pi}{2\gamma_u^{\max}} \qquad (3.40)$$

where σ_{fu} is the uniaxial tensile strength of the fibre.

From test results on hooked end and straight steel fibres by [26, 27, 31-33] proposed:

$$\tau_{bu,i} = k_b \sqrt{f_{cm}} + f\left[1 - \cos\left(\frac{\gamma_{u,i}}{2}\right)\right] \qquad (3.41)$$

where f_{cm} is the average value of the concrete compressive strength, $f = 4.5$ MPa is the maximum frictional resistance of the fibre due to the snubbing effect, and k_b is given in Table 3.1.

3.2.4 Coupling the modified compression field theory with the FOP and FPCL

To evaluate the crack opening at the half of the effective shear depth (z/2) at shear failure stage, wu, (a value normal to the CDC plane), the MCFT is used. The MCFT is based on the following iterative procedure:

1) Assume an initial value for ε_x (denoted as $\varepsilon_{x,i}$).

2) Calculate k_v by Eq. (3.13), by considering Eqs. (3.14) to (3.17),

3) Evaluation of θ according to Eq. (3.18),

4) Calculate of the crack width at z/2, orthogonal to the CDC, w_u:

$$w_u = \left(0.2 + 1000\varepsilon_x\right)\left(\frac{1000 + zk_{dg}}{1300}\right) \geq 0.125 \text{ mm} \quad (3.42)$$

and its component in the vertical direction, wuv (direction of crack opening at shear failure condition of this type of beams, Fig. 3.4), according to Eq. (3.38).

5) Calculate k_p from Eq. (3.12).

6) Calculate $V_{Rd,f}$ from Eq. (3.3).

7) Calculate $V_{Rd,f}$ from Eq. (3.4), with $F_{fuk}(w_u)$ obtained by Eq. (3.22) in combination with the FOP and FPCL models described in Sections 3.2.2 and 3.2.3.

8) Calculate k_f according to Eq. (3.6).

9) Calculate $V_{Rd,F}$ according to Eq. (3.2), and adding the $V_{Rd,s}$ from Eq. (3.5) if beam includes steel stirrups.

10) Calculate V_{Rd} according to Eq. (3.1). Check V_{Rd} does not exceed web crushing limit, $V_{Rd,max}$, calculated from Eqs. (3.19) to (3.21).

11) Determine the new estimate of the mid-depth longitudinal strain (ε_x) for current iteration, $\varepsilon_{x,i+1}$, according to Eq. (3.14), by adopting: $V_{Ed} = V_{Rd}$, $M_{Ed} = V_{Rd}\left(a - d_{eq}\right)$ and the applied prestressed force for N_{Ed}.

12) If $\left|\left(\varepsilon_{x,i+1} - \varepsilon_{x,i}\right)\right| / \varepsilon_{lyk} \leq \varepsilon_{tol}$, the solution is converged, else return to step 2 with

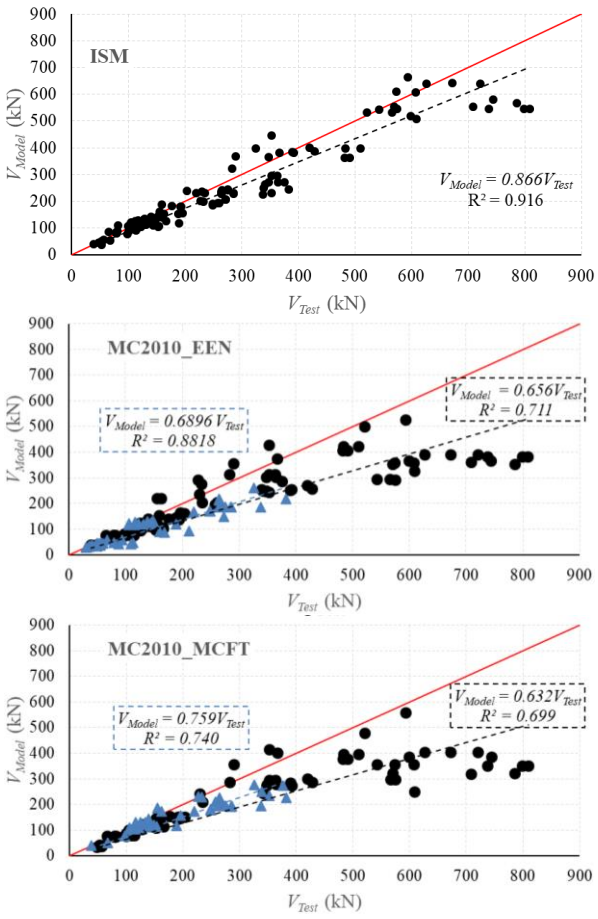

Fig. 3.5 – Test to model comparisons for shear strength: a) ISM; b) MC2010_EEN; c) MC2010_MCFT

$\varepsilon_{x,i} = \varepsilon_{x,i+1}$. ($\varepsilon_{tol} = 1\times10^{-6}$) and repeat until converged.

At the conclusion of the iterative procedure the shear strength on the member V_{Rd} is determined, together with each of the sub-components $V_{Rd,F}$ (consisting of $V_{Rd,c}$ and $V_{Rd,f}$) and $V_{Rd,s}$. The capacity of the member is determined as the lesser of its shear and flexural strength.

3.3. MODEL ASSESSMENT AND VALIDATION

To evaluate performance of the model an already available database [34] was expanded; additional tests included prestressed concrete members and beams reinforced with crimped (C), and flat end (FH) fibres, as well as high-strength (HS) fibres. A large database in this regards was also recently published [35], which includes many of the beams considered in this work for the assessment of the predictive performance of the ISM. After having eliminated the tests of R/SFRC beams of the flexural capacity (evaluated according the recommendation of MC2010) less than the maximum actuating bending at the registered experimental ultimate shear load, i.e. yield initiation of the flexural reinforcement has already occurred, the database was composed of 122 R/SFRC beams from 21 experimental research programs. Thirty seven beams have I- and T-section shapes, with the remaining beams of rectangular cross section. None of the R/SFRC beams have conventional shear reinforcement (stirrups). Twenty three are prestressed and six have hybrid fibre reinforcement (passive and prestress).

Table 3.2 shows the intervals of values (minimum and maximum) of the database for the model parameters, demonstrating to cover a large spectrum of R/SFRC beams possible to find in real applications. In the analysis undertaken nine equal intervals of 10° were used ($n\Delta\varphi$ = 9).

The results of the analysis of the ISM applied to the database are shown in Fig. 3.5. The performance of the ISM is also compared with that of two approaches set out in the Model Code 2010, one where the contribution of fibres is obtained through the value of the ultimate residual tensile strength of FRC (f_{Ftu}), herein designated as MC2010_EEN, and the other based on the MCFT approach, named by MC2010_MCFT.

In all the analysis performed unit values were used for the safety factors, and average values were adopted for the material properties. The higher safety and smaller dispersion of the predictions obtained with the developed ISM is visible.

4 – CONCLUSIONS

The first part of this paper was dedicated to the description of a model to predict the moment-rotation response of FRC elements reinforced flexurally with conventional bars, which is designated by R/FRC members. The model has predicted with good accuracy the relationship between the bending moment *vs* crack width. This predictive performance was better than the ones obtained by applying the recommendations of RILEM TC 162-TDF and *fib* Model Code 2010.

The second part of the paper was devoted to the presentation of model for predicting the shear capacity of R/SFRC beams. A database comprising 122 SFRC beams was assembled for evaluating the performance of the ISM. The predictive performance of the ISM was also compared with that of two approaches available in the *fib* Model Code 2010 (MC2010_EEN that uses the concept f_{Ftu} for considering the contribution of fibre reinforcement, and the MC2010_MCFT, based on the MCFT). For evaluating and comparing the performance of each model, the average test to model prediction ratio ($\lambda=V_{test}/V_{model}$) and its coefficient of variation (CoV) were determined. The average and CoV values for the proposed model are 1.12 and 16.6%, respectively, while for the MC2010_EEN model and MC2010_MCFT model the averages and CoVs were 1.32 and 23.4% and 1.32 and 24.2%, respectively.

5 – ACKNOWLEDGES

The author aims to acknowledge the support provided by FCT through the research project ICoSyTec - Innovative construction system for a new generation of high performance buildings, with reference: POCI-01-0145-FEDER-027990.

REFERENCES

1. *Belletti, B.; Meda, C.A.; Plizzari, G., "Design aspects on steel fiber-reinforced concrete pavements", Journal of Materials in Civil Engineering, 20(9), 599-607, 2008.*
2. *Yang, J.M.; Shin, H.O.; Yoo, D.Y., "Benefits of using amorphous metallic fibers in concrete pavement for longterm performance", Archives of Civil and Mechanical Engineering, 17(4), 2017.*
3. *Tiberti, G., Minelli, F., Plizzari, G. (2014). "Reinforcement optimization of fiber reinforced concrete linings for conventional tunnels", Composites Part B: Engineering, Vol. 58, March 2014.*
4. *Colombo, M.; Martinelli, P.; di Prisco, M., "On the blast resistance of high performance tunnel segments", Materials and Structures, 49 (1-2), pp. 117-131, 2016.*
5. *Craig, R., "Malmo's Construction Starts", Tunnelling & Trenchless Construction, 12-14, 2006.*

6. *Barros, J.A.O.; Taheri, M.; Salehian, H., "A model to simulate the moment-rotation and crack width of FRC members reinforced with longitudinal bars", Engineering Structures, 100, 43-56, October 2015.*
7. *Mazaheripour, H.; Barros, J.A.O.; Soltanzadeh, F.; Sena-Cruz, J.M., "Deflection and cracking behavior of SFRSCC beams reinforced with hybrid prestressed GFRP and steel reinforcements", Engineering Structures journal, 125, 546-565, October 2016.*
8. *Barros, J.A.O.; Taheri, M.; Salehian, H., Mendes, P.J.D., "A design model for fibre reinforced concrete beams pre-stressed with steel and FRP bars", Composite Structures Journal, 94(8), 2494-2512, 2012.*
9. *Taheri, M.; Barros, J.A.O.; Salehian, H.R., "A design model for strain-softening and strain-hardening fiber reinforced elements reinforced longitudinally with steel and FRP bars", Composites - part B Journal, 42 1630-1640, 2011.*
10. *Soranakom C., Multi scale modeling of fibre and fabric reinforced cement based composites, PhD thesis, Arizona State University, 2008.*
11. *Soranakom C, Mobasher B. Correlation of tensile and flexural response of strain softening and strain hardening cement composites. Cement & Concrete Composites 2008; 30: 465-477.*
12. *Ortiz Navas, F., J. Navarro-Gregori, G. Leiva Herdocia, P. Serna, and E. Cuenca, An experimental study on the shear behaviour of reinforced concrete beams with macro-synthetic fibres. Construction and Building Materials, 2018.169: p. 888-899.*
13. *Soltanzadeh, F.; Behbahani, A.E.; Barros, J.A.O.; Mazaheripour, H., "Effect of fiber dosage and prestress level on shear behavior of hybrid GFRP-steel reinforced concrete I shape beams without stirrups", Composites Part B Journal, 102, 57-77, October 2016.*
14. *Soetens, T. "Design models for the shear strength of prestressed precast steel fibre reinforced concrete girders", PhD dissertation, Gent University, Belguim; 2015.*
15. *Foster, S.J., "The application of steel-fibres as concrete reinforcement in Australia: from material to structure. Materials and Structures", 42(9): 1209-1220, 2009.*
16. *Meda. A.; Minelli. F.; Plizzari, G.P.; Riva, P., "Shear behaviour of steel fibre reinforced concrete beams", Materials and Structures Journal, 38, 343-353, 2005.*
17. *Casanova, P.; Rossi, P.; Schaller, I., "Can steel fibres replace transverse reinforcement in reinforced concrete beams?", ACI Material Journal, 94, 341-354, 2000.*
18. *fib Model Code 2010. 2011: CEB and FIP - Final Draft.*
19. *Vandewalle, et al., RILEM TC 162-TDF: Test and design methods for steel fibre reinforced concrete, σ-ε design method - Final Recommendation. Materials and Structures, 36,. 560-567, 2003.*
20. *Barros, J.A.O.; Taheri, M., Salehian, H., "A model to predict the crack width of FRC members reinforced with longitudinal bars", ACI SP-319 Technical Publication, Symposium Volume on the Reduction of Crack Width with Fiber, Editors: Corina-Maria Aldea and Mahmut Ekenel, ACI, ISBN-13: 978-1-945487-68-2, SP-319-2 chapter, 2017.*
21. *EN 206-1, Concrete - Part 1: Specification, performance, production and conformity. p. 69, 2000.*
22. *Salehian, H., "Evaluation of the Performance of Steel Fibre Reinforced Self-Compacting Concrete in Elevated Slab Systems - from the Material to the Structure", PhD thesis, University of Minho. p. 308, 2015.*
23. *ASTM A370, Standard Test Methods and Definitions for Mechanical Testing of Steel Products. 2014.*
24. *Barros, J.A.O.; Foster, S., "An integrated approach for predicting the shear capacity of fibre reinforced concrete beams", Engineering Structures Journal, 174, 346-357, 2018.*
25. *Oliveira, F.L., "Design-oriented constitutive model for steel fiber reinforced concrete", PhD dissertation. Department of Project and Construction Engineering, Polytechnic University of Catalonia, Catalonia, Spain; 2010.*
26. *Ng, T.S.; Htut, T.N.S.; Foster, S.J., "Fracture of steel fibre reinforced concrete – the unified variable engagement model", UNICIV Report R-460, The University of New South Wales, UNSW Sydney, Australia; 2012.*
27. *Ng, T.S.; Foster, S.J.; Htet, M.L.; Htut, T.N.S., "Mixed mode fracture behaviour of steel fibre reinforced concrete", Materials and Structures, 47, 67–76, 2014.*
28. *Bentz, E.C.; Vecchio, F.J.; Collins, M.P., "Simplified modified compression field theory for calculating shear strength of reinforced concrete elements", ACI Structural Journal, 103,614–624, 2006.*
29. *Krenchel, H., "Fibre spacing and specific fibre surface", In: Neville A, editor. Fibre reinforced cement and concrete, UK: The Construction Press, 69-79, 1975.*
30. *Htut, T.N.S., "Fracture processes in steel fibre reinforced concrete", PhD dissertation. School of Civil and Environmental Engineering, The University of New South Wales, UNSW Sydney, Australia, 2010.*
31. *Lee, G.G.; Foster, S.J., "Behaviour of steel fibre reinforced mortar in shear I: Direct shear testing", UNICIV Report No. R-444. The University of New South Wales, UNSW Sydney, Australia, 2006a.*

32. *Lee, G.G.; Foster, S.J., "Behaviour of steel fibre reinforced mortar in shear II: Gamma ray imaging", UNICIV Report No. R-445. The University of New South Wales, UNSW Sydney, Australia, 2006b.*
33. *Lee, G.G.; Foster, S.J., "Behaviour of steel fibre reinforced mortar in shear III: Variable engagement model II", UNICIV Report No. R-448. The University of New South Wales, UNSW Sydney, Australia, 2007.*
34. *Foster, S.J.; Agarwal, A.; Amin, A. "Design of SFRC beams for shear using inverse analysis for determination of residual tensile strength", Structural Concrete, 19, 129–140. 2018.*
35. *Cuenca, E.; Conforti, A.; Minelli, F.; Plizzari, G.A.; Gregori, J.N.; Serna, P., "A material-performance-based database for FRC and RC elements under shear loading", Materials and Structures, 51(11), 1130-1137 2018*

FRC Structures in the next EC2: advances and open questions

MAB konstrukcije v naslednjem EC2 (Eurocode 2): napredki in odprta vprašanja

Marco di Prisco

Politecnico di Milano, Department of Civil and Environmental Engineering, Italy

Abstract

After several decades of research work and some years of pioneer applications, Fiber Reinforced Concrete (FRC) is nowadays a material ready for the world community, also considering that design rules are already available in several countries and a first draft of the Annex L to Eurocode 2 has been already submitted to the Project Team for a first writing. The Annex L is mainly based on the two chapters introduced in the Model Code and is aimed at considering only Steel Fibre Reinforced Concrete (SFRC). SFRC can be a suitable solution, especially for statically indeterminate structures, where stress redistribution occurs. In addition to the structural bearing capacity, SFRC is particularly useful for better controlling crack opening in service conditions, which has a particular influence on structural durability, especially in aggressive environments. Furthermore, structural robustness is nowadays a major concern among structural engineer: also in this perspective, SFRC could improve structural behavior since it provides to the cementitious material a specific toughness both in compression and in tension, i.e. in all the regions of the structural element. In the present paper, the main advances and the open questions are introduced and briefly discussed, profiting of the applied research and the design experience already carried out.

Povzetek

Po več desetletjih raziskovalnega dela in nekaj let pionirskih aplikacij je mikroarmirani beton (MAB) danes material, pripravljen za svetovno skupnost, ob upoštevanju, da so pravila projektiranja že na voljo v več državah in prvi osnutek Priloge L k Eurocode 2 je bil že predložen projektni skupini za prvo pisanje. Priloga L večinoma temelji na dveh poglavjih, ki sta bili uvedeni v Model Code. Namenjena je samo mikroarmiranemu betonu z jeklenimi vlakni (MAB-JV). MAB-JV je lahko primerna rešitev, zlasti za statično nedoločene konstrukcije, kjer pride do prerazporeditve napetosti. Poleg nosilnosti konstrukcije je MAB-JV še posebej uporaben za boljše nadzorovanje odpiranja razpok v pogojih uporabe, kar še posebej vpliva na trajnost konstrukcije, zlasti v agresivnih okoljih. Poleg tega je stabilnost konstrukcije danes glavna skrb projektanta: tudi s tega vidika bi lahko MAB-JV izboljšal obnašanje konstrukcije, saj daje cementnemu materialu specifično žilavost tako pri tlaku kot pri nategu, to je v celotnem konstrukcijskem elementu. V pričujočem članku se predstavlja in na kratko razpravlja o glavnih napredkih in odprtih vprašanjih, izkoriščanju že uporabljenih aplikativnih raziskav in projektantskih izkušenj.

Keywords: Conceptual design, ductility, SFRC beams, elevated slabs, D-regions
Ključne besede: idejna zasnova, duktilnost, nosilci iz MAB-JV, dvignjene plošče, D-razporeditve

1. INTRODUCTION

After several decades of research work (ACI, 1996; Rossi and Chanvillard, 2000; di Prisco et. al, 2004; Reinhardt and Naaman, 2007; Gettu, 2008; Barros, 2012, Banthia 2016) and around twenty years of pioneer applications, Steel Fiber Reinforced Concrete (SFRC) is becoming in several countries an interesting option to conventional R/C material (Bull. 79).

In fact, after a long time where concrete was specified prescribing the cement content, we passed to the compressive strength classes; nowadays, after many years of fibre content prescriptions, the designer can simply, long last, assign a performance class added to the compressive strength, that is a toughness measure in bending. SFRC does not consist only in the addition of steel fibres to concrete, but it is a composite, whose properties must be specified by engineers and controlled at the construction site.

The material performance is determined with EN 14651 standard test. The peculiar property of FRC is the residual post-cracking strength, directly correlated to the toughness measure, which makes FRC very promising in elements subjected to diffused stresses, where its enhanced residual post-cracking strength can better resist tensile stresses diffused in the structural element. After cracking, depending on the properties of the concrete matrix and of the fibres (type, material, content), FRC can have a hardening behavior or a softening behavior (either in bending or in uniaxial tension); being the latter significantly different than Reinforced Concrete (RC), FRC can be a suitable solution for statically indeterminate structures, where stress redistribution occurs. For this reason, MC 2010 (2012) introduced special ductility requirements for FRC structures that can be satisfied when the structure has a high degree of redundancy. The Annex L modifies partially this approach to guarantee also at local level the ductility of the mechanical behaviour, with few exceptions; otherwise, some rebars should be introduced along lines where stresses tend to concentrate.

Another significant aspect of FRC concerns the fibre orientation. Although a 3D distribution of fibres in the structure is generally the desired solution, there are particular elements, as thin-walled ones, where fibres tend to orient (depending on their length with respect to the element thickness) along the main element plane. These elements can take advantage from fibre orientation, since they may be aligned to the main structural stresses. In order to better evaluate the material properties, special “structural specimens”, that better represent the real structure, may be adopted as suggested by Model Code (MC 2010, 2012): this effect is taken into account by the same coefficient K introduced in the Model Code, but some suggestions on the minimum value as well as on special cases is suggested. The Model Code introduced also another significant coefficient (K_{Rd}) that takes into account the observed alignment of the structural response to the average strength values rather than to the characteristic ones: Eurocode modifies partially the formal approach by suggesting different design values according to the specific resistant mechanism evaluated.

In addition to the structural bearing capacity, FRC is particularly useful to better control crack opening in serviceability conditions, which has a particular influence on structural durability, especially in aggressive environments (Vasanelli et al. 2013). Annex L introduces a new computation of the crack width that is able to better take into account fibre pull-out contribution. Last but not least, structural robustness is nowadays a major concern among structural engineers; also in this perspective, FRC could enhance structural behaviour since it provides structural resistance, both in compression and in tension, in the whole volume of the structural element.

Some recent applications, proposed in Italy to show a successful use of FRC in Civil Engineering, are used to highlight the recent advances and the open questions in EC2: the construction of several types of elevated slabs in a new industrial building, in a private residential house in Como region and in existing industrial buildings in Piacenza pre-Alps; new precast roof elements made of FRC and HPFRC for industrial buildings; post-tensioned foundation beams on piles, 750 m long, for a bridge-crane in Piacenza; a SFRC partially-precast retaining wall to secure a bank of the Idroscalo basin in Milan and a retaining wall to secure a slope in the foothills of Como-Lake region; a HPFRC footbridge at south of Oslo; a composite prefabricated tunnel segment to improve fire and blast protection in tunnel linings.

According to the Model Code 2010, FRC represents a new opportunity to simplify and make more efficient the reinforcement of concrete structures. In the all cases discussed, a cost reduction of at least 15% of steel reinforcement is achieved with FRC elements when compared to conventional R/C structures: it comes from a reduction of labour time for placing the reinforcement, from structure maintenance due to an enhancing of local toughness and durability caused by the reduction of the crack opening, an improvement of fire resistance due to the good performance of steel fibres at high temperatures and a significant increase in robustness for statically indeterminate structures.

general conclusion about this comparison can argue that, due to the isotropic randomly distributed fibre reinforcement, fibres can act in any direction giving a significant contribution both to positive and negative bending reinforcement as well as to punching and shear in any point (that significantly enhance robustness). This means that fibres are really able to contribute along any cracked plane in a three dimensional reference and, in statically indeterminate structures, they appear very efficient in terms of resistance and robustness when compared to bars which provide only a significant contribution in one direction.

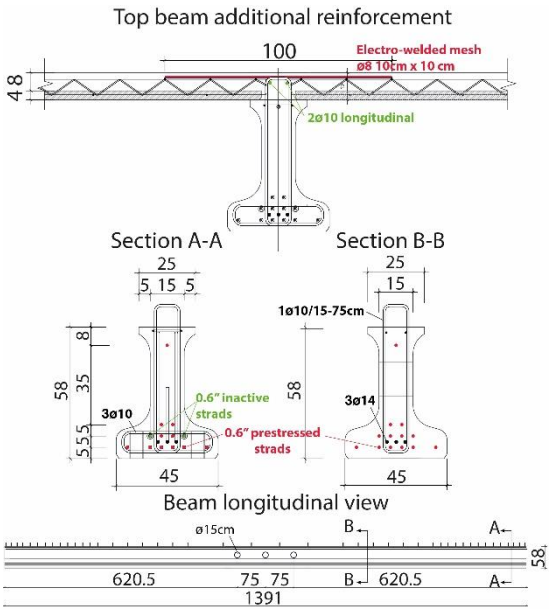

Partially precast slabs

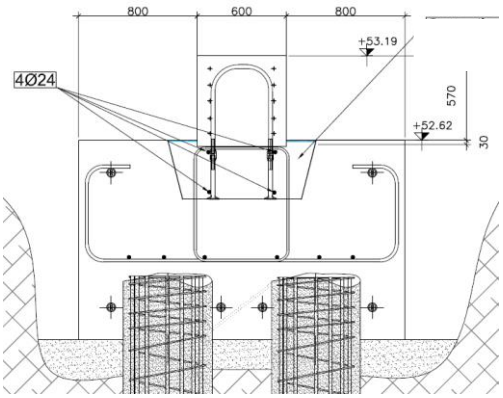

Foundation beams and slabs

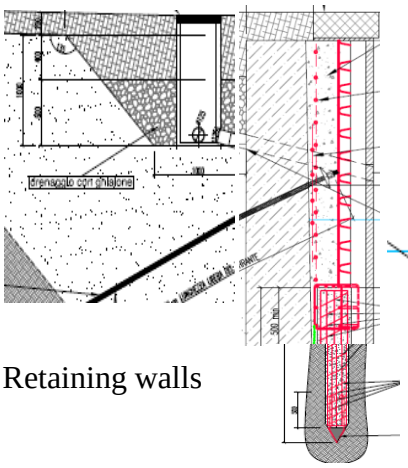

Retaining walls

REFERENCES

1. *ACI Committee 544 (1996), Design considerations for steel Fiber Reinforced Concrete, ACI 544.4R-88, American Concrete Institute, ACI Farmington Hills.*
2. *Barros J. (ed.), Fibre Reinforced Concrete: challenges and opportunities, Proc. of the 8th Int. Symp. Bagneux, France, RILEM Publications S.A.R.L., PRO88., 2012.*
3. *Fib Bull. 79, Fibre-reinforced concrete: from design to structural applications. FRC 2014: ACI-fib International Workshop Proceedings - ACI SP-310, 480 pages, ISBN 978-2-88394-119-9, May 2016.*
4. *Conforti, A., Minelli, F., and Plizzari G.A. (2013), "Wide-shallow beams with and without steel fibres: a peculiar behaviour in shear and flexure", Composites Part B: Engineering, V. 51, pp. 282-290, http://dx.doi.org/10.1016/j.compositesb.2013.03.033.*
5. *Cuenca, E., and Serna, P. (2013), "Shear behavior of prestressed precast beams made of self-compacting Fiber Reinforced Concrete", Construction and Building Materials, V. 45, pp. 145-156, http://dx.doi.org/10.1016/j.conbuildmat.2013.03.096.*
6. *Cuenca, E., and Serna, P. (2013), "Failure modes and shear design of prestressed hollow core slabs made of Fiber-Reinforced Concrete," Composites Part B: Engineering, Vol. 45, No. 1, ISSN 1359-8368, pp. 952-964.*
7. *di Prisco M., Felicetti R., Plizzari G. (eds) (2004), Fibre Reinforced Concrete, BEFIB 2004, Bagneux, France, RILEM Publications S.A.R.L., PRO39.*
8. *di Prisco, M., Colombo, M., Dozio, D. (2013), Fibre-reinforced concrete in fib Model Code 2010: principles, models and test validation, Structural Concrete 14 (4), 342-361.*
9. *di Prisco, M., Martinelli, P. (2014), A numerical approach for the evaluation of the structural redistribution coefficient KRd, Comp. Modelling of Concrete Structures – Proc. EURO-C 2014, Vol. 1, 2014, pp. 503-512, St. Anton am Arlberg; Austria.*
10. *di Prisco, G., Plizzari, G., Vandewalle, L. (2009), Fibre reinforced concrete: new design perspectives, Materials & Structures, 42(9), 1261-1281.*
11. *Dinh, H.H., Parra-Montesinos, G.J., and Wight, J. (2010), "Shear Behaviour of Steel Fibre-Reinforced Concrete Beams without Stirrup Reinforcement", ACI Structural Journal, V. 107, No. 5, pp. 597-606.*
12. *fib Bulletin 65 (2012), "Model Code 2010 - Final draft", Volume 1, 350 pages, ISBN 978-2-88394-105-2.*
13. *fib Bulletin 66 (2012), "Model Code 2010 - Final draft", Volume 2, 370 pages, ISBN 978-2-88394-106-9.*
14. *Gettu R. (ed.) (2008), Fibre Reinforced Concrete: design and applications, BEFIB 2008, Bagneux, France, RILEM Publications S.A.R.L., PRO60.*
15. *Hedebratt, J., Silfwerbrand, J. (2013), Full-scale test of a pile supported steel fibre concrete slab.*
16. *Maya, L.F., Fernández Ruiz, M., Muttoni, A., Foster, S. (2012), Punching shear strength of steel fibre reinforced concrete slabs, Engineering Structures, Vol.40, pp. 83-94.*
17. *Minelli, F., Conforti, A., Cuenca, E., and Plizzari, G.A. (2014), "Are steel fibres able to mitigate or eliminate size effect in shear?", Materials and Structures, V. 47, No. 3, pp. 459-473, doi: 10.1617/s11527-013-0072-y.*
18. *Reinhardt H.W., Naaman A.E. (eds) (2007), High Performance Fibre Reinforced Cement Composites (HPFRCC5), Rilem Publication S.A.R.L., PRO53.*
19. *Vasanelli, E., Micelli, F., Aiello, M.A., Plizzari, G. (2013), Long term behavior of FRC flexural beams under sustained load, Engineering structures, Vol. 56, pp. 1858, 1867.*

Fibre Concrete – Tests, Design and Applications

Betoni z vlakni – preskusi, projektiranje in aplikacije

Johan L. Silfwerbrand

KTH Royal Institute of Technology, Stockholm, Sweden

Abstract

Fibre concrete was invented during the second half of the 19th century in USA, but it was not before the 1950s that it received any practical use. Today, fibre concrete is used for rock strengthening, industrial floors, overlays, and small-size precast concrete products. The use of fibre concrete in typical load-carrying structures, e.g., beams and elevated slabs, has, however, been limited. The major reasons are limited experience and lack of codes. In recent years, several structural tests on fibre concrete beams and slabs have been carried out in several countries. The outcome has been mainly promising and some countries have also developed guidelines. The next version of Eurocode 2 is likely to contain an appendix on structural fibre concrete. Steel fibres is the traditional alternative but there are several alternatives, e.g., synthetic (mainly polypropylene), carbon, glass, hemp, and basalt. They have different advantages and disadvantages. In recent years, the use of basalt fibres has increased. Compared with steel fibres, basalt fibres have two advantages; (i) they have similar density as concrete implying less segregation risk and (ii) they do not corrode. This paper covers some Swedish experiences with fibre concrete structures by summarizing some tests, design specifications, and applications.

Povzetek

V ZDA je bil v drugi polovici 19. stoletja izumljen beton z vlakni, toda pred letom 1950 ni bilo praktične uporabe. Danes se beton z vlakni uporablja za utrjevanje kamnin, industrijske tlake, prekrivne površine in gotove betonske izdelke manjših dimenzij. Uporaba betona z vlakni v značilnih nosilnih konstrukcijah, na primer: nosilci in dvignjene plošče, pa je bila omejena. Glavna razloga sta omejene izkušnje in pomanjkanje standardov. V zadnjih letih je bilo v več državah izvedenih več konstrukcijskih preizkusov na nosilcih in ploščah iz betona z vlakni. Rezultat je bil večinoma obetaven in nekatere države so razvile tudi smernice. Naslednja različica Eurocode 2 bo verjetno vsebovala prilogo o betonskih konstrukcijah z vlakni. Jeklena vlakna so tradicionalna alternativa, vendar obstaja več alternativ, na primer: sintetična (predvsem polipropilenska), ogljikova, steklena, konopljina in bazaltna. Imajo različne prednosti in slabosti. V zadnjih letih se je povečala uporaba bazaltnih vlaken. V primerjavi z jeklenimi vlakni imajo bazaltna vlakna dve prednosti; (i) imajo podobno gostoto kot beton, kar pomeni manjše tveganje segregacije in (ii) ne korodirajo. Ta članek obravnava nekatere švedske izkušnje z betonskimi konstrukcijami z vlakni, s povzetkom nekaterih preskusov, specifikacij za projektiranje in aplikacij.

Keywords: Fibre concrete, Industrial concrete floors, Standards, Steel fibre concrete, Basalt fibre concrete, Tests
Ključne besede: beton z vlakni, industrijski betonski tlaki, standardi, beton z jeklenimi vlakni, beton z bazaltnimi vlakni, preskusi

1 INTRODUCTION

1.1 General

Fibre concrete, or more specifically, steel fibre concrete (SFC) has both technical and economic advantages, e.g., improved ductility and corrosion resistance and substantial reduction of laborious reinforcement work. Despite its extensive and long-term use in specific areas, e.g., underground shotcrete structures and industrial floors, it has not conquered the general market of concrete structures. One reason is that the

major international and national concrete codes have not covered SFC structures. This is presently going to change since both national standards and international standards are available. The aim of this paper is to summarize some Swedish tests on steel and basalt fibre concrete followed by a brief summary of the Swedish design guide and some application fields. The focus of this paper is on cast fibre concrete. Fibre shotcrete has a long tradition in Sweden, both in research and practice. However, the interested reader is recommended to other literature sources, e.g., Holmgren (2010).

1.2 Brief history

Already in 1874 the American A. Berard obtained a patent for steel fibre concrete. Steel fibre concrete was further developed after the 2nd World War in order to make concrete airfield pavements more resistant against bombs than ordinary reinforced concrete pavements. Steel fibre concrete has also been used to improve the energy consumption ability of concrete shelters. In Sweden, steel fibre concrete has been used in 50 years especially in two applications; shotcrete for rock strengthening and industrial floors. Recommendations have been developed in both these areas (Holmgren, 1992; Swedish Concrete Association, 1997 & 2008).

1.3 Fibre materials

The predominant fibre material is steel but other fibre materials, e.g., synthetic (polymers), glass, carbon, basalt, and hemp, are also or have been in use to various degree.

The second most frequent fibre is the synthetic fibre. It exists in two types; (i) macro fibres and (ii) micro fibres. Macro synthetic fibres have similar sizes as steel fibres and are also used to improve the concrete's post-cracking behaviour in tension and flexure. Research on synthetic fibre concrete has shown that a volume content equal to twice the steel fibre volume content is

Figure 1. Full-scale tests on elevated fibre concrete slab on columns. From Hedebratt (2012).

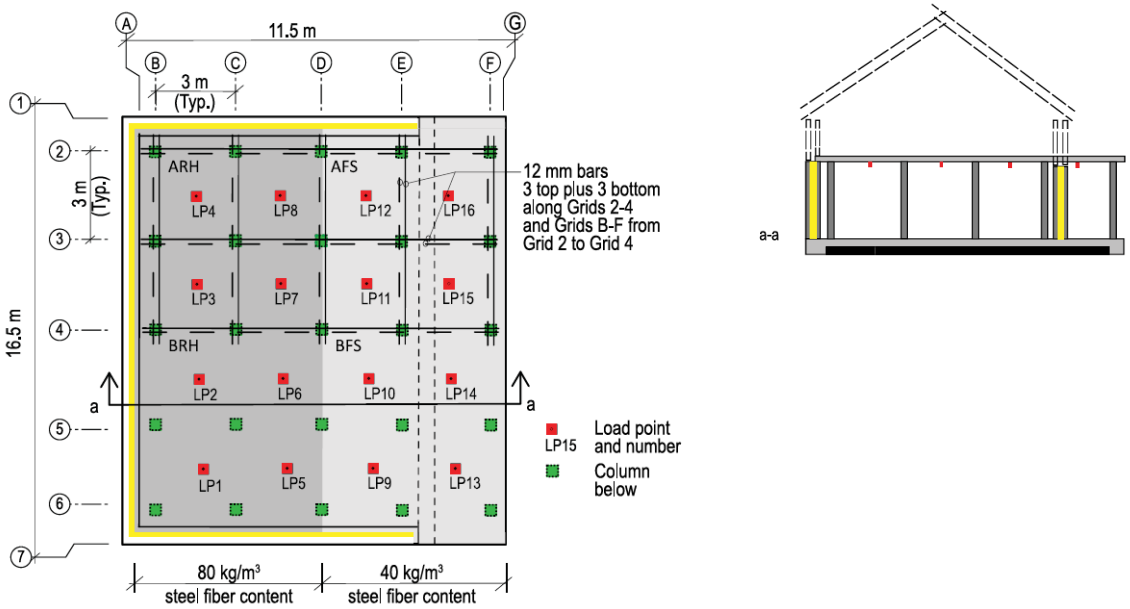

Figure 2. Slab geometry, load point (LP) numbers and reinforcing (left). ARH = 80 kg/m^3 fibres + bars, BRH = solely 80 kg/m^3 fibres, AFS = 40 kg/m^3 fibres + bars. BRS = solely 40 kg/m^3 fibres. Elevation of the test slab (right). From Hedebratt & Silfwerbrand (2015).

needed for equivalent structural performance (Døssland, 2008).

Micro synthetic fibres (polypropylene fibres) have been shown to have an excellent ability to prevent explosive spalling in moist and dense concrete structures (e.g., tunnels) exposed to fire temperature (Jansson, 2013).

Basalt fibres have recently shown up as a realistic alternative, see Section 2.2.

2 SWEDISH TESTS ON FIBRE CONCRETE STRUCTURES

2.1 Tests on elevated slabs

In 2007-2009, unique load tests were carried out near the town of Västerås, Sweden, about 100 km from Stockholm (Hedebratt, 2012; Hedebratt & Silfwerbrand, 2012; Hedebratt & Silfwerbrand, 2015). The tests were subjected to an elevated slab constructed for private home. The slab was designed as a half scale model of a pile supported industrial floor slab (**Figure 1**).

The slab is supported by 25 reinforced concrete columns on a 3x3 m rectangular grid and sandwich wall panels on three of the four perimeter edges (**Figure 2**). The thickness of the slab is 130 mm, resulting in a span/depth ratio of just over 23 to 1.

One-half of the test slab, from Grid 4 to 6, was reinforced only with steel fibres. The other half was reinforced with a combination of steel fibres and reinforcing bars. The bars were designed to carry section moments from a uniformly distributed load of 10 kN/m^2 in the ultimate limit state. Top and bottom layers each comprised three 12 mm diameter bars

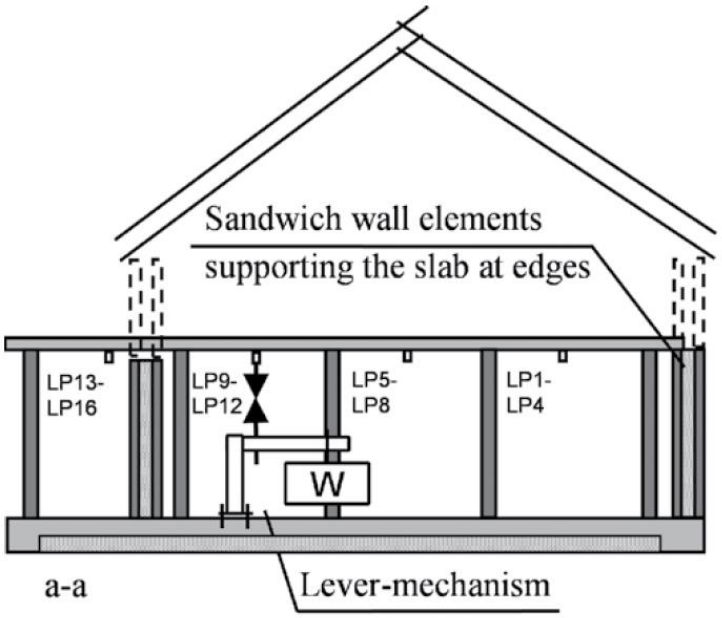

Figure 3. Construction of the roof structure and upper level sandwich walls took place during the long-term period. From Hedebratt & Silfwerbrand (2015).

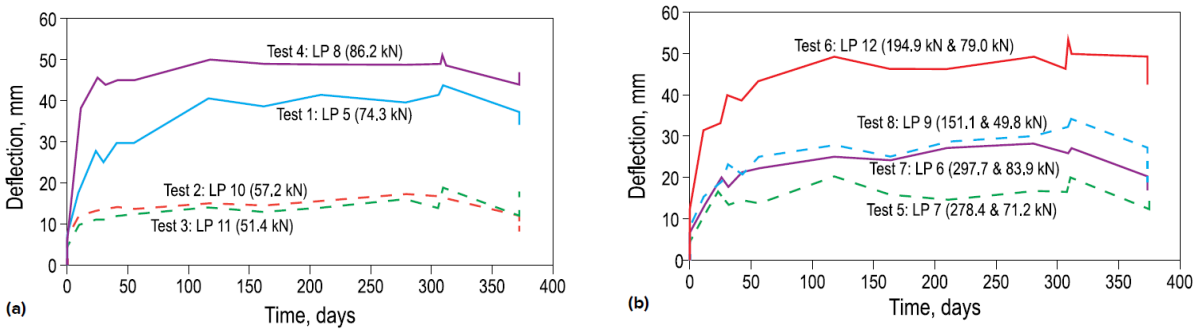

Figure 4. Deflection as a function of time identified by loading test number. Notation includes load number, load point (LP) number, and short-time loading (if any). Tests in slab regions not previously loaded during short-time tests (a); and tets in slab regions that were loaded during the short-time tests (b). From Hedebratt & Silfwerbrand (2015).

spaced at 100 mm. Bars were placed along column lines as indicated in **Figure 2**.

In the test program, selected panels of the slab were subjected to short-term and long-term loadings comprising concentrated loads applied at the panel midpoints. Corner panels were not loaded during the long-term tests.

The slab was constructed using fibre dosages of 40 or 80 kg/m^3 (**Figure 2**) with the objective of obtaining a residual strength factor $R_{10,30}$ ranging from 60 to more than 100%. We estimated the strain hardening/softening properties (here defined as $R_{10,30}$ > 100%) of the concrete based on our experience with similar mixtures, information obtained in the research literature, and extrapolation of the fibre supplier's unofficial tabulated values of flexural toughness and $R_{10,30}$ (the latter are provided for guidance but are not guaranteed by the supplier).

The test building was constructed between November 2007 and February 2008. The slab-on-ground was completed on November 13. After walls and columns were constructed, the elevated slab was cast on February 18, 2008. The slab was water-cured for one week, the forms were stripped at 15 days, and the first short-term load test was conducted on March 18. Thereafter, two to three individual tests were conducted per testing day. The short-term load tests ended on May 31, 2008.

The short term tests showed that structural capacity and crack arresting performance increased with fibre dosage. Also, the tests showed that the addition of conventional reinforcing bars along the column lines increased slab capacity by 10 to 40%. Although there was large scatter in the physical properties of the delivered SFC, the slab test results indicated that SFC can be used with verifiable results in structural applications. Detailed test results for the short-term testing program are presented in Hedebratt (2012) and Hedebratt & Silfwerbrand (2012).

In the second phase, four of the previously loaded slab panels and an additional four panels were subjected to long-term point loads of about 50 or 75 kN. Loading mechanisms (**Figure 3**) were installed on the slab-on-ground and pulled downward on the elevated slab using a 30 mm diameter all-thread rod, a lever arm, and a concrete block that had been cast on site. These tests were started in May 2008 and continued until May 2009.

After nearly one year of loading at 50 to 75% of the initial cracking load, the data show that the rate of change in the deflection appears to be approaching zero (**Figure 4**). This is also indicated by beam tests according to Tan & Saha (2005), where only 7% deflection growth occurred in about ten years of sustained loading.

2.2 Tests on basalt fibre concrete specimens

2.2.1 The basalt fibre

The basalt fibre is relatively new in concrete applications despite that it has its origin in the 1920s in USA. It is used in various fields, e.g., fire-proof textiles for the automobile and aircraft industries.

Figure 5 – Two types of basalt fibres. To the left chopped fibres (here denoted type C). To the right, bar-shaped fibres (often called Minibars, here denoted type M). Photo: A M Mohaghegh.

The basalt fibre is produced of crushed and washed basalt that is taken from carefully selected rock quarries. The basalt melts at 1500°C. Extremely thin, continuous basalt fibres – filament – are extruded through very thin nuzzles. From the filament, thicker basalt fibres are produced. The basalt material is encapsulated within a matrix consisting of a thermoset vinyl ester resin or another similar resin.

In concrete mixes, basalt fibres with similar geometrical dimensions as straight steel fibres without hooked ends are usually used (**Figure 5**, right). The anchorage to the surrounding concrete is provided by a rough, irregular surface. In these investigations, a basalt fibre with diameter = 0.65 mm and length = 43 or 55 mm. The fibre is a small, slender bar, the product name is *Minibar* (here denoted M type).

Also another basalt fibre can be used in concrete. It is chopped from the melt. The fibres of this type (here denoted C type) used in current investigation had the length = 13 mm (**Figure 5**, left).

As stated above, the basalt fibre cannot corrode. Another advantage is that it has almost the same density as the surrounding concrete mix. It means that it is less prone to segregation. In concrete with a segregation risk, the heavy steel fibre may sink whereas the light polypropylene fibre may flow to the surface.

2.2.2 Norwegian-Swedish research project

The technical universities KTH in Stockholm (Sweden) and NTNU in Ålesund (Norway) have carried out a PhD project on basalt fibre concrete. The project was carried out between 2013 and 2018. The PhD student and later the graduated doctor was Mr Ali Mohammadi Mohaghegh and he carried out all tests in Ålesund but was registered as a PhD student at KTH. Both NTNU in Ålesund and KTH in Stockholm participated in the supervision.

The project was mainly experimental and it consisted of four test series in order to study flexural moment, shear, punching shear, and fire. The various parts are summarized in the following subsections.

2.2.3 Concrete mix design

The background to the project was efforts to develop concrete structures that are resistant in the very harsh marine environment at the Norwegian west coast. Therefore, a concrete with low permeability and high durability constituted the basis. In the latter test series, the selected concrete mix consisted of 495 kg cement and 63 kg silica per cubic meter and a w/b = 0.33. In the first test series, slightly less cement and silica were used resulting in a w/b = 0.40. The fibre content varied between 0 and 2 volume percent or between 0 and 42 kg/m^3. Maximum aggregate size was in all test series d_{max} = 16 mm.

2.2.4 Flexural moment capacity

The ground for assessment when designing fibre concrete structures is the flexural concrete strength that is determined through flexural testing of beam specimens. Here, the method recommended by EN 14651 was used. **Figure 6** shows the result from the tests on eight basalt fibre concrete beam specimens where the so called residual flexural strength (the residual strength after cracking and at a given displacement) has been plotted versus the fibre content. We may observe that the values increase approximately linearly with increasing fibre content. This is similar to the relationship that lot of researchers have found for steel fibre concrete beams.

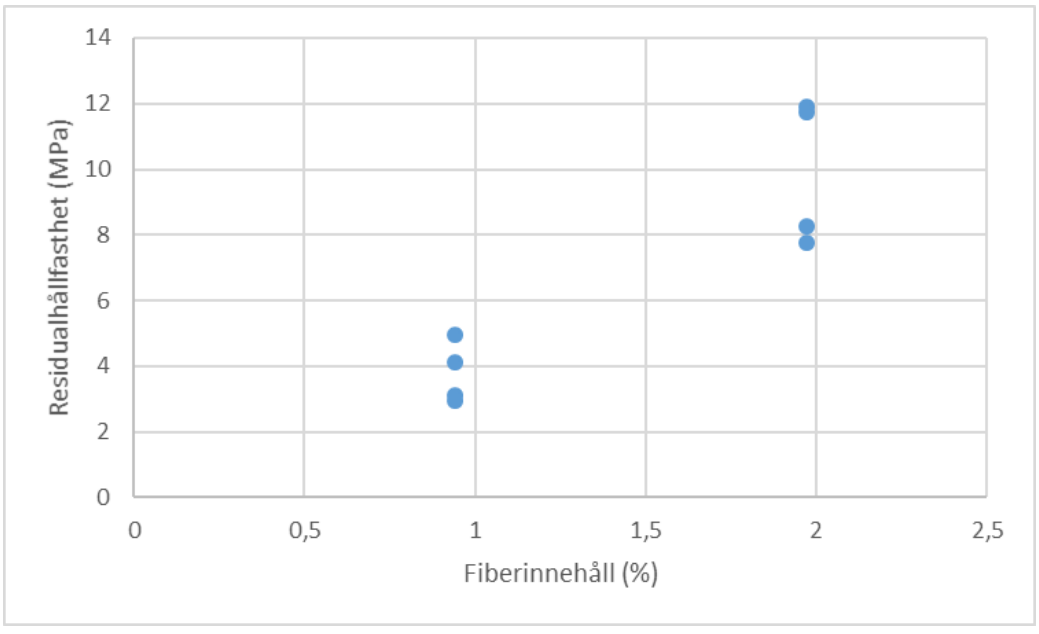

Figure 6 – Residual flexural strength as a function of fibre content.

2.2.5 Shear capacity

According to Eurocode 2, the designer usually needs to insert a certain amount of shear reinforcement (= minimum reinforcement) in order to handle the shear force in the concrete beam. The shear reinforcement usually consists of vertical stirrups but the installation of these units is more laborious and time-consuming than installing the horizontal flexural reinforcement. Many research papers have shown that a combination of conventional reinforcement for flexural moment and steel fibres for shear force results in a very good shear capacity.

The shear test series consisted of seven concrete beam with the measures $L \times b \times h$ = 1200×100×200 mm^3. All beams were reinforced with four basalt fibre bars with diameter = 8.9 mm and mean tensile strength = 1095 MPa. The basalt fibre content varied between 0 and 2 volume percent. At the tests, a substantial enhancement of the load-carrying capacity or shear capacity was measured; 30% at 1 volume percent and 50% at 2 volume percent.

The project also contained a test series on small circular concrete slabs to study the punching shear capacity, see Mohaghegh et al. (2018b). Here, the results only showed a slight improvement for specimens containing basalt fibres. The somewhat disappointing result can be explained by the selection of the small specimens that in turn was a result of a very limited budget. The specimen geometry did not allow the most beneficial crack orientation to develop.

2.2.6 Fire spalling

There is a risk of explosive fire spalling in dense concrete in a moist environment. There are several examples from tunnel fires that have resulted in spalling of the surface layer of the concrete lining. One example is the Euro tunnel between Great Britain and France. Research and experience show that there is a very good precaution: polypropylene fibres. Here, we are talking about very small and thin so-called micro fibres and it has been shown that an amount as small as 1 to 1 kg/m^3 is sufficient to prevent fire spalling. The reason for this success is not fully clear but the fact is that the polypropylene fibres are melting at 165°C and the most frequent hypothesis is that the melting fibres open up channels that enable the vapour, that otherwise would spall the concrete, to release.

As mentioned above, the basalt fibre does not solely consist of rock basalt but also of a matrix of thermoset vinyl ester resin. Vinyl ester starts to degenerate at its glass transfer temperature about 120°C and the degeneration of the matrix continues at temperatures around 350-450°C. The hypothesis was that the basalt fibres should improve the fire spalling resistance, partly due to a process similar to that of the polypropylene fibres, partly due to their possibility to bridge the cracks that arise during the spalling process.

The fire tests were carried out in the oven in RISE fire laboratory in Borås in the west of Sweden. Three concrete specimens with the dimensions 500×600×200 mm^3 were exposed to the so-called standard test fire curve with a maximum temperature of 900°C. One specimen without basalt fibres was used as a reference, the second specimen contained 0.5 volume percent fibres of type C and the third one contained 0.5 volume percent fibres of type M. All specimens spalled and no significant difference could be observed (**Figure 7**). The average spalling depth was 73, 73, and 62 mm, respectively. One reason to the observed spalling could be the very low *w/b* (= 0.34). On one hand, it may be stated that the basalt fibres did not make any improvement in this case. On the other hand, it could be concluded that the basalt fibre did not cause any impairment. More research would be beneficial on concrete mixes with slightly higher *w/b*, i.e., between 0.4 and 0.45. These values would be more representative for modern concrete tunnels.

Figure 7 – Test specimens after fire testing. Left = reference concrete. Centre = concrete with 0.5 % fibres of type C. Right = concrete with 0.5 % fibres of type M. Photo: A M Mohaghegh.

3 DESIGN

One reason for the limited use of fibre concrete (FC) in load-carrying structures is that the major international and national concrete codes do not cover FC structures. In Sweden, the Swedish Concrete Association (SCA) developed its first recommendations for SFC in 1995 (SCA, 1997). In 2008, SCA published recommendations on industrial concrete floors (SCA, 2008). They cover both plain, conventionally reinforced and SFR concrete floors and both slabs-on-grade, pile-supported slabs, and overlays. Pile-supported slabs are generally regarded as a load-carrying structure and since the Swedish code for concrete structures does not cover SFC solutions without conventional reinforcement ("SFC only") have not been possible to design. The new SCA recommendations have tried to fill this gap and have consequently developed guidelines for pile-supported slabs of SFC only. The guidelines also present straight-forward methods to design SFC floors and overlays for crack control. Together, the two SCA reports will facilitate the proper design and probably increase the future use of SFC structures.

In order to develop guidelines for designing load-carrying fibre concrete structures, the Swedish Standards Institute (SIS) established a Committee in 2007. The original object was to develop an addition to the Swedish structural concrete handbook BBK 04 (Swedish National Board of Housing, Building & Planning, 2004). In 2009, Eurocode 2 (SS-EN 1992-1-1, 2005) was introduced in Sweden. The object of the Committee was then changed to develop an addition to Eurocode 2. A draft version was completed in summer 2013 and in spring 2014, the printed version was completed, SS 812310:2014 (2014).

The Standard applies to the design of buildings and other civil engineering works with steel or synthetic fibres. The Standard does not cover glass, carbon, basalt or any other type of fibres. It is intended to be used in conjunction with Eurocode 2. This section describes the most important items in the standard and discusses how it can be used in order to simplify the design and production of fibre concrete structures with maintained safety level.

Fibre concrete is characterized through its flexural strength. The Standard bases the design on flexural strength values determined through tests on the European notched fibre concrete beam that has a height to span ratio = 150/550 and is tested in three point bending according to SS-EN 14651 (2007) at 28 days (**Figure 8,** left). Flexural strength classes R_1, R_2, R_3, and R_4 are defined from the characteristic values (lower 5% fractile) of the residual flexural tensile strength. For all four classes, six levels of the strength are given (1.0, 2.0, …6.0 MPa). That means a total of 24 classes.

The design of fibre concrete members is based on pure tensile strength. In order to obtain design values, the characteristic residual flexural tensile strength must be (1) transferred to a characteristic residual tensile strength and (2) transferred to a design residual tensile strength (**Figure 8**, right).

The second transformation contains two new factors, the fibre factor taking the fibre orientation into account (more unilateral distribution gives higher values) and a factor considering the degree of static determination.

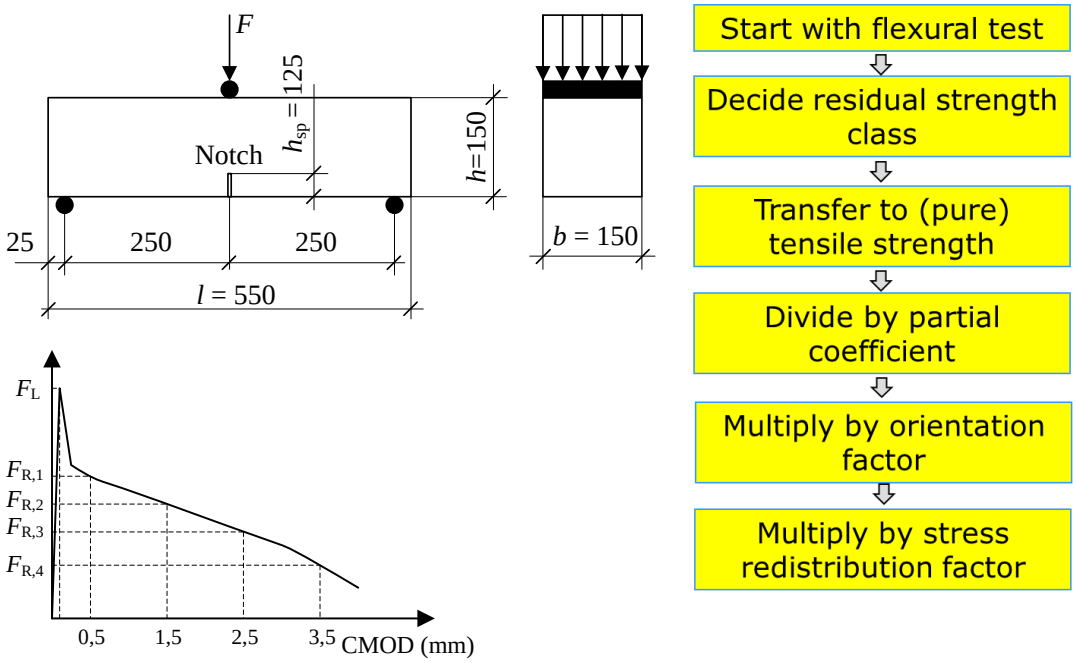

Figure 8. The design values for tensile strength is based on flexural tests on according to SS-EN 14651 (left) and transformations in several steps (right).

Statically indeterminate structures provide possible stress redistribution reducing the failure probability. This beneficial condition is considered by setting a value > 1 for this factor. A theoretical background is given in Silfwerbrand (2017).

The overall conclusion is that the new Swedish Standard will remove an obstacle that has restrained the use of fibre concrete in structural beams and elevated slabs. However, full use of FC in applications where it is suitable and economic will hardly be the case before the introduction of next version of Eurocode 2 that probably will contain an appendix devoted to FC structures.

4 APPLICATIONS

4.1 Shotcrete

For shotcrete in tunnels, fibre reinforcement has become nearly the only type of reinforcement that is used (**Figure 9**), at least in Sweden where the rock quality to a large majority is very high. The fibre reinforced shotcrete used is normally strain softening, which is a shortcoming in certain cases as, e.g., drainage structures. Otherwise the experiences are good.

The spraying technique also makes it easier to produce thin walled structures like shells and domes, where fibre reinforcement also gives large advantages, **Figure 10**.

4.2 Precast concrete elements

Reinforcing with fibres allows for the use of thinner sections than when bar reinforcement is used because no concrete cover is needed. The fibre reinforced elements are also less sensitive to damages since there are fibres everywhere. A very good example is a vault door with both fibres and bars. The fibres make it more difficult to crack the door into pieces with hydraulic tools. Some examples are given in **Figure 11** below.

4.3 Industrial floors

The industrial floor is one of the major applications of fibre concrete and especially steel fibre concrete. Most industrial concrete floors are regarded as a simple

Figure 9. Tunnel lining of steel fibre reinforced shotcrete. Picture by courtesy of BESAB, Gothenburg, Sweden.

Figure 10. Examples of thin-walled roof structures in fibre reinforced shotcrete.

structure (**Figure 12**). Traditionally, the industrial concrete floor has been produced as a slab-on-grade which is not regarded as a load-carrying structure. However, during the ongoing urbanization industrial buildings, distributions centres, and shopping malls, that all include large concrete floors placed close to or on the ground level, have been placed outside the cities, often in rural areas and often in areas with rather soft subgrade, e.g., silt and clay. If high mechanical loads are anticipated, the floor is often strengthened by a pile grid, e.g., a pile-supported slab. The question is if the pile-supported slab is a load-carrying structure or not.

Industrial floor slabs constructed in Sweden typically comprise concrete with a water-cementitious material ratio *w*/*cm* of 0.55 to 0.58. The concrete strength class normally ranges from C30/37 to C32/40. The concrete is preferably of Consistency Class S3 to S4 per SS-EN 206:2013 (2015). That is, it has a slump of 80 to 210 mm, although higher slumps are sometimes used.

Traditionally, pile supported industrial floor slabs have been reinforced with two layers of welded wire reinforcing or distributed deformed bars, with the top and bottom layers anchored outside and inside the moment inflection points, respectively. The reinforcement has been installed in bands crossing the pile heads. The areas between has been relying solely on the fibre concrete.

Such floors span 4.0 to 6.0 m, comprise slabs that are generally 180 to 300 mm thick, and are designed for loads ranging from 10 to 30 kN/m^2 in the ultimate limit state (SCA, 2008).

In Sweden, there has been a competition between two different design strategies; one Swedish based on Swedish praxis expressed in Swedish handbooks, recommendations, and standards, and one based on continental experience. The difference has been quantified and highlighted in a paper written co-written by representatives of the both strategies (Destrée & Silfwerbrand, 2012). The Swedish traditional design leads to thicker SFC floors with adherent higher safety against cracking and other damages. This finding does not state that the safety using the continental strategy is too low. Beneficial effects, e.g., arch action and membrane effects, are not taken into account in any of the two methods and may provide the sufficient safety margin. However, in all cases, the importance of meticulous operations in structural design, detailing, concrete mix design, concrete delivery, concrete production, casting, curing, loading, operation, and maintenance cannot be overestimated.

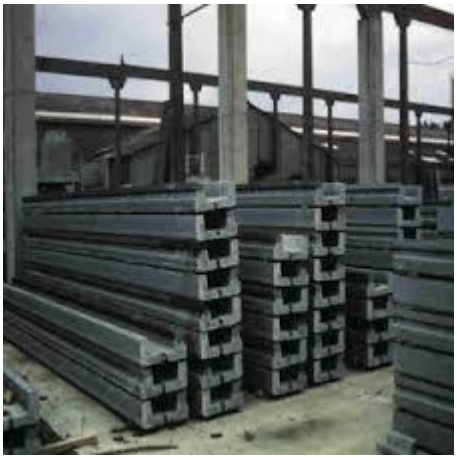

Beam elements.

Pipes

Tunnel elements.

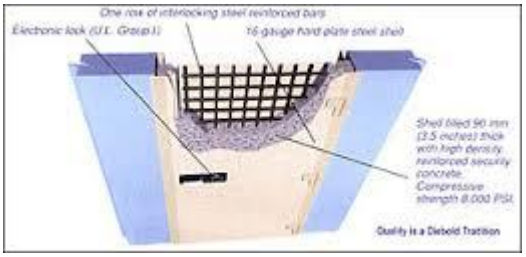

Vault door.

Figure 11. Examples of fibre reinforced precast concrete elements.

4.4 Overlays

Overlays – bonded or unbonded – are often used in bridge deck repair (**Figure 13**), as a part of the pavement system (**Figure 14**) or as a part of the industrial floor. The idea with the bonded overlay is to secure composite action between the existing layer (substrate) and the overlay. If the bond is ensured, the two layers act as a monolith. Unbonded overlays lack bond between the existing layer and the overlay, but usually the absence of bond is intentional. The designer may wish to minimize the stresses in either the overlay or in the substrate. This condition could be secured through introducing a specific interlayer between the two layers.

Bonded overlays are the most common case in bridge deck repair. A thin bonded overlay may be cast in plain concrete (i.e., without reinforcement), but steel fibre concrete is quite often selected since this solution diminishes the risk of uncontrolled cracking. (There are, of course, also solutions in conventional reinforced concrete.)

Figure 12. Example of an industrial concrete floor in a storage building. Photographer: J. Hedebratt.

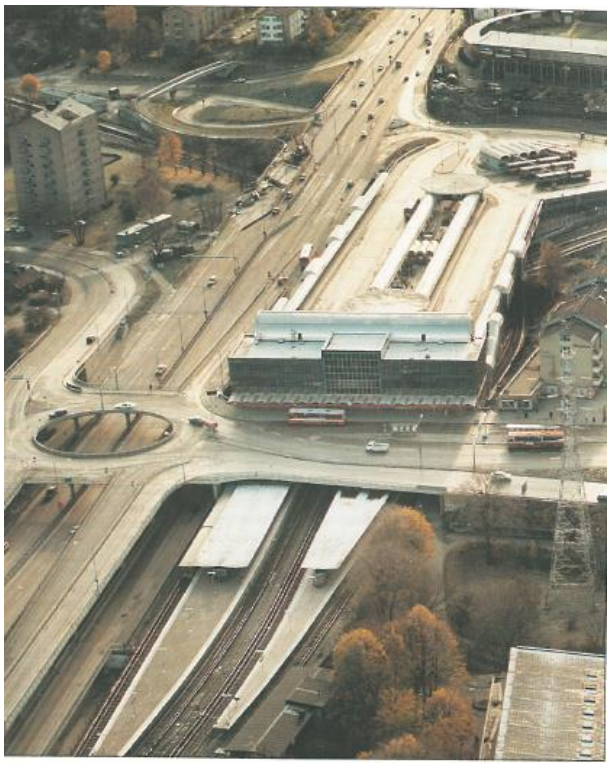

Figure 13. Gullmarsplan's traffic interchange was repaired with a bonded SFC overlay in 1995 (Paulsson & Silfwerbrand, 1995).

Figure 14. Whitetopping. Steel fibre concrete overlay on an old asphalt road (Silfwerbrand, 1995).

Both bonded overlays and unbonded overlays are used in pavement design and pavement restoration. Concrete pavements are often cast in two lifts, a thick bottom layer of ordinary concrete and a thin top layer of wear resistant concrete with high quality aggregates. Thin concrete overlays can also be used to repair old asphalt pavements with extensive rutting. This solution is called whitetopping and may contain a steel fibre concrete overlay (**Figure 14**).

4.5 Beams and elevated slabs

As stated above, the lack of standards and legal recommendations has prevented the use of fibre concrete in structural applications such as beams and elevated slabs. Industrial concrete floors, overlays, and minor precast concrete elements are hardly regarded as load-carrying structures making the facilitating the design. However, the benefits of fibre concrete are several and ought to be taken into account also for structural applications. Avoiding the manual work of installing conventional reinforcement would improve the working environment and increase the productivity.

The research in fibre concrete is vast and the allowable space is not sufficient to summarize it here. However, a large part of this research has been devoted to beams, most of them fairly small. We know that fibres substantially contribute to both flexural and shear strength. Tests on large beams and slabs are more scarce but here it may be stated that a combination of conventionally steel reinforcing bars for flexure and steel fibres for shear may be a very interesting solution where bars are localized to areas and section with the highest stresses and fibres will eliminate the need of stirrups and its adherent laborious installation.

During the latest ten years, more research has been devoted to tests on larger SFC elements. In Norway, Døssland (2008) conducted tests on slabs both indoors and outdoors. Field tests on elevated SFC slabs have been conducted in Luxemburg, Estonia, and Latvia (Hedebratt, 2012). Personally, Hedebratt also conducted tests on elevated SFC slabs (Section 2.1). The overall conclusion is that SFC slabs have a substantial load-carrying capacity. This has been an important prerequisite for the development of standards for load-carrying SFC structures.

4.6 Marine structures

As stated above, the project on basalt fibre concrete (Section 2.2) was originally developed for the harsh environment at the Norwegian west coast and especially for floating structures. The aim was to develop a basalt fibre concrete meeting high demands on durability. **Figure 15** shows an example of a floating structure that would be possible to make in basalt fibre concrete.

5 CONCLUDING REMARKS

Fibre concrete (FC) is a versatile alternative for many applications, e.g., shotcrete, precast elements, industrial floors, and overlays. The lack of standards and recommendations have prevented the use of FC for beams and elevated slabs. Recent research has resulted in new standards for FC for structural applications. In Sweden, a new standard was published in 2014.

As stated above, there are several alternatives to steel fibres. The two most important ones for structural applications are synthetic fibres and basalt fibres. The new Swedish standard is written in a material-independent way regarding fibres, but in order to use it for other materials than SFC, we need more test results and experience. At KTH, a recent doctoral thesis (Mohaghegh, 2018), summarized in Section 2.2, shows that basalt fibre concrete has similar properties as SFC regarding flexure, shear, and punching shear if the fibre dosages are the same. The basalt fibre has equal density as concrete (making it easier to avoid segregation) and does not corrode.

Generally, it is good to have many alternatives when we are making our material selection. Having lots of alternatives makes it easier to optimize load-carrying capacity, function, sustainability, and aesthetics. The above cited research project shows that basalt fibre concrete (BFC) constitutes an additional alternative. The test results indicate that the basalt fibres provide the concrete properties that are similar to the ones steel fibres give. The fact that basalt fibres do not corrode leads to an advantage in concrete structures in severely aggressive environments like the one along the Norwegian west coast. The project was carried out with a very limited budget leading to test series with a small number of small-size specimens. More tests with larger test specimens and preferably including parallel tests with steel fibre concrete would be desirable. However, BSF is already used in Sweden, e.g., by a couple of precast concrete producers.

Finally, it ought to be repeated that FC hardly may replace RC in structural applications. Reinforcing steel is in many cases more economical since it can be localized to areas and sections subjected to the highest stresses. However, combinations of steel fibres and reinforcing bars and meshes may provide an interesting alternative; e.g., FC with additional reinforcing meshes above the pile heads in pile-supported slabs or reinforcing bars for flexure and fibres for shear.

Figure 15 – Floating fish factory in the North Sea. Photo: Ulstein Betong Marine Company.

REFERENCES

1. *ACI Committee 544, "Measurement of Properties of Fiber Reinforced Concrete (ACI 544.2R-89 [Reapproved 2009]),"* American Concrete Institute, Farmington Hills, MI, 2009, 11 pp.
2. *BBK 2004 (2004): "Handbook of Concrete Structures. Part 1 Design" ("Boverkets handbok om betongkonstruktioner. Band 1 Konstruktion"),* National Board of Housing, Building and Planning, Karlskrona, Sweden, 271 pp. (In Swedish).
3. *Destrée X & Silfwerbrand J (2012): "Steel Fibre Reinforced Concrete in Free Suspended Slabs: Case Study of the Swedbank Arena in Stockholm". Proceedings, fib Symposium on "Concrete Structures for Sustainable Community",* Stockholm, Sweden, June 11-14, 2012, p. 97-100.
4. *Døssland Å L (2008): "Fibre Reinforcement in Load-carrying Concrete Structures. Laboratory and Field Investigations Compared with Theory and Finite Element Analysis". Doctoral Thesis 2008:50,* Norwegian University of Science and Technology, Faculty of Engineering Science and Technology, Dept. of Structural Engineering, Trondheim, Norway, 254 pp.
5. *Hedebratt J (2012): "Industrial Fibre Concrete Floors – Experiences and Tests on Pile-Supported Slabs". Bulletin No. 113 (Doctoral Thesis), Div. of* Structural Design & Bridges, Dept. of Civil & Architectural Engineering, School of Architecture & Built Environment, KTH Royal Institute of Technology, Stockholm, Sweden.
6. *Hedebratt J & Silfwerbrand J (2012): "Lessons Learned – Swedish Design and Construction of Industrial Concrete Floors",* Nordic Concrete Research, NCR, June 2012, p. 75-92.
7. *Hedebratt J & Silfwerbrand J (2015): "Time-Dependent Deflections of a Steel Fiber Concrete Slab."* Concrete International, Vol. 37, No. 7, July 2015, p. 46-52.
8. *Holmgren J (1992): "Rock Strengthening with Shotcrete" ("Bergförstärkning med sprutbetong"),* Vattenfall Vattenkraft, Stockholm, Sweden, 74 pp. (In Swedish).
9. *Holmgren J (2010): "Shotcrete Research and Practice in Sweden—Development over 35 Years". From: "Shotcrete: Elements of a System", CRC* Press, London, 310 pp. Edited by E S Bernard.
10. *Jansson R (2013):"Fires Spalling of Concrete. Theoretical and Experimental Studies". Bulletin No. 117 (Doctoral Thesis), Div. of Concrete Structures, Dept. of Civil & Architectural Engineering, School of Architecture & Built Environment, KTH Royal Institute of Technology, Stockholm, Sweden.*
11. *Mohaghegh A M (2018): "Structural Properties of High-Performance Macro Basalt Fibre Concrete; Flexure, Shear, Punching Shear and Fire Spalling". Bulletin No. 152 (Doctoral Thesis), Div. of Concrete Structures, Dept. of Civil & Architectural Engineering, School of Architecture & Built Environment, KTH Royal Institute of Technology, Stockholm, Sweden.*
12. *Mohaghegh A M, Silfwerbrand J & Årskog V (2017): "Flexural Behaviour of Medium-Strength and High-Performance Macro Basalt Fibre Concrete Aimed for Marine Applications". Nordic Concrete Research, Vol. 57, No. 2/2017, p. 103-123.*
13. *Mohaghegh A M, Silfwerbrand J, Årskog V & Jansson McNamee R (2017) "Fire Spalling of High-Performance Basalt Fibre Concrete". Nordic Concrete Research, Vol. 57, No. 2/2017, p. 89-102.*
14. *Mohaghegh A M, Silfwerbrand J & Årskog V (2018a): "Shear Behaviour of High-Performance Basalt Fiber Concrete – Part I: Laboratory Shear Tests on Beams with Macrofibers without Bars". Structural Concrete, Vol. 19, No. 1, p. 246-254.*
15. *Mohaghegh A M, Silfwerbrand J & Årskog V (2018b): "Shear Behaviour of High-Performance Basalt Fiber Concrete – Part II: Laboratory Punching Shear Tests on Small Slabs with Macro Fibers and Bars". Structural Concrete, Vol. 19, No. 2, p. 331-339.*
16. *Paulsson J & Silfwerbrand J (1995): "Förnyelse av Gullmarsplans trafikplats - vidhäftande slitskikt av stålfiberbetong". Tidskriften Betong, No. 2, 1995, p. 22-27. (In Swedish).*
17. *Silfwerbrand J (1995): "Whitetoppings - Swedish Field Tests 1993-1995". CBI Report No. 1:95,* Swedish Cement and Concrete Research Institute, Stockholm, 77 pp.
18. *Silfwerbrand J (2017): "Safety Levels in Concrete Slabs-on-Grade". Proceedings, fib Symposium 2017, Maastricht, The Netherlands, June 12-14, 2017, 8 pp.*
19. *SS-EN 14651 (2007): "Test Method for Metallic Fibre Concrete — Measuring the Flexural Tensile Strength (Limit of Proportionality (LOP), Residual)".* Swedish Standards Institute, Stockholm, Sweden.
20. *SS-EN 1992-1-1 (2005): "Eurocode 2: Design of Concrete Structures – Part 1-1: General Rules and Rules for Buildings". Swedish Standards Institute,* Stockholm, Sweden, 225 pp.
21. *SS-EN 206:2013 (2015): "Concrete – Specification, Performance, Production and Conformity". Swedish Standards Institute,* Stockholm, Sweden, 15 pp.
22. *SS 812310:2014 (2014): "Fibre Concrete – Design of Fibre Concrete Structures". Swedish Standards Institute, Stockholm, Sweden, 38 pp.*
23. *Swedish Concrete Association (1997): "Steel Fibre Concrete – Recommendations for Design, Construction and Testing" ("Stålfiberbetong – rekommendationer för konstruktion, utförande och*

provning"), Concrete Report No. 4, 2nd edition, Stockholm, Sweden, 135 pp. (In Swedish).

24. *Swedish Concrete Association (2008): "Industrial Floors – Recommendations for Design, Material Selection, Execution, Operation and Maintenance" ("Industrigolv – Rekommendationer för projektering, materialval, produktion, drift och underhåll"), Concrete Report No. 13, 1st Edition, Stockholm, Sweden, 296 pp. (In Swedish).*
25. *Tan K H & Saha M K (2005): "Ten-Year Study on Steel Fiber-Reinforced Concrete Beams Under Sustained Loads," ACI Structural Journal, American Concrete Institute, V 102, No. 3, May-June 2005, p. 472-480.*

Basalt fibers and basalt-carbon fibre reinforced polymers for reinforcement of concrete structures

Bazaltna vlakna in polimeri ojačeni z bazalt-karbonskimi vlakni za armiranje betonskih konstrukcij

Andrzej Garbacz

Warsaw University of Technology

Marta Kosior-Kazberuk

Bialystok University of Technology

Kostiantyn Protchenko, Marek Urbański, Maria Włodarczyk, Elżbieta Szmigiera

Warsaw University of Technology, Poland

Abstract

The paper describes recent developments in the area of Fibre-Reinforced Polymers (FRP) reinforcement implemented in concrete structures. Durability, strength and stability are the main criteria when selecting FRP reinforcement. A major motive for the implementation of FRP lies in the unique characteristics of these materials and their constituents when they used to its considered design purpose. Extensive research on Hybrid FRP (HFRP) bars is being conducted at the Warsaw University of Technology in conjunction with an FRP manufacturing company under the programme of the National Centre for Research and Development in Poland. This research aims at investigating the mechanical and physical behaviour of HFRP bars, and the possibilities of using these types of reinforcement in structural systems for both flexural and compression members

Povzetek

Članek opisuje najnovejši razvoj armature iz polimerov ojačenih z vlakni (POV), ki se uporablja v betonskih konstrukcijah. Trajnost, trdnost in stabilnost so glavna merila pri izbiri armature iz POV. Glavni motiv za uporabo POV je v edinstvenih značilnostih teh materialov in njihovih sestavnih delov, ko so se uporabljali za načrtovani namen. Na Tehniški univerzi v Varšavi potekajo obsežne raziskave o palicah iz hibridnih POV (HPOV) v povezavi s proizvajalcem POV v okviru programa Nacionalnega centra za raziskave in razvoj na Poljskem. Namen raziskave je raziskati mehansko in fizikalno obnašanje palic iz HPOV ter možnosti uporabe teh vrst armiranja v konstrukcijskih sistemih za upogibne in tlačne elemente.

Keywords: FRP reinforcement, basalt fibres, HFRP bars, FRP-RC members, Fire resistance of FRP, FRC Structures
Ključne besede: armatura iz POV, bazaltna vlakna, palice iz HPOV, POV-AB elementi, požarna odpornost POV, MAB konstrukcije

1. INTRODUCTION

The service life of reinforced concrete (RC) structures is drastically affected by the corrosion of internal steel reinforcement, particularly in cases where de-icing salts are used. The same problem of steel corrosion was observed in marine structures where chlorides and seawater are present [1].

Therefore, routine maintenance is needed to counter this problem, however, the cost of repair, rehabilitation, strengthening of steel reinforced concrete structures, as well as delaying and detouring traffic can be as high as two times the original construction cost [2, 3].

The advantage of fibre reinforced polymer (FRP) composites lies in their high-strength, lightweight, noncorrosive, nonconducting, and nonmagnetic properties. In addition, FRP manufacturing, using various cross-sectional shapes and material combinations, offers unique opportunities for the development of shapes and forms that would be difficult or impossible with conventional steel materials [4]. The widespread implementation of FRP as a reinforcement for reinforced concrete elements requires: a comprehensive understanding of how each of these materials behaves alone as well as the behaviour of the structural system as a whole. [5].

Fibre Reinforced Concrete (FRC) has been widely used in different applications in constructions, such as geotechnical structures(dam, tunnels), roads (bridges, pavements, railways objects), marine and industrial structures (cooling towers, floors, overlays), etc., where the major concern is toughness and first-crack strength in flexure. For engineering applications, the tension-weak nature of concrete is usually reduced by using different types of fibres. A recent development has been the introduction of various types of non-metallic fibres, which can provide a similar post-cracking performance [6-9].

Basalt fibre is an inorganic fibre that is assumed to be one of the most ecologically friendly type of fibres. Basalt fibre is formed from basalt rock, which is a ubiquitous natural resource covering nearly one-third of the earth's surface, including much of the ocean floor [10]. The manufacture of basalt fibre involves the melting of the crushed and washed basalt rock at about 1500 °C (2,730 °F). The manufacturing process requires two distinct procedures, at the first the molten rock is extruded through small nozzles to obtain continuous filaments of basalt fibre. The second is whereby the fibres are bonded with the matrix during moulding to produce ready products, BFRP bars.

The basalt fibres are characterised as weak anisotropic materials with high tensile strength, improved chemical resistance, extended operating temperature range, and environmental friendliness. Moreover, basalt fibre has a good impact resistance, and a fire with less poisonous fumes [11, 12]. In addition, the basalt fibres do not need any other additives in the one-step producing process, adding a distinct benefit in cost.

Therefore, these advantages make basalt fibre a promising alternative to other types of fibres [13]. BFRP composite is expected to provide benefits that are comparable or superior to other types of FRP while being significantly cost-effective [14-16].

The current situation on the market shows that using of BFRP bars will be confined to applications where their unique characteristics will be the most appropriate. Nevertheless, the data currently available on the behaviour of BFRP-RC members are relatively scarce. North American design codes and guidelines such as CAN/CSA S806 (2012) [17], CAN/CSA S6 (2014) [18] and ACI 440.1R (2015) [19] have been developed to regulate the design conditions for structural elements reinforced with GFRP, CFRP and AFRP bars, but do not consider BFRP reinforcement.[20, 21].

Therefore, BFRP bars are characterised as a new variety of material whose properties are still have not been completely investigated and consequently this research is aimed at investigating the mechanical and physical behaviour of HFRP bars, and the possibilities to use these types of reinforcement in structural systems for both flexural and compression members.

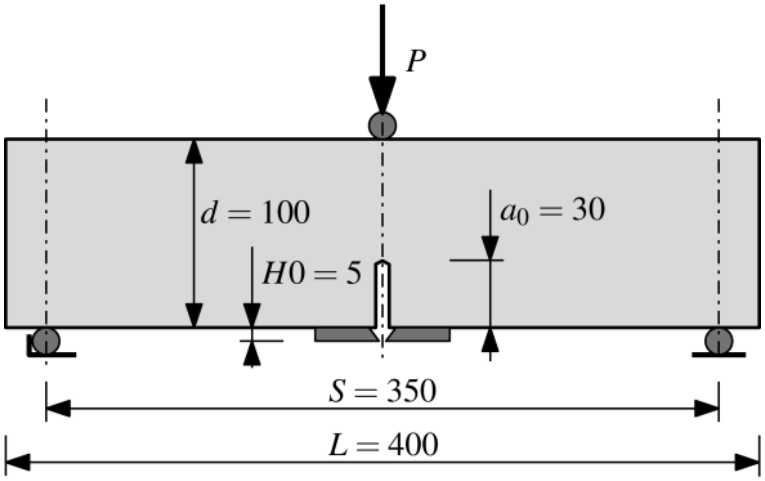

Fig. 1: Fracture testing configuration and geometry of notched specimen.

Table 1. Measured average values of concretes with various fibre contents V_f: compressive strength f_{cm} and flexural strength f_{ctm}.

Cement	*w/c*	V_f (kg/m^3)	f_{cm} (MPa)	f_{ctm} (MPa)
CEM I 42.5 R	0.40	0.0	67.54	4.51
		2.0	65.73	5.48
		4.0	72.77	4.89
		8.0	75.63	5.62
	0.50	0.0	65.17	4.14
		2.0	66.26	4.18
		4.0	70.67	5.00
		8.0	72.50	5.28
CEM II/A-V 42.5 R	0.40	0.0	52.28	5.03
		2.0	55.78	5.10
		4.0	58.26	5.64
		8.0	60.19	5.89
	0.50	0.0	51.09	4.84
		2.0	54.52	4.65
		4.0	54.87	4.89
		8.0	58.88	5.55

2. FRACTURE TOUGHNESS OF CONCRETE WITH BASALT FIBRE

2.1 Characteristics of the materials and specimens

The aim of the investigation was to evaluate the effect of basalt fibre content on the toughness and post-cracking behaviour of concrete. The details of the experiment are presented in the work of M. Kosior-Kozberuk and J.Krassowska [22]

Concrete mixtures were made with two cement types CEM I 42.5 R and CEM II/A-V 42.5 R (usually used in concrete pavements). The cement content in all mixtures tested was *320 kg/m^3*. The water to cement ratio was equal to *0.40* and *0.50*, respectively. For the aggregate, a mixture of sand (fraction *0-2 mm*) and natural aggregate with a maximum diameter of up to *16 mm* was used. The basalt fibres with a diameter of *0.02 mm* and a length of *50 mm* were characterized by a tensile strength of *1680 MPa*, elastic modulus of *89 GPa* and density of *2600 kg/m^3*.

The basalt fibres were added to concrete at three contents, V_f of *2.0*, *4.0* and *8.0 kg/m^3*, which gave volume fractions *0.075%; 0.15%* and *0.31%*, respectively. The fibres were added as a replacement for part of the coarse aggregate by volume. Comparatively, the properties of concretes with no added fibres were also tested. The polycarboxylate polymer based super-plasticizer was used to minimize fibres clumping and enhance fibre dispersion in concrete mix. The super-plasticizer was applied in the amount of *1.0%* of cement mass.

For each fibre-dosage combination notched beams of size *100×100×400* mm were prepared for fracture parameters determination. Every series was composed of four replicates. Moreover, the beams (*100×100×400 mm*) for flexural strength were also cast and cubes (*100×100×100 mm*) for the compressive strength test were cut from them. After demoulding all specimens were cured in water at the temperature of *18±2°C* until they were tested.

The fracture performance of concretes with fibres and the control concrete without reinforcement was tested in accordance with the recommendations of the RILEM Fracture Mechanics Committee [19, 20]. The notched beams of size *100×100×400* mm were used for a three-point bending test corresponding to Mode I conditions. An initial saw-cut notch with a depth equal to *30 mm* and width of *3 mm* was located in the middle of the span (Fig. 1). The elongated U-notches ($a_0/d = 0.30$) were sawn under wet conditions one day before the test. Each series was composed of four replicates.

The fracture parameters considered were the critical stress intensity factor K_{Ic} and the critical tip opening displacement $CTOD_c$. The critical stress intensity factor K_{Ic} is defined as the stress intensity factor calculated at the critical effective crack tip, using the measured maximum load. The critical crack tip opening displacement $CTOD_c$ is defined as the crack tip opening displacement calculated at the original notch tip of the specimen, using the measured maximum load and the critical effective crack length a_c. The values of K_{Ic} and $CTOD_c$ were determined using the procedure and equations given in RILEM TC 89-FMT Recommendation [23], based on the fracture model (*TPFM*) elaborated by Jenq and Shah [24], assuming a cyclic loading-unloading test procedure. Both parameters are related to the critical stress σ_c initiating the crack propagation and the effective length of the critical crack a_c. The assessments for LEFM application by Jenq and Shah were described in detail in [25].

The fracture energy, G_F, is defined as the area under the load-deflection curve per unit fractured surface area. The fracture energy of concretes tested in this experimental study, was evaluated using the procedure given by RILEM TC 50-FMT Recommendation [23], in which energy was calculated from load-deflection curves obtained by performing a three-point bending test, dividing by the area of ligament, which is defined as the projection of the fracture zone on a plane perpendicular to the beam axis. The scatter of the calculated values of G_F results from the inevitable random length of the tail region of the P-δ curve and also from the uncertainty in extrapolating the curve`s descent toward zero. To reduce the impact of factors mentioned on the scatter of G_F, the plot was turned down when the load was approximately equal to $0.05\ P_{max}$ *(100÷200 N)*. The area of the cross section of the specimen, which the total energy value was referred to, was determined based on the width of the test specimen b and the depth d excluding the notch ($a_0 = 30$ *mm*).

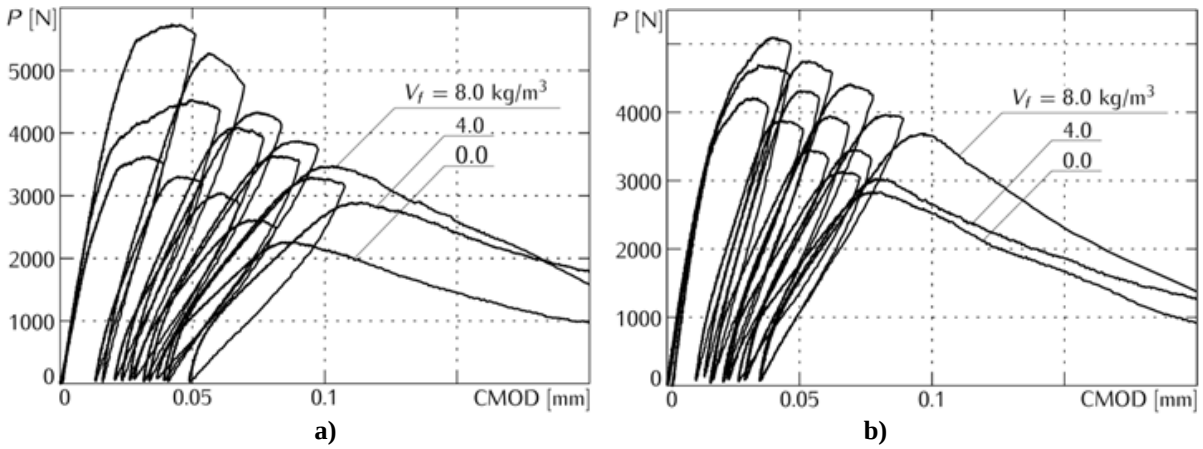

Fig. 2: Load *P-CMOD* plots for concretes with different content of basalt fibres V_f for concretes with: a) *w/c = 0.40* (CEM I 42,5 R) and b) *w/c = 0.40* (CEM II/A-V 42,5 R).

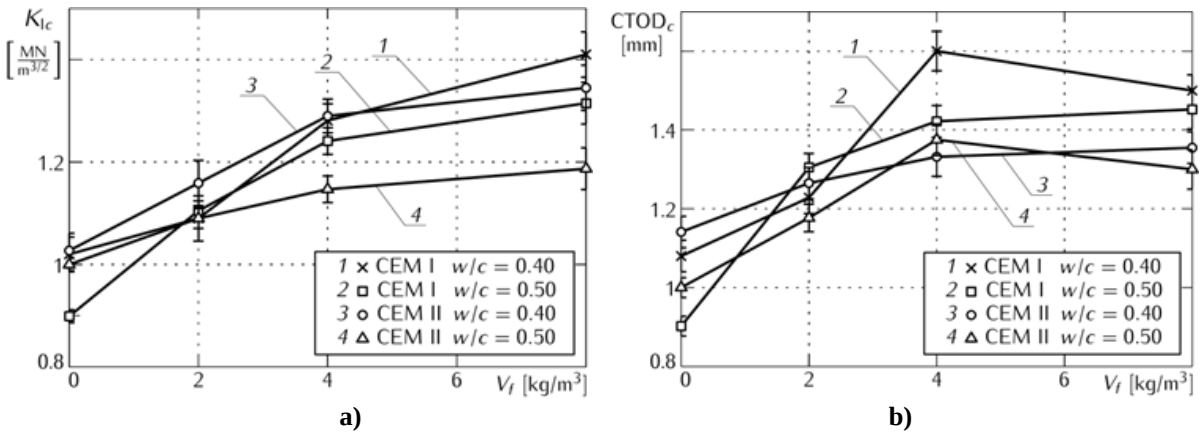

Fig. 3: Effect of fibre volume fraction V_f (%), cement type and *w/c* ratio on: a) fracture toughness K_{Ic} b) $CTOD_c$

Table 2: Elastic G_{Fel} and plastic G_{Fpl} part of the fracture energy until crack propagation, G_F– total fracture energy.

Cement	*w/c*	V_f (kg/m^3)	G_F (Nm/m^2)	G_{Fpl} (Nm/m^2)	G_{Fel} (Nm/m^2)
CEM I 42.5 R	0.40	0.0	147.8	9.0	52.0
		2.0	159.8	16.0	53.0
		4.0	190.3	27.0	78.0
		8.0	210.4	33.6	88.0
	0.50	0.0	128.0	7.0	39.0
		2.0	154.6	15.0	54.0
		4.0	185.7	24.0	71.0
		8.0	200.2	30.0	84.0
CEM II/A-V 42.5 R	0.40	0.0	144.8	7.2	49.0
		2.0	175.3	16.0	54.0
		4.0	180.0	23.0	72.0
		8.0	188.4	28.0	77.0
	0.50	0.0	150.5	10.0	49.5
		2.0	170.5	14.0	54.5
		4.0	166.5	20.0	59.5
		8.0	185.5	21.0	70.0

2.2 Results

The flexural strength of concrete was defined by the load capacity at the first crack. The compressive strength was determined according to EN 12390-3 [26] using cubes of size *100 mm* (Tab.1).

The fracture toughness, K_{Ic} and the critical crack tip opening displacement ($CTOD_c$) were determined on the basis of load *P* vs. *CMOD* curves obtained for the concrete specimens subjected to cyclic loading-unloading (Fig.2)

The results of the critical stress intensity factor, K_{Ic} and the critical value of the crack tip opening displacement *CTODc*, derived from the *P–CMOD* relationships for different fibre content, were shown in Figure 3.

The incorporation of the basalt fibre does not only influence the post-peak behaviour of concrete beams but also the pre-peak part of both load-CMOD and load-deflection curves. The values of fracture energy given in Table 2 were calculated according to load-deflection diagrams containing both the plastic and elastic part of the fracture energy, up to the breaking load. To give an idea about the proportion of the elastic part of the fracture energy, Table 2 illustrates the elastic G_{Fel} and plastic G_{Fpl} part of energy until crack propagation related to the total measured energy G_F.

3. BFRP REINFORCED BEAMS

The first stage of this research project involved the fabrication of several series of beams reinforced with BFRP bars to test their flexural capacity. In order to determine bending resistance, deflections and cracks, concrete beams reinforced with BFRP bars and reference beams reinforced with steel bars of various reinforcement ratios were subjected to flexural loading in a four-point bending test. All specimens had rectangular cross-section with dimensions *140 mm* wide and *260 mm* high and were *3000 mm* long. Every series contained a two samples.

(1 and 2 series) Top reinforcement (compression zone) and shear reinforcement (stirrups) were kept constant for all beams. Two BFRP bars with a diameter of *8 mm* were used as longitudinal top reinforcement for beams reinforced with FRP reinforcement and *4 mm* BFRP

Table 3: Specimen Details

Series No.	Mechanical reinforcement ratio $\rho_{me} = \rho(f_u/f_{ck})$		Bottom reinforcement		Tensile Strength f_u MPa	Elastic Modulus, E GPa		Srain at break ε_u %
	BFRP	Steel	BFRP	Steel	BFRP	BFRP	Steel	BFRP
1	0,166	0,163	2Ø10	2Ø14	1020	49,4	200	2,06
2	0,250	0,244	3Ø10	3Ø14				
3	0,326	0,322	2Ø14	2Ø20	943	42,8		2,36

stirrups, and two *10 mm* steel bars for steel reference beams. The stirrups of reference beams were made of *6 mm* steel bars of class *B500SP*. The stirrup spacing was assumed as *100 mm* and the mid part of the beam did not have stirrups to simulate clear bending. The bottom reinforcement (tensile zone) was changing depending on the series.

The average modulus of elasticity of BFRP bars with the diameter of *10 mm* was determined in the uniaxial tensile test and equals *49.4 GPa*, average tensile strength *1019,83 MPa*, and average strain at breaking was defined as *2.4%*.

(3 series) The average modulus of elasticity of BFRP bars with the diameter of *14 mm* was determined in the uniaxial tensile test and equals *42,76 GPa*, average tensile strength *942,98* MPa, and average strain at break was defined as *2,36 %*.

The average concrete strength was $f_{ck,\,cube} = 43.82\ MPa$. Table 3 shows specimens characteristics and a detailed overview of the flexural testing of beams reinforced with BFRP bars as is given in companion papers [27-29].

Loading was placed in a four-point system made of steel traverse, at one third and two thirds of the beam span. Loading was performed in several cycles. During the first cycle of loading, the beams were subjected to load equal to *10 kN* and then the load was reduced to *5 kN*. In each following cycle loading was increased by *10 kN*, and then reduced again to *5 kN*, till the failure of the structure.

It has been stated in this study that in contrast to the bilinear stress-strain dependence for steel reinforcement, basalt reinforcement has a linear dependence until failure.

The failure of beams with BFRP reinforcement did not occur suddenly and this effect was a result of the transformation of the beam into a tie system since the flexural basalt reinforcement remained unbroken.

Deflections of beams with BFRP reinforcement were significantly higher than the reference beam deflection, which can be caused by the much lower modulus of BFRP bars compared to steel bars. However, in the final phase of the loading, the difference in deflections was decreased to *40%*.

Average width of cracks on the constant cross-section in beams with basalt reinforcement was *4* times higher than in the reference beams.

The obtained results confirm the need to develop Hybrid FRP bars that are made by a material hybridization concept. This can reduce or eliminate excessive deflections in beams reinforced with FRP bars.

4. DEVELOPMENT OF HFRP BARS

4.1 Analytical and Numerical Considerations

The HFRP bars were created by a physical substitution of part of the basalt fibres by carbon fibres and then embedded in a single epoxy resin during the pultrusion process. During the development, several parameters of proposed Hybrid Carbon/Basalt FRP (HFRP) bars were changed to investigate their performance, such as: the location of fibres, technological aspects, different volume fraction ratio of fibres.

The carbon fibres are characterized by a strong anisotropy and were selected due to their strong properties in the longitudinal direction. Low Strength (LS) carbon fibres were chosen because their strain is approximately the same as for the basalt fibres. The combination of basalt and LS carbon fibres and their appropriate volume fractions can result in adjusting parameters of HFRP bars to desirable values.

The properties of FRP bars in the longitudinal direction can be calculated using the Rule of Mixtures (ROM) (axial loading - Voigt model) as it comes from the literature. The transverse properties can be obtained with Halpin-Tsai and other semi-empirical models [30-32]. However, these formulas do not consider bars

Table 4. Results of Experimental Testing for BFRP and HFRP Bars

HC/BFRP Ø8mm				
	Maximum strength, F_u [kN]	Tensile strength, f_u [MPa]	Tensile strain at rupture, ε_u [%]	Modulus of elasticity, E_L [GPa]
Average	**77,21**	**1277,92**	**1,73**	**73,89**
Standard deviation σ	3,35	55,4	0,07	3,07
Variation	4,34%	4,34%	4,33%	4,15%
BFRP Ø8mm				
Average	**60,03**	**1103,3**	**2,52**	**43,87**
Standard deviation σ	1,24	22,87	0,05	0,86
Variation	2,07%	2,07%	2,09%	1,95%

configuration, i.e. location of fibres, so, it was agreed to prepare a numerical simulation for this purpose.

The numerical simulation of tensile strength test for HFRP bars was performed in Finite Element Analysis FEA software ANSYS. Two different bar configurations were proposed, one where carbon fibres were substituting basalt fibres in the core region, the other one with carbon fibres located in the near-surface region.

The bars were modelled as cylindrical elements with a diameter of *8 mm* and a length of *850 mm*. A constant pressure of *500 MPa* was applied on the side edges. One central point was fixed in the y and z directions. The structure of the HFRP bars consisted of a core and surface region, which were perfectly interconnected.

The results showed that bar configuration is less important than the volume fraction of fibres. The difference between various bar configurations can be a maximum of *2%*, meanwhile, the volume fraction of all analysed combinations can influence the final stiffness by *74.6%*.

More detailed description on HFRP development is provided in [33-35]

4.2 Experimental Testing of HFRP Bars

Two possible bar configurations were produced, but manufacturing companies faced some technological problems while placing carbon fibres in the near-surface layer. These issues include an increased heterogeneity in fibre distribution and local scorching of carbon fibres caused by temperature increases.

Therefore, it was decided to produce HFRP bars with a preferable distribution of carbon fibres in the core region. The selected volume fractions of carbon-to-basalt fibres were *1:4* (i.e. *16%* of carbon fibres, *64%* of basalt fibres, *20%* epoxy resin to ensure correct bonding).

The tensile strength test was carried out in accordance with ACI 440.3R (2012) [36] standard for pultruded FRP bars. The average values of tensile strength (limit stress), f_u, modulus of elasticity, E_L, and the limit strain,

Fig. 4. Destruction of 8 mm diameter HFRP bar.

ε_u, for HFRP and BFRP bars were obtained and are shown in the Table 4.

The samples were destroyed by splitting and the destruction mechanism of bars had a brittle character (Figure 4).

BFRP and HFRP bars showed high tensile strength in the longitudinal direction. However, the mechanical characteristics were lower than predicted by analytical and numerical simulations by approximately *20%*.

In accordance with several studies [37-39] adding silica nanoparticles into the epoxy resin can improve the general performance of composite HFRP, chemical cohesion between constituents, and fire resistance of bars etc.

For the experimental tests, it was decided to modify epoxy resin (a four-component *1300 System®)*, which was added during the pultrusion process. The silica nanoparticles were used as a concentrated sol of nanosilica with a concentration of *25* to *30%* by weight. The structure of nano Hybrid FRP (nHFRP) is shown in the SEM image in the Figure 5.

However, the obtained results showed small reductions in mechanical properties for bars with the diameter *8mm*. The authors suggest that it can be related to the improper distribution of nanoparticles in epoxy resin for such diameters, however for bars with bigger diameters, the addition of nanosilica particles improved the overall strength properties for the nHFRP bars.

5. FIRE RESISTANCE OF FRP RC MEMBERS

Consequently, hybridization of constituents of hybrid FRP bars showed that properties of FRP bars are dependent on the properties of their constituents and the relative proportions of the fibre, known as the fibre-volume ratio. The matrix can be seriously affected at elevated temperatures, therefore it is needed to examine the behaviour of bars subjected to fire exposure as well as structures reinforced with these materials [40]. Currently, the use of FRP reinforcement in RC structures is limited and only includes cases when fire resistance aspects are not particularly meaningful.

Therefore, it was agreed to analyse two possible situations, when beams were subjected to temperature and then tested, and when beam were heated and loaded with a sustained load simultaneously. In the case of the first type of testing, the required output was to analyse the residual behaviour of FRP-RC beams and to find the level of reduction of the beam's strength capacity. For the second type of experiments, the task was to check for the duration of the period in which the structure can withstand loading and elevated temperatures, reflecting the conditions of a fire.

The reinforcement in the compression zone and shear reinforcement (stirrups) were assumed to be consistent for all beams. The stirrups made of *6 mm* diameter BFRP bars have a spacing assumed to be *100 mm*. The longitudinal top reinforcement is composed of two *8 mm* diameter BFRP bars. For the tensile reinforcement (bottom zone) different reinforcement types and amounts were used. Either *2* bars with a diameter of *14*

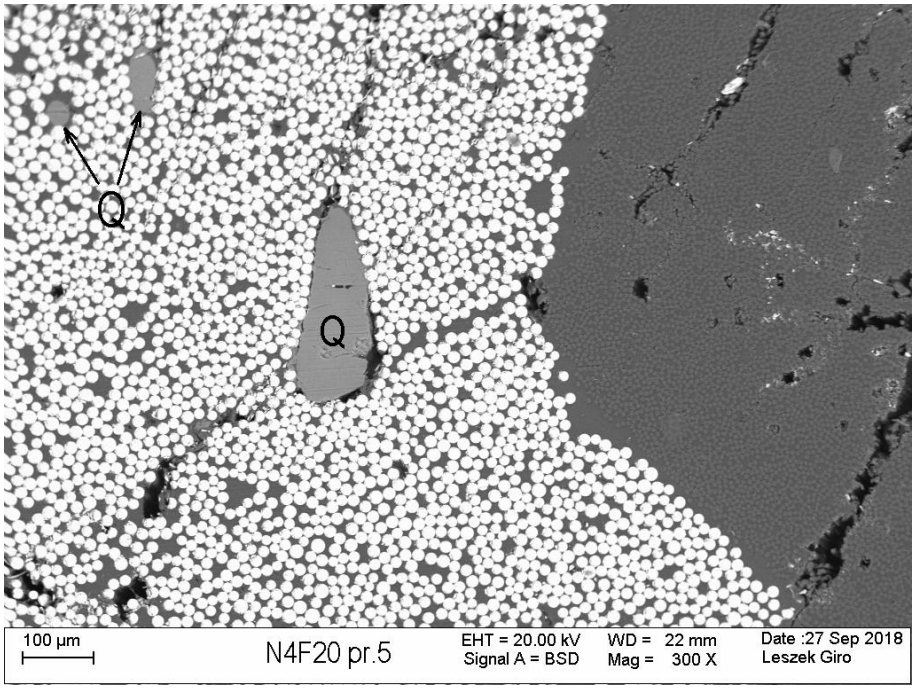

Fig. 5. nHFRP rod after cooling down to -20 °C. The figure shows a visible silica nanoparticles (Q) distribution. Bright points represent basalt fibres, darker area shows carbon fibres, space between nanoparticles and fibres is filled by epoxy resin.

mm or *4* bars with a diameter of *8 mm* of BFRP/HFRP/nHFRP were used for the tensile reinforcement.

During the testing of residual behaviour of the beams, all tested specimens were destroyed due to failure in the tensile zone, unlike reference beams, where the destruction took place due to concrete crushing in compression zone. The overall strength capacity of the FRP reinforced beams was reduced by approximately *42.4%* after being subjected to fire exposure.

The highest strength capacity was obtained by beams reinforced with HFRP bars. The beams` strength capacity after applying elevated temperatures was reduced by *40.34%* and was equal to *50.71 kN*. It is worth to mention that the post-fire behaviour of FRP-RC beams was similar to beams not subjected to fire exposure until failure as it can be seen from force-deflection curves.

As for the beams subjected to the simultaneous application of temperature and loading, the beams were loaded by *50%* of their ultimate load. The loading and heating were applied until the beams' failure. Figure 6 shows the test Setup during the heating phase.

Unlike the reference specimens, which were destroyed due to concrete being crushed in the compression zone, the failure of beams subjected to heating and loading occurred in different ways. Two beams reinforced with BFRP bars were destroyed due to failure of the reinforcement in the tension zone and four beams reinforced with hybrid FRP bars failed because of concrete crushing.

Fig. 6. Test Setup of Specimen, Beam Reinforced With *14 mm* Two BFRP Bars, Being Heated and Loaded

Fig. 7. HFRP Bars After the Matrix Evaporated in Specimen Reinforced with 14 mm HFRP Bars

Table 5. The test results and specimens characteristics

Description **Type / #×Ø / stirrups spacing**	**Tensile strength/ Elastic modulus** **[MPa]**	**N_n – average experimental ultimate force** **[kN]**
Axially loaded		
HFRP/4×8/150 mm	1139/73.57·10^3	905.50
HFRP/4×10/150 mm	1278/73.89·10^3	972.20
HFRP/4×10/75 mm	1278/73.89·10^3	980.60
BFRP/4×8/150 mm	1103/43.87·10^3	906.00
BFRP/4×8/75 mm	1103/43.87·10^3	1001.00
BFRP/4×10/75 mm	1153/48.18·10^3	1001.50
Steel /4×10/150 mm	556/210·10^3	999.00
Loaded with eccentricity e = 40 mm		
HFRP/4×10/75 mm	1278/73.89·10^3	491.00
BFRP/4×10/75 mm	1153/48.18·10^3	375.90
Steel/4×10/75 mm	556/210·10^3	465.00

As it can be seen in Figure 7, after the hybrid FRP bars were uncovered by removing the clear cover, it showed that the temperature caused a burning of the FRP bars. This resulted in the evaporation of the matrix in the middle of the bars. A major part of the fibres stayed in the same place and continued to sustain the load.

The highest temperature and the longest period of heating was achieved by beams reinforced with BFRP bars as opposed to beams reinforced with hybrid FRP bars in the same sets. The duration of the heating phase for the sample reinforced with four BFRP bars with the diameter *8 mm* was approximately *98 min*.; deflections were *162 mm*, and the temperature in the bars, measured by thermocouples, was approximately *900 ^{0}C*.

6. FRP RC COMPRESSION MEMBERS

The experimental process of testing compression members involved the fabrication of samples with dimensions *150x150 mm* and a height of *750 mm* reinforced with BFRP, HFRP bars and reference members reinforced with conventional steel reinforcement.

The research project consisted of two series of experimental tests which differ in the setup of applied loading, for the first series the loading was applying axially and for the second with the loading applied at a big eccentricity. The load was gradually increasing until the ultimate force was reached; and after reaching the limit point, the loading program was continued in order to obtain a full course of the static equilibrium path, including the post-critical range.

Figure 8a shows the destruction modes of axially loaded compressed members and Figure 8b describes the damage modes for elements loaded with eccentricity of *e =40 mm*.

Table 5 shows the values of tensile strength of reinforcement and values of elasticity modules of reinforcement and results of average experimental ultimate force of tested columns.

The compression members with BFRP and HFRP reinforcement collapsed by the crushing of concrete under an axial compression load. However, the destruction of the steel reinforced concrete elements took place due to reaching the capacity of steel bars of longitudinal reinforcement, which in consequence also caused the crushing of concrete. In the case of the eccentrically loaded samples, the destruction occurred in the shear mode due to concrete cutting. Steel reinforcement and FRP bars have significantly different mechanical properties represented by stiffness, strength, plasticity or brittleness, and a symmetrical or asymmetrical response in uniaxial tension or compression tests. The reported discrepancy in the stress-strain relationships for the materials results in a

different response from concrete members reinforced by steel or FRP bars. More detailed description is provided in companion papers [41].

7. CONCLUSION

The widespread application of FRP reinforcement can become possible after a comprehensive analysis of the mechanical and physical properties of these materials. In addition, it is quite important to examine the performance of FRP-RC members, particularly in accidental situations, such as being exposed to fire or an aggressive chemical environment.

The results of from measuring the toughness and the energy-absorption characteristics showed that basalt fibre reinforced concrete specimens acquire a great highly ductile behavior and energy absorption capacity, compared to ordinary concrete specimens. The addition of basalt fibre in the tested amount of *2-8 kg/m*^{3} has a significant influence on the fracture mechanics parameters of concrete, with relatively little impact on the compressive strength of concrete. The presence of fibres has improved the fracture mechanics parameters such as *KIc*, *CTODc*, G_F and recorded maximum values of load. The analysis of the *P-CMOD* relationships show that dispersed reinforcement can significantly change the nature of the behaviour of concrete elements subjected to bending in both pre-cracking and post-cracking phases. The changes in fracture mechanics parameters and the modification of P-CMOD plots, recorded under loading, indicate that basalt fibres can increase concrete resistance to initiation and propagation of cracks.

This work outlines the mechanical behaviour of FRP bars made with basalt fibres BFRP, carbon-basalt fibres HFRP and carbon-basalt fibres with modified epoxy resin nHFRP. The possible application of the aforementioned types of reinforcement was checked by applying them in flexural and compression members. Additionally, the specimens were completely reinforced with FRP reinforcement to eliminate the influence of conventional steel reinforcement.

Fire resistant aspects were examined for flexural members, where they were tested by using a standard fire endurance test, i.e. the specimens where heated and loaded simultaneously. Moreover, the residual properties of the beams were checked by applying elevated temperatures for some period of time and allowing them to have a cooling phase, and finally reloaded flexurally until failure.

Based on experimental testing on the mechanical behaviour of BFRP and hybrid FRP bars, it is possible to conclude that their properties can become predictable with the concept of material hybridization. Experimental testing of flexural and compression members, and analyses related to fire resistance aspects suggest that the considered reinforcement can be a promising alternative to steel bars, however, a comprehensive investigation is still required.

a) **b)**

Fig. 8. Destruction mechanisms (a) axially loaded members (with HFRP reinforcement) (b) members loaded with eccentric force (with BFRP reinforcement).

REFERENCES

1. *Protchenko, K. Młodzik, M. Urbański, E. D. Szmigiera, and A. Garbacz, "Numerical estimation of concrete beams reinforced with FRP bars," MATEC Web of Conferences, vol. 86, pp. 1–8, 2016.*
2. *H.C. Boyle, V.M. Karbhari, "Investigation of Bond Behavior between Glass Fiber Composite Reinforcements and Concrete." Polymer-Plastics Technology and Engineering, 33(6), 733-753, 1994.*
3. *B. Benmokrane, F. Elgabbas, E. Ahmed, and P. Cousin, "Characterization and comparative durability study of glass/vinylester, basalt/vinylester, and basalt/epoxy FRP bars." J. Compos. Constr., 2015. https://doi.org/10.1061/(ASCE)CC.1943-5614.0000564*
4. *ACI 440.4R-04: Prestressing Concrete Structures with FRP Tendons (Reapproved 2011), American Concrete Institute, the USA, 2011.*
5. *M. Włodarczyk, E. D. Szmigiera, and K. Protchenko, "Analysis of interface between FRP strip and concrete in structural systems," in Theoretical Foundations of Civil Engineering. Structural Mechanics, vol. 7, S. Jemioło and M. D. Gajewski, Eds. Oficyna Wydawnicza Politechniki Warszawskiej, pp. 111–120, 2016.*
6. *ACI 544. IR-96. State-of-the-art report on fibre reinforced concrete. Manual of concrete practice. Farmington Hills, 1998.*
7. *J. Branston, S. Das, S.Y. Kenno, C. Taylor, "Mechanical behaviour of basalt fibre reinforced concrete". Construction and Building Materials, 124, 878-886, 2016.*
8. *N. Buratti, C. Mazzotti, M. Savoia, "Post-cracking behaviour of steel and macro-synthetic fibre-reinforced concretes" Construction and Building Materials 25, 2713 – 2722, 2011.*
9. *J.L. Clarke, "Design guidance for fibre-reinforced concrete". In: Harnessing Fibres for Concrete Construction, IHS BRE Press, University of Dundee, 311-322 (2008) Concrete Society Technical Report No 34, Concrete Industrial Ground Floors – A guide to their Design and Construction, Ed. 3, 2003.*
10. *https://www.cosmodermic.nl/ball/4209-design-aspects-basalt-rock-fibres.html*
11. *InfoMine Research Group 2007*
12. *K. Protchenko, J. Dobosz, M. Urbański, & A. Garbacz, „Wpływ substytucji włókien bazaltowych przez włókna węglowe na właściwości mechaniczne prętów B/CFRP (HFRP)". Czasopismo Inżynierii Lądowej, Środowiska i Architektury, JCEEA, 63(1/1), 149–156, 2016.*
13. *W. M. Mingchao, Z. Zuoguang, L. Yubin, L. Min, and S. Zhijie, "Chemical Durability and Mechanical Properties of Alkali-Proof Basalt Fiber and Its Reinforced Epoxy Composites." Journal of Reinforced Plastics and Composites, 27 (4), 393–407., 2008.*
14. *R. Parnas, M. Shaw and Q. Liu, "Basalt Fiber Reinforced Polymer Composites." Technical Report No. NETCR63, Prepared for the New England Transportation Consortium, Institute of Materials Science, University of Connecticut, 2007.*
15. *X. Wang, G. Wu, and Z. Wu, "Tensile Property of Prestressing Basalt and Hybrid FRP Tendons under Salt Solution." Proceeding of the 6th International Conference on FRP Composites in Civil Engineering (CICE), Rome, Italy, 8 pp., 2012.*
16. *V. Lopresto, C. Leone and I. De Iorio, "Mechanical Characterization of Basalt Fiber Reinforced Plastic." Journal of Composites Part B: Engineering, 42 (4), 717–723, 2011.*
17. *Canadian Standards Association, "Design and Construction of Building Structures with Fiber Reinforced Polymers (CAN/CSA S806-12)." Rexdale, ON, Canada, 2012.*
18. *Canadian Standards Association, "Canadian Highway Bridge Design Code (CAN/CSA S6–14)." Rexdale, ON, Canada, 2014.*
19. *ACI Committee 440, "Guide for the Design and Construction of Concrete Reinforced with FRP Bars (ACI 440.1R-15)." ACI, Farmington Hills, Michigan, USA, 2015.*
20. *F. Elgabbas, P. Cousin, E. Ahmed, and B. Benmokrane "Development and Characterization of Basalt FRP Reinforcing Bars for Concrete Structures." Proceedings of the 7th International Conference on FRP Composites in Civil Engineering (CICE), Vancouver, Canada. August 20–22, 6 pp, 2014.*
21. *V. Dhand, G. Mittal, K.Y. Rhee, D Hui, "A Short Review on Basalt Fiber Reinforced Polymer Composites." Journal of Composites Part B: Engineering, 73, 166–180, 2015.*
22. *M. Kosior-Kazberuk, J. Krassowska and Carolina Piña Ramírez. "Post cracking behaviour of fibre reinforced concrete with mineral wool fibers residues". ECCE 2018, MATEC Web of Conferences 174, 02016, 2018. https://doi.org/10.1051/matecconf/201817402016*
23. *Recommendation TC 89-FMT RILEM Determination of fracture parameters (KIc and CTODc) of plain concrete using three-point bend test. Materials and Structures 23, 457-460, 1990.*
24. *Y.S. Jenq, S.P. Shah, Journal of Engineering Mechanics 111, 1227-1241,1985,*
25. *S.P. Shah, S.E. Swartz, Ch. Ouyang, "Fracture mechanics of concrete: Applications of fracture mechanics to concrete, rock and other quasi-brittle materials. John Wiley & Sons, Inc., New York, 552, 1995.*
26. *EN 12390-3. "Testing Hardened Concrete: Compressive strength of test specimens", 2011*
27. *M. Urbański and A. Łapko, "Effectiveness of flexural basalt reinforcement application in RC beam structures," in Modern materials,*

installations and construction technologies, S. Fic, Ed. John Paul II State School of Higher Education, 2013, pp. 113–123.

28. *E. D. Szmigiera, M. Urbański & K. Protchenko, "Strength Performance of Concrete Beams Reinforced with BFRP Bars." In M. M. Reda Taha, U. Girum, & G. Moneeb, M. M. Reda Taha, U. Girum, & G. Moneeb (Eds.), International Congress on Polymers in Concrete (ICPIC 2018) : Polymers for Resilient and Sustainable Concrete Infrastructure (pp. 667–674), 2018. http://doi.org/10.1007/978-3-319-78175-4_85*
29. *A.Garbacz, M. Urbański & A. Łapko"BFRP bars as an alternative reinforcement of concrete structures - Compatibility and adhesion issues. Advanced Materials Research, 1129, 233–241, 201. http://doi.org/10.4028/www.scientific.net/AMR.1129.233*
30. *W. Voigt Uber die beziehung zwischen den beiden elasticitatsconstanten isotroperkorper. Ann Phys; 38:573–87 [in German], 1989.*
31. *T. Black, R. Kosher, "Non Metallic Materials: Plastic, Elastomers, Ceramics and Composites (tenth edition)". In Materials and Processing in Manufacturing, (162-194), JohnWiley & Sons, Inc., ISBN 978-0470-05512-0, USA, 2008.*
32. *Barbero, E. J. "Introduction to composite materials design". 2nd ed. Boca Raton, FL: CRC Press, Taylor & Francis Group, 2011.*
33. *K. Protchenko, E.D. Szmigiera, M. Urbański & A. Garbacz, "Development of Innovative HFRP Bars". MATEC Web of Conferences, 196, 1-6, 2018. http://doi.org/10.1051/matecconf/201819604087*
34. *A. Garbacz, E.D. Szmigiera, K. Protchenko, & M. Urbański, M. "On Mechanical Characteristics of HFRP Bars with Various Types of Hybridization". In M. M. Reda Taha, U. Girum, & G. Moneeb, M. M. Reda Taha, U. Girum, & G. Moneeb (Eds.), International Congress on Polymers in Concrete (ICPIC 2018) : Polymers for Resilient and Sustainable Concrete Infrastructure, pp. 653–658, 2018. http://doi.org/10.1007/978-3-319-78175-4_83*
35. *K. Protchenko, M. Włodarczyk & E.D. Szmigiera, "Investigation of Behavior of Reinforced Concrete Elements Strengthened with FRP". Procedia Engineering, 111, 679–686, 2015.. http://doi.org/10.1016/j.proeng.2015.07.132*
36. *ACI Committee 440. "Guide Test Methods for Fiber-Reinforced Polymers (FRPs) for Reinforcing or Strengthening Concrete Structures (ACI 440.3R-12)." ACI, Farmington Hills, Michigan, USA, 2012.*
37. *H.N. Dhakal, Z.Y. Zhang, R. Guthrie, J. MacMullen, N. "Bennett Development of flax/carbon fibre hybrid composites for enhanced properties". Carbohyd Polym, 96, pp. 1-8, 2013.*
38. *T. Jesionowski, R. Pilawka, „Kompozyty epoksydowe z krzemionką sieciowane 1-etylomimidazolem". Kompozyty 11: 1, pp. 14-17, 2011.*
39. *J.W. Baur, C. Chen, R.S. Justice, D.W. Schaefer "Highly dispersed nanosilica-epoxy resins with enhanced mechanical properties." Polymer 49, 3805–3815, 2008.*
40. *D.S. Ellis, H. Tabatabai, A. Nabizadeh, "Residual tensile strength and bond properties of GFRP bars after exposure to elevated temperatures". Materials 11, 346, 2018.*
41. *M. Włodarczyk, D. Trofimczuk, "Prediction of ultimate capacity of FRP reinforced concrete compression members. fib Symposium, Kraków (accepted) 2019 (Symposium w dniach 27-29/05/2019).*

Primena cementnih kompozita na bazi sintetičkih vlakana za prefabrikovane fasadne panele

Application of synthetic fibre reinforced cement composites for prefabricated façade panels

Tijana Vojnović Ćalić

Coburg University of Applied Sciences and Arts, School of Design, Department of Architecture, Coburg, Germany

Dragica Jevtić, Dimitrije Zakić

Univerzitet u Beogradu, Građevinski fakultet, Beograd, Srbija

Rezime

Mikroarmirani cementni kompoziti su duže vreme u upotrebi u sastavu različitih fasadnih panela dostupnih na tržištu. To su uglavnom jednoslojne tanke vlaknasto-cementne ploče. U okviru ovog rada će biti prikazan fasadni panel sa podlogom od mikroarmiranog cementnog kompozita i dekorativnim licem od kamena. Specifičnost cementnih kompozita u ovom slučaju je to što sadrže i laki agregat u vidu drobljene opeke. Razmatraće se fizičko-mehanička svojstva primenjenih mikroarmiranih cementnih kompozita i pojedine karakteristike pomenutog fasadnog panela bitne za njegovu primenu. U skladu sa održivim pristupom u građevinskoj industriji, posebnu vrednost ovog panela predstavlja upotreba lokalnih i recikliranih materijala.

Abstract

Fibre reinforced cement composites are used in a longer period for production of various façade panels that are available on the market. These are mainly single-layer thin fiber-cement boards. The paper deals with façade panels composed of fibre reinforced cement composite substrate and a decorative face of stone. Specific for the cement composite in this case is that it contains light aggregate in the form of crushed brick particles. The physical-mechanical properties of the applied fibre reinforced cement composites and the particular properties of the aforementioned façade panel essential for its application are given. In accordance with the sustainable approach in the construction industry, the additional value of this research represents the application of local and recycled materials.

Ključne besede: fasadni panel, mikroarmirani cementni kompoziti, fizičko-mehanička svojstva, primena
Keywords: façade panel, fibre reinforced cement composites, physical-mechanical properties, application

1. UVOD

Mikroarmirani cementni kompoziti nalaze sve širu primenu kod različitih fasadnih panela, od kojih su mnogi već prisutni na tržištu. To su, na primer, vlaknasto-cementni paneli poznatih proizvođača Rieder ili Eternit. Takođe je zastupljen i višeslojni panel firme Alsecco, koji se sastoji od lakoagregatnog cementnog kompozita armiranog tkaninom od staklenih vlakana. Lice ovog panela sačinjeno je od kamene obloge.

U ovom radu se predlaže primena mikroarmiranog cementnog kompozita u okviru višeslojnog fasadnog panela. Uvodi se novi fasadni element koji može naći primenu u okviru provetravanog fasadnog sklopa. Kao sastavni materijali, razmatraju se podloga panela od

Tabela 1: Tehnički podaci za polipropilenska i polivinil-alkoholna vlakna [8],[9]

Svojstva vlakana	Sika *Sika Fibers*	Kuraray *Kuralon RMS702*
Materijal	polipropilen	polivinil-alkohol
Tip vlakna	monofilamentna	monofilamentna
Oblik poprečnog preseka	kružni	bubrežasti
Prečnik d (mm)	0,040	0,026
Dužina l (mm)	6	6
Faktor oblika l/d	150	230
Specifična masa γ_s (g/cm³)	0,91	1,30
Čvrstoća pri zatezanju f_z (MPa)	360	1600
Modul elastičnosti E (GPa)	2,5	37,0
Izduženje pri lomu δ (%)	22	6
Preporučeno doziranje (kg/m³)	0,6-0,9	1,3-19,5
Otpornost u alkalnoj sredini	otporna	otporna

lakoagregatnog mikroarmiranog maltera i usvaja obloga od kamenog mozaika.

Vodeći se trendom održivosti, evropska direktiva - *The European Commission Waste Framework Directive,* opisuje poželjnu hijerarhiju pri upravljanju otpadom: prevenciju, ponovnu upotrebu, reciklažu, ponovno izdvajanje resursa poput energije i konačno, odlaganje otpada [1]. U skladu sa tim, kao laki agregat u sastavu podloge predloženog panela usvojena je drobljena opeka.

Eksperimentalna istraživanja lakoagregatnih mikroarmiranih cementnih kompozita su relativno malobrojna. Istraživanja maltera zasnovanih na agregatu od drobljene opeke armiranih polipropilenskim vlakanima sa umerenim učešćem mikroarmature (~0,1% od ukupne zapremine) pokazuju neznatne promene vrednosti čvrstoća pri pritisku u odnosu na kompozite bez vlakana. Pri većem doziranju vlakana od 0,5% i 1%, ova vrednost opada i za 25%. Čvrstoća pri savijanju raste sa umerenim učešćem vlakana od 0,1% za 5%, a od 1% učešća čak i za 50% [2], [3], [4]. S druge strane, ispitivanja potvrđuju porast vrednosti čvrstoće pri pritisku maltera (frakcija 0/8 mm) od 5-16% i čvrstoće pri savijanju od 4-25% u odnosu na uzorke bez polipropilenske mikroarmature, a u zavisnosti od učešća sitne frakcije (0/4 mm) rečnog agregata. Istraživanja ukazuju da dodatak vlakana unutar maltera sa agregatom od reciklirane opeke u količinama od 1% mogu smanjiti deformacije skupljanja i do 17% [5], [6]. Takođe je primećeno da dodatak polipropilenske mikroarmature malterima na bazi drobljene opeke praktično ne utiče na svojstvo upijanja vode postepenim potapanjem [7].

U radu je prikazan deo rezultata dobijen prilikom istraživanja za potrebe izrade doktorske disertacije [24]. Radi se o rezultatima sopstvenih eksperimentalnih istraživanja osnovnih fizičko-mehaničkih svojstava mikroarmiranih cementnih kompozita namenjenih za izradu fasadnih panela.

2. MATERIJALI I METODE

2.1 Komponentni materijali

U svrhu eksperimentalnih ispitivanja mikroarmiranih maltera korišćen je portland-kompozitni cement na bazi cementnog klinkera sa dodatkom granulisane zgure i krečnjaka oznake *PC 20M (S-L) 42.5R (CEM II/A-M (S-L) 42.5R)* proizvođača "Lafarge" iz Beočina, Srbija, koji se odlikuje visokim ranim i krajnjim čvrstoćama. Kao agregat je upotrebljen rečni pesak („Dunavac“) frakcije 0/2 i 0/4 i drobljena opeka frakcije 2/4, koja je izdrobljena za potrebe izvođenja eksperimentalnih istraživanja u Laboratoriji za materijale Instituta za materijale i konstrukcije Građevinskog fakulteta Univerziteta u Beogradu. U svrhu mikroarmiranja korišćena su dva tipa vlakana dužine 6 mm: polipropilenska vlakna niskog modula elastičnosti - *Sika Fibers* proizvođača Sika, i polivinil-alkoholna vlakna višeg modula elastičnosti - *Kuralon RMS702* japanskog proizvođača Kuraray (tabela 1).

Tabela 2: Sastav malterskih mešavina

Oznaka serije	E	E_1	E_2	M_1	M_2
Komponenta (g)					
CEM II 42,5R(S-L)	450	450	450	450	450
Rečni pesak 0/4	1350	1350	1350	/	/
Rečni pesak 0/2	/	/	/	810	810
Drobljena opeka 2/4	/	/	/	270	270
Polipropilensla vlakna	/	0,9	/	0,9	/
Polivinil-alkoholna vlakna	/	/	1,5	/	1,5
Superplastifikator	/	3,6	3,6	3,6	3,6
Lateks	/	9	9	9	9
Voda	225	180	180	193	203
Svojstvo					
Vodocementni faktor m_v/m_c	0,5	0,4	0,4	0,43	0,45
Fluidnocementni faktor m_f/m_c	0,5	0,43	0,43	0,46	0,48
Agregatnocementni faktor m_a/m_c	3	3	3	2,4	2,4

Tabela 3: Rezultati ispitivanja svežeg maltera

Oznaka serije Svojstvo	E	E_1	E_2	M_1	M_2
Konzistencija (mm)	120	130	110	110	110
Zapreminska masa $\gamma_{m,sv}$ (kg/m³)	2201	2161	2275	2135	2110

U svrhu redukcije količine vode i bolje ugradljivosti svežeg maltera, primenjen je superplastifikator na bazi polikarboksilata *Sika Viscocrete Techno 20* proizvođača Sika. Predmetni malteri su takođe modifikovani tečnim polimernim lateksom *Sika Latex* istog proizvođača. Ovaj dodatak u istom smislu (u funkciji plastifikatora) utiče na konzistenciju i ugradljivost malterskih smeša, ali i na vodonepropustljivost, odnosno otpornost na mraz, i redukciju napona skupljanja kod tankih elemenata. Vodeni rastvor lateksa je pripremljen sa zapreminskim udelom lateksa od 5%. Za spravljanje svih malterskih mešavina u okviru ovog eksperimentalnog istraživanja, korišćena je voda iz gradskog vodovoda.

U vidu kamena primenjenog za lice fasadnog pilot elementa korišćen je lokalni kamen – granit "Šutica".

2.2 Primenjene metode

Malterske mešavine su spravljene mašinskim putem po standardnom postupku, s produženim vremenom mešanja do 5 minuta, odnosno do ravnomernog dispergovanja vlakana. Ugrađene su u kalupe dimenzija 4x4x16 cm uz primenu postupka vibriranja. Prizmatične epruvete su 7 dana negovane pod vlažnom sargijom, a potom 21 dan na vazduhu u laboratorijskim uslovima na temperaturi 20±2ºC.

Konzistencija svežeg maltera je utvrđena metodom rasprostiranja uz pomoć potresnog stola (prema SRPS EN 1015-3 [10]). Nakon utvrđivanja čvrstoće pri savijanju, na delovima prizmi dobijenim prilikom loma, vršeno je ispitivanje čvrstoće maltera pri pritisku (prema SRPS EN 1015-11 [11]). Određivanje skupljanja na prizmatičnim uzorcima je vršeno nabazi odredbi standarda SRPS B.C8.029 [12].

Tabela 4: Rezultati ispitivanja očvrslog maltera

Oznaka serije		E	E_1	E_2	M_1	M_2
Svojstvo	Starost (dani)					
Zapreminska masa	7	2171	2139	2249	2101	2083
γ_m(kg/m³)	28	2138	2067	2156	2059	2065
Čvrstoća pri pritisku	7	44,8	48,4	59,1	49,4	49,5
f_p (MPa)	28	61,0	60,8	73,0	67,4	66,5
Čvrstoća pri savijanju	7	6,8	7,2	8,0	7,2	6,8
f_{zs} (MPa)	28	8,9	9,3	10,9	9,8	9,6
Skupljanje (mm/m)	28	0,541	0,520	0,593	0,614	0,666

Ispitivanje upijanja vode pod atmosferskim pritiskom je vršeno nakon 28 dana u vodi, u svemu prema odredbama standarda SRPS B.B8.010 [13]. Otpornost prema mrazu je ispitivana u saglasnosti sa standardom SRPS U.M8.002 [14]. Opitna tela su nakon nege od 28 dana podvrgnuta ciklusima naizmeničnog smrzavanja (4h), te odmrzavanja u vodi (4h). Nakon 25 ciklusa je vršeno ispitivanje čvrstoće pri savijanju i pritisku ovih opitnih tela prema SRPS EN 1015-11 [11].

Dalja eksperimentalna istraživanja su obavljana na uzorcima specifičnih dimenzija čija će izrada detaljnije biti opisana u nastavku rada. Ispitivanje prianjanja maltera za kamenu podlogu metodom pull-off je vršeno u skladu sa standardom SRPS EN 1015-12 [15]. Čvrstoća pilot panela pri savijanju je ispitivana prema prilagođenoj metodi u okviru Laboratorije za materijale Instituta za materijale i konstrukcije Građevinskog fakulteta Univerziteta u Beogradu, nanošenjem ravnomernog opterećenja na površinu lica panela. Ispitivanje eflorescencije je vršeno prema američkom standardu ASTM C67-14 [16] koji je prvenstveno namenjen proizvodima od opeke.

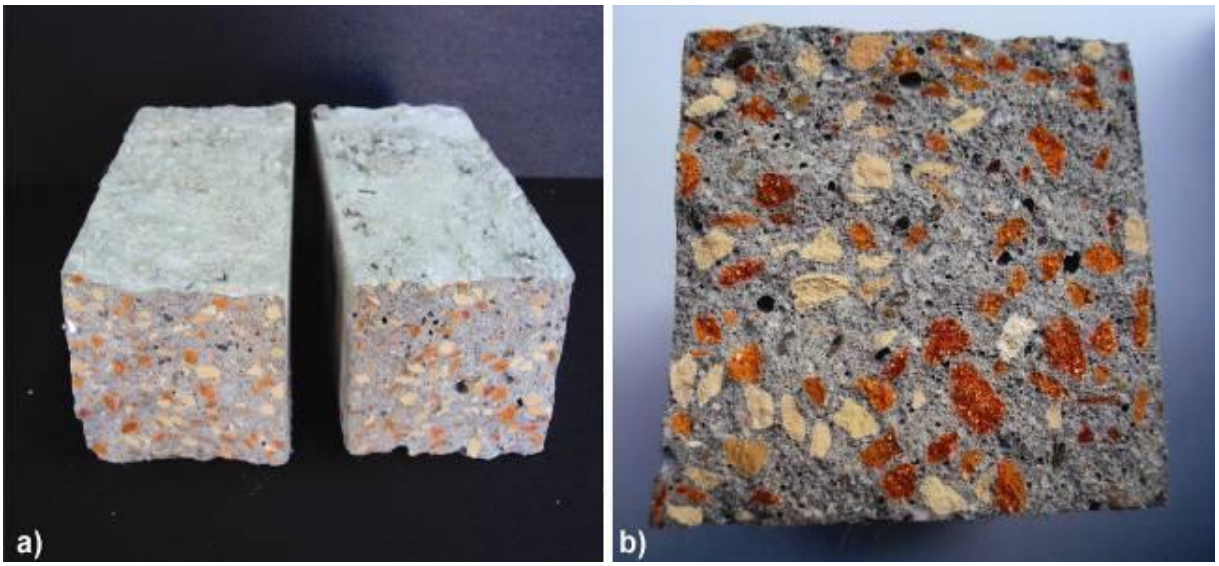

Slika 1. Prizmatični uzorak sa drobljenom opekom:

a) polutke nakon ispitivanja čvrstoće pri savijanju; b) površina loma

3. SPROVEDENA EKSPERIMENTALNA ISPITIVANJA

3.1 Sastav cementnih kompozita

U okviru eksperimentalnih ispitivanja spravljeno je pet serija maltera, čiji se sastav razlikovao po vrsti i količini izabranih agregata i vlakana. Etalonska mešavina E predstavlja klasičnu maltersku mešavinu u masenoj razmeri cementa, agregata i vode m_c:m_a:m_v=1:3:0,5. Etalonske mešavine E1 i E2 su unapređene dodatkom preporučene količine polipropilenskih (0,9 kg/m³; ~0,1%Vol), odnosno polivinil-alkoholnih (1,5 kg/m³; ~0,1%Vol) vlakana uz dodatak superplastifikatora i lateksa. U odnosu na prethodnu recepturu, pri spravljanju mešavina M1 i M2, frakcija 2/4 rečnog peska je zapreminski zamenjena lakim agregatom u vidu drobljene opeke. Količine cementa (450 kg/m³), lateksa (9 kg/m³) i superplastifikatora (3,6 kg/m³) su bile konstantne. Količina vode je dozirana zasebno za svaku seriju u svrhu postizanja krute konzistencije sveže malterske mešavine (rasprostiranje manje od 140 mm, prema SRPS EN 1015-6 [17]). Recepture pojedinačnih serija su prikazane u tabeli 2. Sa primenom superplastifikatora i lateksa može se uočiti trend umanjenja vodocementnog faktora m_v /m_c. Primenom agregata manje specifične mase, može se uočiti i umanjenje agregatnocementnog faktora m_a/m_c (tabela 2).

3.2 Svojstva mikroarmiranih cementnih kompozita u svežem stanju

Ispitivanjem konzistencije malterskih mešavina metodom rasprostiranja, zabeleženo je rasprostiranje od 110-130 mm, odnosno kruta konzistencija svih serija maltera (manje od 140 mm, prema SRPS EN 1015-6 [17]). Takođe je uočena neznatna razlika u vrednostima zapremniske mase etalona E i preostalih ispitivanih malterskih mešavina sa različitim sastavom agregata i vlakana (videti tabelu 3).

3.3 Svojstva mikroarmiranih cementnih kompozita u očvrslom stanju

U okviru tabele 4. prikazani su rezultati ispitivanja očvrslog maltera pet serija maltera starosti od 7 i 28 dana (slika 1). Na osnovu merenja, može se uočiti jedino jasan porast vrednosti skupljanja kod prizmatičnih uzoraka pri zameni određene zapremine peska agregatom od drobljene opeke kod uzoraka M1 i M2.

U tabeli 5 su prikazani rezultati ispitivanja upijanja vode i otpornosti maltera pri dejstvu mraza. Na osnovu rezultata ispitivanja mogu se uočiti viši procenti upijanja kod maltera sa drobljenom opekom, zahvaljujući upijanju samog agregata koji u ovom slučaju iznosi 18% za 30 s i 21% za 24 h (tabela 5).

Otpornost pri dejstvu mraza predmetnih maltera određena je iz odnosa računskih vrednosti čvrstoće uzoraka pri ekvivalentnoj starosti i laboratorijskog ispitivanja nakon 25 ciklusa smrzavanja/odmrzavanja. Čvrstoće pri savijanju pri ekvivalentnoj starosti su određene na osnovu čvrstoća pri pritisku, odnosno aproksimacije njihovog odnosa preko izraza:

$$f_{zs} = 0{,}566 \cdot f_p^{2/3} \quad (R^2 = 0{,}85)$$

a) b)

Slika 2. *Ispitivanje uzoraka metodom Pull-off: a) isecanje cilindričnih zareza, b) testiranje uzoraka metodom pull-off*

Tabela 5: Rezultati ispitivanja upijanja nakon 28 dana i čvrstoće nakon 25 ciklusa mraza

Oznaka serije / Svojstvo	E	E_1	E_2	M_1	M_2
Upijanje vode u procentima mase (%)	8,23	6,75	6,83	8,54	9,01
Čvrstoća pri pritisku pri ekvivalentnoj starosti $f_{p,e}$ (MPa)	64,2	67,0	76,6	70,6	69,7
Čvrstoća pri pritisku nakon dejstva mraza $f_{p,m}$ (MPa)	52,7	53,5	64,8	57,7	56,1
Čvrstoća pri pritisku nakon opita mraza u odnosu na etalon – Δfp (%)	82,1	79,8	84,6	81,7	80,5
Čvrstoća pri savijanju pri ekvivalentnoj starosti $f_{zs,e}$ (MPa)	9,1	9,3	10,2	9,7	9,6
Čvrstoća pri savijanju nakon dejstva mraza $f_{zs,m}$ (MPa)	9,0	8,4	8,9	8,0	7,9
Čvrstoća pri savijanju nakon opita mraza u odnosu na etalon - Δfs (%)	99,1	89,9	87,1	82,5	82,3

Tabela 6: Rezultati ispitivanja prianjanja

Oznaka serije / Svojstvo	M_1	M_2
Tip loma (%)	90a+10m	95a+5m
Napon prianjanja f_{at} (MPa)	4,19	3,27

Kao uslov otpornosti cementnih kompozita na dejstvo mraza uglavnom se usvaja održanje čvrstoće pri pritisku od 75% (SRPS U.M1.016 [18]). Nakon 25 ciklusa smrzavanja i odmrzavanja, kod opitnih tela nije registrovan gubitak mase. Prilikom vizuelnog pregleda, nije primećeno ljuštenje, niti pojava prslina na površini uzoraka. Na osnovu rezultata ispitivanja može se uočiti da su sve serije maltera zadržale čvrstoću pri pritisku i savijanju u procentu višem od 75%.

3.4 Ispitivanje prianjanja

Ispitivanje prianjanja maltera za kamenu podlogu je vršeno u skladu sa standardom SRPS EN 1015-12 [15]. Kao podloga za ispitivanje prianjanja su korišćene kamene ploče granita "Šutica" dimenzija 30x30x4 cm koje su dobijene standardnim rezanjem. Ispitivanja su vršena na dve vrste lakoagregatnih maltera – serije M1 i M2. Kamene ploče su neposredno pre nanošenja maltera potapane u vodu, a zatim je suvišna voda uklonjena kako bi se malterska mešavina nanela na površinski suvu podlogu u sloju od 10±1 mm. Nakon 28 dana mešovite nege, na svakoj ploči je urezano 5 cilindričnih zareza koji zalaze i u masu kamena (slika 2). Za ocenu adhezije (prionljivosti), po standardu SRPS EN 1015-12 [15] su dovoljna 3 uspešna ispitivanja uzoraka.

Na površinu maltera je uz pomoć epoksi smole zalepljen metalni pečat. Nakon montiranja ispitne aparature, nanosi se normalna sila zatezanja i beleže se sile loma uzoraka (slika 2). Rezultati ispitivanja prianjanja su prikazani u okviru tabele 6.

Kao minimalni napon prianjanja preporučuje se vrednost od 0,5 MPa, odnosno, da napon prianjanja pri adhezionom lomu bude veći od čvrstoće pri zatezanju samog maltera [19]. U ovom slučaju pogodno je da čvrstoće pri zatezanju komponentnih materijala budu veće od iznosa adhezije, a takođe i ostvarenje mešovitog loma.

Prikazani rezultati ispitivanja ukazuju da napon prianjanja kod svih uzoraka prelazi granicu od

preporučenih 0,5 MPa. Uzorci pokazuju mešoviti tip loma - sa dominantnim adhezionim tipom loma preko dodirne površine dva materijala i propratnim lomom preko površine kamena.

3.5 Ispitivanje eflorescencije

Mogućnost pojave eflorescencije je ispitivana na uzorcima dimenzija 10x60 cm. U sastav uzoraka ulaze granitne pločice dimenzija 10x10x1 cm i malterska smeša sa polipropilenskim vlaknima M1. Uzorci su spravljeni u kalupima od blažujke unutrašnjih dimenzija 10x60x3,5 cm. Kamene pločice su pripremljene potapanjem u vodu iz gradskog vodovoda. Nakon ukljanjanja viška vode sa pločica, one se površinski suve polažu u kalup sa licem na dole. Malter se nanosi preko pločica i ugrađuje u kalupe na vibro-stolu. Mešovita nega od 28 dana se vrši po prethodno utvrđenom režimu. Lice od kamena je polirano, da bi preko tako obrađene površine uzorci kapilarno upijali vodu.

Ispitivanje eflorescencije je vršeno prema američkom standardu ASTM C67-14 [16] koji je namenjen proizvodima od opeke. Tri uzorka su postavljena na distancere i potopljena sa licem od kamena na dole u destilovanu vodu, tako da je svaki bio 15 mm pod vodom. U vodu je uronjena cela kamena pločica i cementni malter u visini od 5 mm. Nakon 7 dana u vodi, uzorci su sušeni u sušnici na temperaturi od 110-115 ºC

a) **b)**

Slika 3: Ispitivanje uzoraka na potencijalnu pojavu eflorescencije: a)i spitni uzorci, b) kapilarno upijanje vode preko finalno obrađenog – poliranog lica od kamena .

Slika 4. Izrađen fasadni panel

do konstantne mase (slika 3). Nakon ispitivanja uzoraka vizuelno-makroskopskim pregledom, ustanovljeno je da oni nisu pokazali znake eflorescencije.

3.6 Ispitivanje čvrstoće pri savijanju

Nakon izvršenih ispitivanja serija cementnih kompozita, pristupilo se planiranju i izradi fasadnog pilot elementa. Ovaj element je projektovan kao

dvoslojni sistem. Podloga je sačinjena od lakoagregatnog cementnog kompozita sa polipropilenskim vlaknima tipa M1, dok je lice sačinjeno od lokalnog kamena – granita "Šutica". Obloga od kamenih pločica (10x10 cm) je projektovana debljine 1 cm, podloga od primenjenog maltera 2,5 cm, a konačne dimenzije fasadnog pilot elementa su iznosile 60x60x3,5cm. Prianjanje dva sloja panela je ostvarivano polaganjem svežeg cementnog maltera direktno na poleđinu kamenih pločica prilikom procesa izrade. Postupak izrade je sledio isti tok kao kod izrade uzoraka za ispitivanje eflorescencije (slika 4).

Što se tiče fasadnih ploča od kamena, kao minimalan obim ispitivanja se pominju čvrstoća pri savijanju i sila loma na mestu veze sa potkonstrukcijom [20], [21], [22], [23]. Povlačeći paralelu sa predmetnim panelom, pristupilo se ispitivanju postepenim dodavanjem opterećenja na lice od kamena. Pri ispitivanju, fasadni pilot element je postavljen na linearne oslonce na međusobnom razmaku od 55 cm. Postignuta je zbirna sila od 5,13 kN, a naneto jednako podeljeno opterećenje nije dovelo do loma ispitivanog elementa (slika 5).

4. ZAKLJUČAK

U radu su prikazani rezultati sopstvenih istraživanja osnovnih fizičko-mehaničkih svojstava lakoagregatnih mikroarmiranih cementnih kompozita koji mogu ući u sastav predloženog fasadnog panela, kao i osnovne karakteristike pomenutog pilot elementa. Na osnovu istraživanja maltera može se jasno uočiti porast vrednosti skupljanja usled sušenja i upijanja vode uzoraka sa agregatom od drobljene opeke u odnosu na etalonske mešavine. I pored povećanog upijanja, može se zaključiti da su svi ispitani uzorci otporni na mraz.

Adhezija lakoagregatnih mikroarmiranih cementnih kompozita za površinu od kamena je ocenjena kao povoljna, sa vrednošću višom od 0,5 MPa i mešovitim tipom loma. Nakon ispitivanja, pripremljeni uzorci nisu pokazali znake eflorescencije. Ispitivanjem pilot fasadnog elementa dimenzija 60x60x3,5cm postignuto je zbirno opterećenje od 5,13 kN.

U skladu sa trendom održivosti, u okviru predloženog fasadnog panela korišćeni su reciklirani materijali u vidu agregata od drobljene opeke i lokalni kamen – granit "Šutica". Dalje se predlaže se da se fasadni element primeni u okviru ventilisanog fasadnog sklopa. Tako bi se, cirkulacijom vazduha unutar provetrenog međuprostora, omogućavalo pasivno hlađenje fasadnog zida tokom letnjeg perioda. U smislu životnog ciklusa materijala, ovi paneli se takođe mogu dalje reciklirati i ponovo upotrebiti u vidu agregata.

a) b)

Slika 5. Ispitivanje fasadnog pilot elementa: a) ispitna kompozicijai, b) tok ispitivanja

ZAHVALNOST

U radu je prikazan deo istraživanja koje je pomoglo Ministarstvo prosvete, nauke i tehnološkog razvoja Republike Srbije u okviru tehnološkog projekta TR 36017 pod nazivom: „Istraživanje mogućnosti primene otpadnih i recikliranih materijala u betonskim kompozitima, sa ocenom uticaja na životnu sredinu, u cilju promocije održivog građevinarstva u Srbiji“.

LITERATURA

1. *European Commission. Directive 2008/98/EC of the European Parliament and of the Council of 19 November 2008 on Waste and Repealing Certain Directives (Waste Framework Directive) (2008). European Commission: Brussels, Belgium, pp. 3–30.*
2. *Corinaldesi, V., Giuggiolini, M., & Moriconi, G. (2002). Use of rubble from building demolition in mortars. Waste Management, 22, 893-899.*
3. *Radoičić, V. (1997). Beton na bazi reciklirane opeke armiran polipropilenskim vlaknima. Magistarska teza, Građevinski fakultet Univerziteta u Beogradu.*
4. *Vytlačilová, V. (2011). The fibre reinforced concrete with using recycled aggregates, International Journal of Systems Applications, Engineering & Development, 5(3), 359-366.*
5. *Jevtić, D., i Zakić, D. (2006). Mikroarmirani malteri i betoni – mogućnost poboljšanja fizičko-mehaničkih svojstava. Materijali i konstrukcije, 49(3/4), 35-44.*
6. *Jevtić, D., Zakić, D., i Harak, S. (2002). Ispitivanje različitih tipova maltera spravljenih na bazi opekarskog loma. Materijali i konstrukcije, 45, 60-63.*
7. *Harak, S. (2001). Izbor građevinskog materijala za malter na bazi opekarskog loma na osnovu ispitivanja tržišta i uzoraka materijala. Diplomski rad, Građevinski fakultet Univerziteta u Beogradu.*
8. *Sika. http://srb.sika.com/*
9. *Kuraray. http://www.kuraray.eu/en/*
10. *SRPS EN 1015-3: Metode ispitivanja maltera za zidanje – Deo 3: Određivanje konzistencije svežeg maltera (pomoću potresnog stola) (2008). Institut za standardizaciju Srbije.*
11. *SRPS EN 1015-11: Metode ispitivanja maltera za zidanje – Deo 11: Određivanje čvrstoće pri savijanju i čvrstoće pri pritisku očvrslog maltera (2008). Institut za standardizaciju Srbije.*
12. *SRPS B.C8.029: Cement – Skupljanje cementnog maltera usled sušenja (1979). Institut za standardizaciju Srbije.*
13. *SRPS B.B8.010: Ispitivanje prirodnog kamena – Određivanje upijanja vode (1980). Institut za standardizaciju Srbije.*
14. *SRPS U.M8.002: Malteri za zidanje i malterisanje – metode ispitivanja (1997). Institut za standardizaciju Srbije.*
15. *SRPS EN 1015-12: Metode ispitivanja maltera za zidanje – Deo 12: Određivanje čvrstoće prianjanja očvrslih maltera za unutrašnja i spoljašnja oblaganja na podloge (2008). Institut za standardizaciju Srbije.*
16. *ASTM C67-14: Standard Test Methods for Sampling and Testing Brick and Structural Clay Tile (2009). ASTM International.*

17. *SRPS EN 1015-6: Metode ispitivanja maltera za zidanje – Deo 6: Određivanje zapreminske mase svežeg maltera (2008). Institut za standardizaciju Srbije.*
18. *SRPS U.M1.016: Beton – Ispitivanje otpornosti betona prema dejstvu mraza (1992). Institut za standardizaciju Srbije.*
19. *German Institute for Construction Engineering. (2008). General approval by the building inspectorate: Ventilated external wall cladding „Airtec Stone".*
20. *Lammert, B. T., & Hoigard, K. R. (2007). Material strength considerations in dimension stone anchorage design. Journal of ASTM International, 4(6), 40-57.*
21. *Pires, V., Amaral, P. M., Rosa, L. G., & Camposinhos, R. S. (2011). State flexural and anchorage considerations in cladding design. Construction and Building Materials, 25, 3966-3971.*
22. *Crnković, B., i Šarić, Lj. (2012). Građenje prirodnim kamenom. Zagreb: UPI.2M PLUS.*
23. *Yu, J. Y. H., & Chan, S. L. (2001). Practice and testing of stone cladding in Hong Kong. http://88.198.249.35/preview/2slqmYRsQTcNraJRvnLlRt2Kw9jhsPE_PvM81GpeswQ,/ Practice-and-testing-of-stone-cladding-in-Hong-Kong.html?query=Granite-Cladding*
24. *Vojnović, T. (2015). Modeli tehnologije oblaganja fasada kompozitnim panelima sa licem od kamena. Doktorska disertacija, Arhitektonski fakultet Univerziteta u Beogradu.Infrastructure: Project description; March 2014*

Effect of types and length of fibres in reinforcement concrete structures

Vpliv vrst in dolžine vlaken v armirano betonskih konstrukcijah

Naser Kabashi, Cene Krasniqi, Enes Krasniqi

Department of Civil Engineering, University of Prishtina, Prishtina, Kosovo

Hysni Morina

Institute of Building Materials and Structures –IBMS, Prishtina, Kosovo

Abstract

Fibre-reinforced concrete (FRC) often referred as micro reinforcing concrete is defined as concrete containing relatively short and discontinuous fibres. Fibres used in FRC may differ in terms of origin (steel, carbon, glass, polypropylene etc.), length (micro-fibres, macro-fibres), shape (straight, hooked, fibrillated etc.) diameter etc. consequently resulting in concrete behavior. The addition of fibres, even at low fibre content, affects in post-cracking toughness and ductility of the concrete. Because of three dimensional dispersing, discrete nature and high mechanical properties, the main application is oriented in concrete elements to control plastic shrinkage cracking, improve fatigue strength, generally in structural parts where reinforcement is not statically required. Fibres improves also the tensile strength of concrete and therefore holds the potential for reducing or even eliminating the conventional bar reinforcement. Nevertheless the application for this tendency is still limited. Firstly there is no generally accepted design method and very complicated determination of post cracking behavior. Various abovementioned parameters tend to influence post cracking behavior and principally complicates to structure a general design method even though there are some design proposals, recommendation or standards. Nowadays fibres are commercially available and affordable. The tendency now is to define the improvement in tensile strength of concrete and if they will partially or fully replace the conventional steel bars in structural members. The experimental program of this study conclude results of 27 standard concrete beams with various fibres in term of origin, shape, length, diameter and fibre content. For comparative approach, reference specimens were cast without fibres. For polypropylene specimens, increasing the fiber ratio affects in pre-cracking behavior but the ratio taken for this experiment, didn't archive the nominal fibre content in order to influence the post-cracking behavior. Specimens with steel fibres excluding the specimens with 0.25% volume, have enhanced post-cracking tensile behavior and improved crack control.

Povzetek

Z vlakni ojačeni beton, ki se pogosto imenuje mikroarmirni beton (MAB), je opredeljen kot beton, ki vsebuje razmeroma kratka in diskontinuirana vlakna. Vlakna, ki se uporabljajo v MAB, se lahko razlikujejo glede na poreklo (jeklo, ogljik, steklo, polipropilen itd.), dolžino (mikro vlakna, makro vlakna), obliko (ravne, kljukaste, fibrilirane itd.), premer itd. in posledično vplivajo na obnašanje betona. Dodana vlakna, tudi pri nizki vsebnosti, vplivajo na žilavost po razpokanju in duktilnost betona. Zaradi tridimenzionalne razporeditve in visokih mehanskih lastnosti je glavna aplikacija usmerjena v betonske elemente za nadzor razpok zaradi plastičnega krčenja, izboljšanje odpornosti na utrujenost, običajno v konstrukcijskih delih, kjer armatura ni statično potrebna. Vlakna izboljšajo tudi natezno trdnost betona in zato imajo potencial za zmanjšanje ali celo odpravo običajne armature. Kljub temu je uporaba te težnje še vedno omejena. Prvič, ni splošno sprejeta metoda projektiranja in zelo zapletena določitev obnašanja po razpokanju. Različni zgoraj navedeni parametri vplivajo na obnašanje po razpokanju in v glavnem zapletajo strukturo splošne metode projektiranja, čeprav obstajajo predlogi, priporočila ali standardi. Danes so vlakna na voljo na tržišču in cenovno dostopna. Zdaj je težnja, da se opredeli izboljšanje natezne trdnosti betona in ali bodo vlakna delno ali v celoti nadomestila konvencionalne jeklene palice v konstrukcijskih elementih. V eksperimentalnem programu te študije so bili ugotovljeni rezultati 27 standardnih betonskih nosilcev z različnimi vlakni glede na izvor, obliko, dolžino, premer in njihovo vsebnost. Zaradi primerjave so bili izdelani referenčni vzorci brez vlaken. Pri vzorcih s polipropilenskimi vlakni, povečanje vsebnosti vlaken vpliva na obnašanja pred razpokanjem, vendar vsebnost,

uporabljena za ta poskus, ni bila takšna, da bi vplivala na obnašanje po razpokanju. Vzorci z jeklenimi vlakni, razen vzorcev z 0,25-odstotnim volumnom, imajo izboljšano natezno obnašanje po razpokanju in boljšo kontrolo razpok.

Keywords: Fibre-reinforced concrete, residual flexural strength, steel fibres, polypropylene fibres
Ključne besede: mikroarmirani beton, rezidualna upogibna trdnost, jeklena vlakna, polipropilenska vlakna

1. INTRODUCTION

Concrete is characterised by brittle-failure, nearly complete loss of loading capacity, from beginning the failure is initiated. This characteristic, which limits the applications of the material in many cases request to improve the behaviour parameters, can be overcome by using the optimal amount different types of fibres with different characteristics (steel, glass, synthetic and natural). The using of fibres can be practiced in remedy weaknesses of concrete such as resistance, shrinkage, cracking, ductility etc.

Steel fibres remains the most used fibres followed by polypropylene, glass and other fibres. Studies have shown that the addition of steel fibres and polypropylene fibres in a concrete matrix improves all the mechanical properties of concrete, especially tensile strength, impact strength, and toughness. The influence of polypropylene fibres with different proportioning and fibre length improve the performance of mechanical characteristics. Different types of fibres used in two different lengths (12mm, 25 mm and 50-60 mm) and different fibre proportions by weight in the mixture design. The resulting material possesses higher tensile strength, consolidated response and better ductility.

This paper describes the results of an extensive experimental work performed at Laboratory of Materials and Structural Engineering of the University of Prishtina. In this test we used the same mix design in order to emphasise the influence of fibres. Several concrete beams were casted using different types and ratios of steel and macro-micro -polypropylene fibres where after curing in determined condition, specimens were tested in a three-point bending scheme.

2. EXPERIMENTAL PROGRAM

The following part of papers describe the most important features of the experimental test. All the tests described in this paper were performed following the guidelines given by EN 14651:2005 and EN 14845:2006.

2.1. Materials

In the present work three different types of fibres were used: macro-synthetic fibres; micro synthetic fibres and a steel fibre. Figure 1 shows the fibres used and Table 1 gives details on their geometry (length, l_f, and diameter, d_f) and on their mechanical properties (elastic modulus, E, and tensile strength, f_t')

For each of type of fibres we apply three different dosage , and in combinations we prepare the nine sets of prismatic samples for testing and one set of plain concrete for comparison during the presentation the results. Paralely we prepare the cubic samples (150 x 150 x 150)mm for verify the compressive strength. The dosage of fibres is calculate in mass for cubic meter of concrete , considering the each type of fibres and also dosage suggesting from the manufacturer.

2.2. Test procedure

The test procedure consist with guidelines given in EN 14651: 2005 using the prismatic specimens with dimension 150x150 x 600 mm, testing in three point bending , presenteded in figure 2. The specimens are notched at mid span with hight of notch 25 mm. The specimens were cured in laboratory conditions and prepared for testing after 28 days. Loading was performed according to a deformation control. The method allows to measure force-displacement or force-CMOD (crack mouth opening displacement) relations. One transducer is installed to the specimen at mid-depth directly over supports to measure corresponding

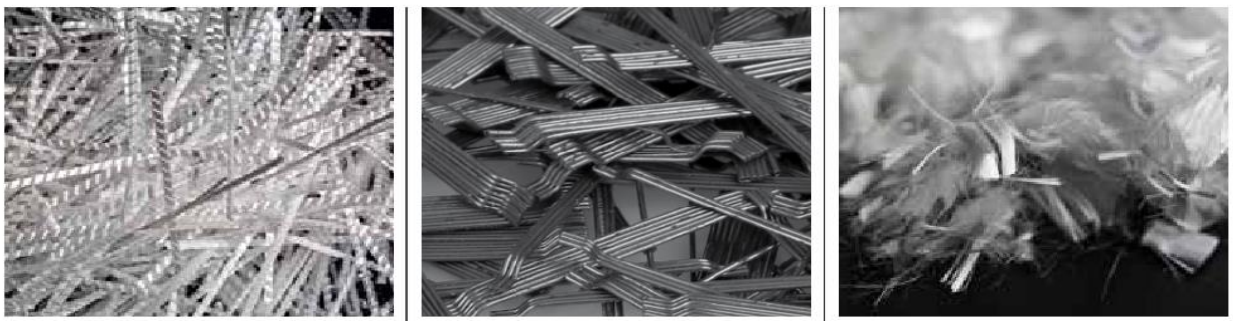

Fig 1: Macro fibres, steel fibres and micro fibres.

Table 1: Type , geometry and mechanical properties of fibres

Series No.	**Reference**	**Fiber type**	**Length *lf (mm)***	**Tensile strength *ft* (Mpa)**	**Modulus of elasticity E (Mpa)**
I	SPPM1	Monofilament polypropylene	12	600-700	3000-3500
II	SPPF1	Fibrillated polypropylene	25	275-415	4100-4200
III	SSF1	Steel	50-63	1000-1100	206000

Table 2: Fibre content in different set of samples

Reference	**No. of specimens**	**Fiber type**	**Amount kg/m3**	**Volume of fibres *%***
SPPM1	3	Monofilament polypropylene	0.6	0.063
SPPM2	3	Monofilament polypropylene	0.7	0.074
SPPM3	3	Monofilament polypropylene	0.9	0.095
SPPF1	3	Fibrillated polypropylene	0.6	0.063
SPPF2	3	Fibrillated polypropylene	0.7	0.074
SPPF3	3	Fibrillated polypropylene	0.9	0.095
SSF1	3	Steel	19.62	0.25
SSF2	3	Steel	39.25	0.5
SSF3	3	Steel	58.87	0.75

deflection. Another transducer mounted at the tip of the notch to measure the crack tip opening displacement (CTOD). During the flexure testing, the same rate of the CMOD is maintained during the process. All the tests were ended when the specimens fails (PPM and PPF beams) or CMOD exceeds 4mm.

3. RESULTS OF THE EXPERIMENTAL ANALYSES

3.1. Properties of the fresh concrete

To compare the mechanical properties using different types of fibres, we take in considerations the stability and workability of fresh concrete matrix in different batches. This parameter is very important parameter and comparison is always with plain concrete . During the casting process some properties of fresh concrete were meseaured: slump and density. The results are presented in table 3. The cementious content in concrete mix was fixed at 370 kg/m^3. The water-cementious ratio (W/C=0.52) and was kept constant in all mixes. All mixures including the control mixture were prepared with same ingredients. The control mixture –plain concrete contained no fibres. Fiber reinforced concrete (FRC) differ from each other (each set) from volume fraction V_f presented in Table 2.. Minor volume fraction V_f for samples with polypropylene is done according to manufacturer

instruction and our intent to see effects of small amount of fibres.

The preparing and maintenance the samples till testing are presented in fig.3.

3.2. Flexural test and residual strength

Testing procedure will lead to evaluate the relations: Load-CMOD (Load-Crack mouth opening Displacement) values were measured in each test. The testing results present the increasing CMOD in the peak load (F_L) with the increasing of volume of fibres V_f. In specimens with minimum volume of fibres (PPM and PPF) especially specimens with amount 0.6 kg/m^3 ratio, in term of Load-CMOD response, just minimum improvement.

For polypropylene specimens, increasing the fiber ratio affects in pre-cracking behavior but the ratio taken for

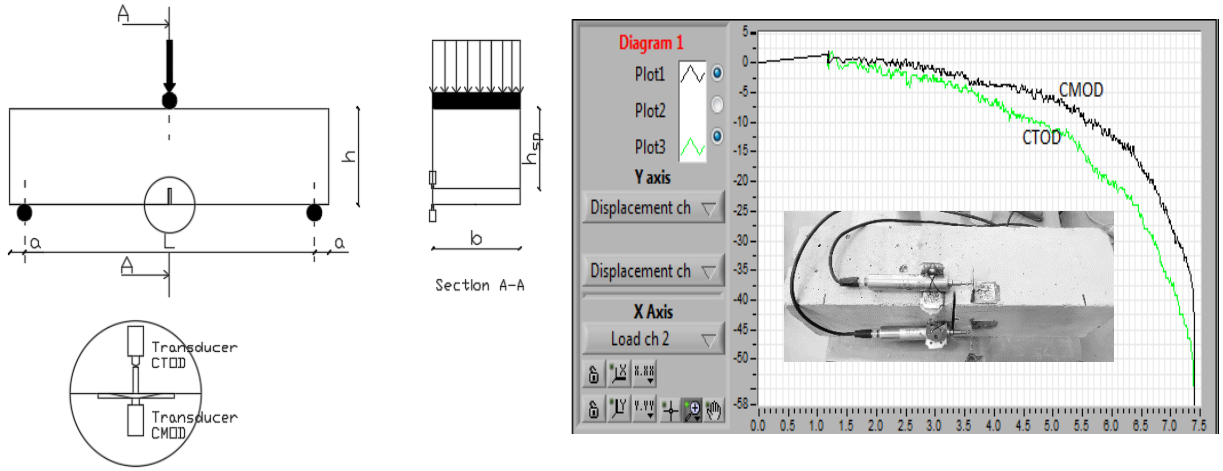

Fig 2: Experimental setup for flexure test of notched specimens.

Fig 3: Preparing, maintaining and examinating FRC specimens

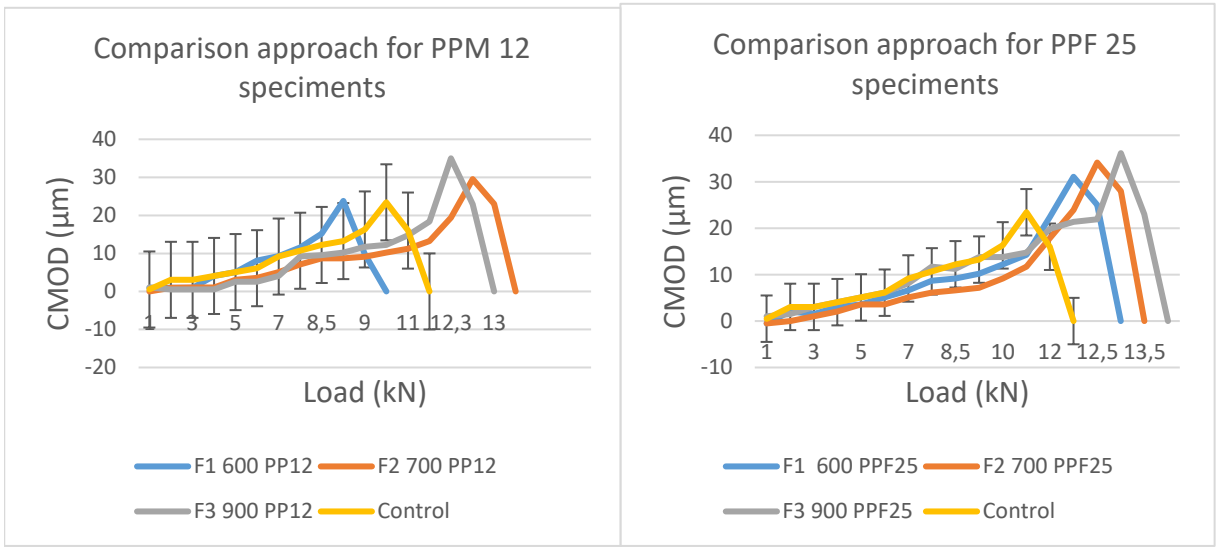

Fig 4: Effect of PPM 12 in relations Load-CMOD

Table 3: Properties of the fresh concrete measured during the casting of the different sets of specimens

Reference	No. of specimens	Fiber type	Slump mm	Density kg/m^3
SPPM1	3	Monofilament polypropylene	60	2380
SPPM2	3	Monofilament polypropylene	65	2380
SPPM3	3	Monofilament polypropylene	63	2380
SPPF1	3	Fibrillated polypropylene	62	2380
SPPF2	3	Fibrillated polypropylene	60	2380
SPPF3	3	Fibrillated polypropylene	63	2380
SSF1	3	Steel	57	2399
SSF2	3	Steel	60	2419
SSF3	3	Steel	61	2438
SPC	3	Plain concrete	60	2380

this experiment, didn't archive the nominal fibre content in order to influence the post-cracking behavior. Specimens with steel fibres excluding the specimens with 0.25% volume, have enhanced post-cracking tensile behavior and improved crack control. Since it is the post-cracking behavior that is affected, the characteristic residual tensile strength is the parameter governing the effects of fibres, presented in fig. 5.

The increase in the residual load carrying capacity with increasing CMOD indicates that the steel fibres are effective in providing crack closing stresses with increasing crack opening. The CTOD provides a qualitative measure of the crack opening when the load recovery is initiated. Increasing the fiber volume content increases the resistance to crack openings.

With reference to the curves experimentally recorded, the load at the limit of proportionality F_L, the corresponding strength $f^{f}_{ct,L}$, and the residual flexural strengths $f_{R,j}$ were evaluated according to EN 14651 . Based on this recommendation, the load limit of proportionality (F_L) is equivalent to the highest value of the load recorded up to CMOD value of 0.05mm, and the strength corresponding to the limit of proportionality (LOP) which can be calculated using the following equations :

$$f^{f}_{ct,L} = \frac{3 \cdot F_l \cdot l}{2 \cdot b \cdot h^2_{sp}} \text{ (Mpa)}, \quad (1)$$

Where: b (150mm), h_{sp} (125mm) and L (450mm) are geometrical parameters of testing samples.

In testing process the residual flexural tensile strengths $f_{R,1}$, $f_{R,2}$, $f_{R,3}$ and $f_{R,4}$ at the CMOD value of 0.025mm, 0.05mm, 0.5mm and 3.5mm were computed using the following equations:

$$f_{R,j} = \frac{3 \cdot F_{R,j} \cdot l}{2 \cdot b \cdot h^2_{sp}} \text{ (Mpa)}, \quad (2)$$

Residual tensile strengths $f_{R,1}$ and $f_{R,2}$ corresponds to specimens with polypropylene fibres and have minor influence in post cracking behavior were in the meantime $f_{R,3}$ can be used in the verification of the serviceability limit states and $f_{R,4}$ is applied in the ultimate limit state analysis.

for different testing sets with results is presented in Table 4.

The strengths at the limit of proportionality reach similar values, and it's not affected by the increase of the fiber volume content, while the residual strengths $f_{R,1}$, $f_{R,2}$, $f_{R,3}$ and $f_{R,4}$ increase about from (10 -23)% for specimens with steel fibers while for specimens with

Table 4: Three point bending tests, tensile strength parameters

	F_L kN	$f^f_{ct,L}$ (Mpa)	$f_{R,1}$ (Mpa)	$f_{R,2}$ (Mpa)	$f_{R,3}$ (Mpa)	$f_{R,4}$ (Mpa)
SPPM1	8.9	2.56	2.02	2.56	N/A	N/A
SPPM2	13.5	3.78	3.65	3.78	N/A	N/A
SPPM3	N/A	N/A	3.53	N/A	N/A	N/A
SPPF1	13.15	3.78	3.72	3.78	N/A	N/A
SPPF2	N/A	N/A	3.47	N/A	N/A	N/A
SPPF3	13.10	3.77	3.69	3.77	N/A	N/A
SSF1	13.60	3.91	3.80	3.92	N/A	N/A
SSF2	12.50	3.60	3.51	3.60	3.70	4.0
SSF3	13.40	3.86	3.96	4.06	4.11	5.21

**Note; N/A not achievable*

polypropylene fibers deviate while and residual strengths $f_{R,3}$ and $f_{R,4}$ are unreachable.

The results of specimens with steel fibres (SFF2 and SFF3) were analyzed using procedure given in UNI 11039-2 because they interfere in post-cracking behavior. The first crack nominal strength represents the matrix behavior:

$$f_{lf} = \frac{P_{lf} \cdot l}{b \cdot (h - a_0)^2} \text{ (Mpa)}, \quad (3)$$

Where b (150 mm), h (150 mm), and l (450 mm) are width, the height, and the span of the specimen, respectively, and a_0 (25mm) is the height of the notch. P_{lf} corresponds to the value of the load recorded for a crack tip opening displacement equal to $CTOD_0$. The parameters $f_{eq(0-0.6)}$ and $f_{eq(0.6-3)}$ are the average nominal

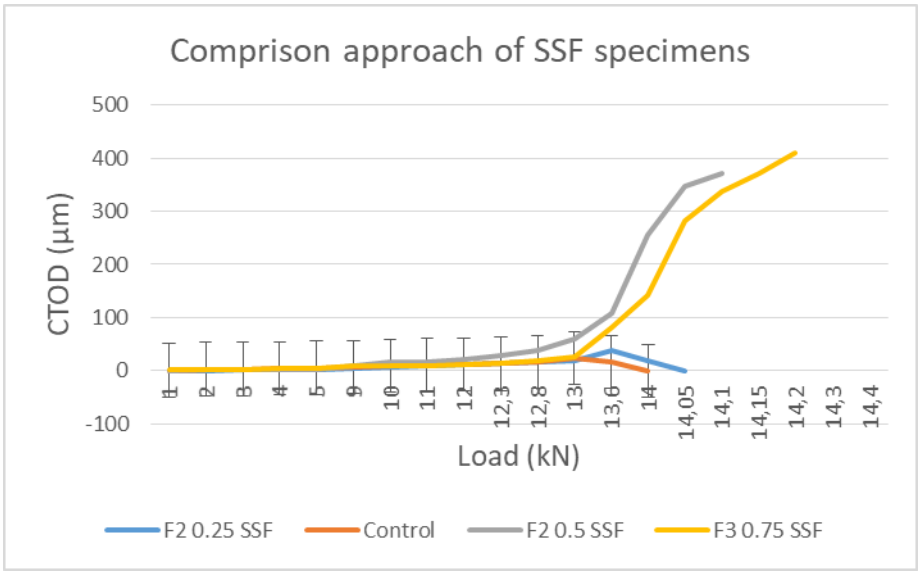

Fig 5: Effect of SSF in relations Load-CTOD.

Table 5: Corresponding strength values according UNI 11039-2

	P_{lf} (kN)	f_{lf} (Mpa)	$f_{eq(0-0.6)}$	$f_{eq(0.6-3)}$
SPC	12.21	3.51		
SFF2	12.50	3.60	2.74	15.21
SFF3	13.40	3.86	3.22	18.17

**SPC-Usually plain Concrete*

stresses in the CTOD range between 0-0.6 mm and 0.6-3 mm, respectively. These two parameters are the post-cracking equivalent strengths useful for the serviceability limit state and for the ultimate limit state that can be computed using the following expressions:

$$f_{eq(0-0.6)} = \frac{l}{b\cdot(h-a_0)^2} \cdot \frac{U_1}{0.6} \text{ (Mpa)}, \quad (4)$$

$$f_{eq(0-0.6)} = \frac{l}{b\cdot(h-a_0)^2} \cdot \frac{U_1}{0.6} \text{ (Mpa)}, \quad (5)$$

where U_1 and U_2 can be evaluated:

$$U_1 = \int_0^{0.6} P(CTOD)d\,(CTOD) \quad (6)$$

$$U_2 = \int_{0.6}^{3} P(CTOD)d\,(CTOD) \quad (7)$$

It can be seen that there is an increasing trend in the first crack strength with increasing fiber content alongside the values of $f_{eq(0-0.6)}$ and $f_{eq(0.6-3)}$ show clear improvement on increasing the V_f from 0.5% to 0.75%.

In the case of plain concrete, a brittle failure occurred by separating the elements into two parts. Adding small fraction of fibres doesn't influent the ductile behavior, in contrary, a few parameters such as volume fraction, fiber length and modulus of elasticity tend to improve brittle failure. Fibres on the fracture surface didn't bridge the cracks and behave inactive like voids or errors in concrete matrix.

4. CONCLUSIONS

The present work investigate the flexural behaviourof notched beams made of concretes fibre-reinforced with different types and amounts of fibres.

- Fiber volume content plays a significant role while small amount of volume fraction tend to have no influence in post-cracking behavior and very small fraction tend to have a negative impact.
- Short, low modulus and small volume fraction of fibres tend to improve the brittle failure of concrete.
- The residual strengths increase about 10% and 23% related to fibre volume content for specimens with steel fibers while for specimens with

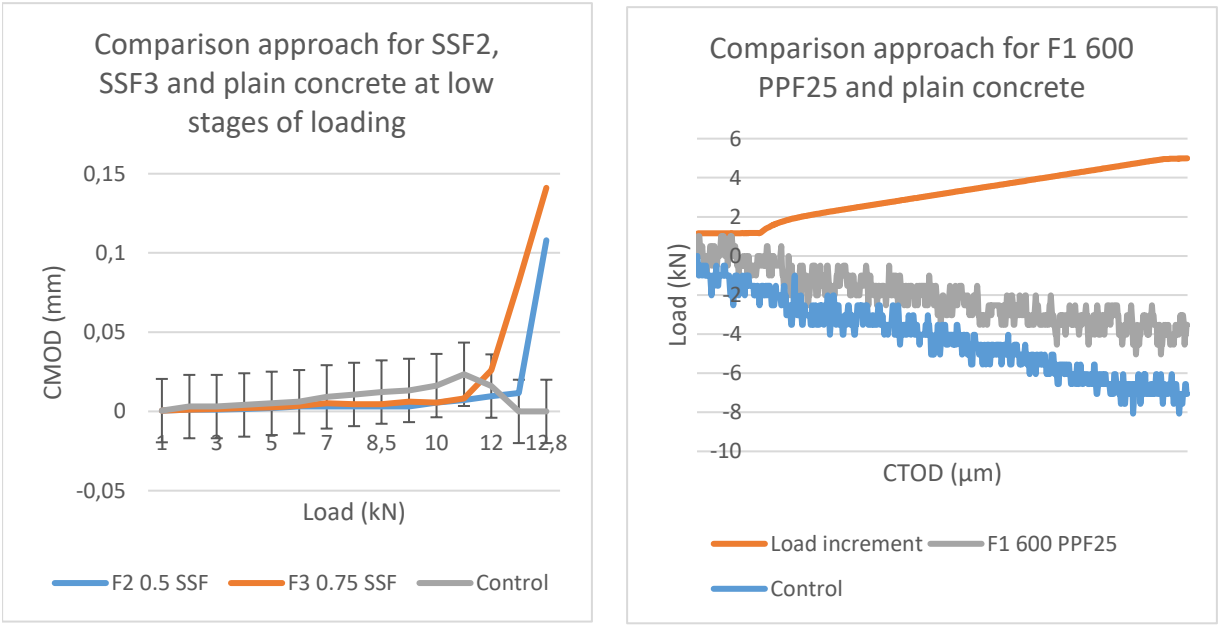

Fig 6: Examples.

polypropylene fibers deviate and the residual strengths for ultimate limit state and service limit state are unreachable.

- Data obtained from experimental work confirmed that the addition of steel fibres with corresponding aspect ration into concrete matrix, significantly improves the post-peak behavior.
- At fiber volume content equal to 0.75% there is a significant decrease in the crack depth for a given crack tip opening displacement which improves the post peak load resistance response in flexure.

SCOPE FOR FURTHER STUDY

Based on results of this study there are many scope for further study, but below are listed only the basic points what is important to know further about used the different types of fibres in improvement the ductility, focused on:

- Improvement the post cracked stage in flexural load applied
- Experimental verifications the amount of different type of fibres , not just orientated amount based on the manufacture specifications
- Analyzing the analytical model of the behavior the beams under loading process for different types of loadings.

REFERENCES

1. *Ahmad, A. Di Prisco, M. Meyer, C. Plizzari, G.A. & Shah, S.P. " Fiber reinforced concrete: from theory to practice" , Bergamo, 24 - 25 September ,2004*
2. *EN 14651:2005."Test method for metallic fibres concrete-Measuring the flexural tensile strength (limit of pro-portinality)(LOP), residual*
3. *Soroushian,P.&Lee,C.D." Distribution and orientation of fibres in steel fiber reinforced concrete ",ACI Materials Journal, 87(5),p.p. 262-278*
4. *Sahith Gali, Kolluru V. L. "Evaluation of crack propagation and Post-cracking Hinge-type Behavior in the Flexural Response of Steel Fiber Reinforced Concrete" , International Journal of Concrete Structures and Materials, Vol.11, No.2, pp.365-375, June 2017*
5. *EN 14651, Test method for metallic fibre concrete-Measuring the flexural tensile strength (limit of proportionality (LOP), residual). European Committee for Standardization, B-1050 Brussels, September 2007.*
6. *N.Kabashi,Sh.Dermaku,C.Krasniqi."The effects of polypropylene fibers on the energy-absorption capabilities of reinforced concrete beams; The Ready Mix Concrete, Istanbul Octomber 20-22.2011; pp 542-549; ISBN:978-975-92122-7-8*
7. *ACI 544.3.Indirect Method for Obtaining a Model Stress-Strain Curve of Strain Softening FRCs;2007*
8. *Miss Komal Bedi" Experimental Study For Flexure Strength On Polypropylene Fiber Reinforced Concrete"IOSR Journal of Mechanical and Civil Engineering (IOSR-JMCE),2014*
9. *F.A.Olutoge, V. Bhashya, G. Ramesh, B. Hanumantharai, S. Sundar Kumar." Evaluation of Residual Strength Properties of Steel Fiber Reinforced Concrete" Journal of Emerging Trends in Engineering and Applied Sciences,2013*
10. *EN 14845-1:2007. Test Methods for Fibres for Concrete-Part 1-Reference Concretes , 2007*
11. *Abbas H. Mohammed, Khattab Saleem Abdul-Razzaq, Raad D. Khalaf, Ali K. Hussein." Suggesting Deflection Expressions for RC Beams" International Journal of Civil Engineering and Technology (IJCIET),2019*
12. *N.Kabashi,Q.Kadir,C.Krasniqi."Flexural Behavior of the Concrete Beams Reinforced with the GFRP and Cracks analyses" Journal: Bulletin of the Transilvania University of Brasov, Romania,CIBv,2017Commission, EUROPE 2020: A strategy for smart, sustainable and inclusive growth, COM(2010)2020.*

Krčenje mikroarmiranih betonov visoke trdnosti v zgodnjem obdobju

Shrinkage of Fiber Reinforced High Strength Concrete at Early Ages

Drago Saje in Jože Lopatič

Univerza v Ljubljani, Fakulteta za gradbeništvo in geodezijo, Ljubljana

Povzetek

V članku je predstavljen in opisan fenomen krčenja mikroarmiranih betonov visoke trdnosti v zgodnjem obdobju, ki smo ga eksperimentalno preiskovali. Znaten del obravnavanega krčenja se odvije v obliki avtogenega krčenja. Različne vrste vlaken na zgodnji reološki pojav vplivajo s svojo togostjo, ki ovira proces krčenja. Vlaka vplivajo na avtogeno krčenje še s svojo sposobnostjo vpijanja vode in oddajanja le te v kompozit v času intenzivne hidratacije. V okviru eksperimentalnega programa smo v betone vgrajevali različne vrste mikroarmature: kratka in dolga jeklena vlakna, suha in predhodno namočena polipropilenska vlakna, predhodno namočena bazaltna vlakna ter predhodno namočena celulozna vlakna. Prostorninski delež vsebovanih vlaken v preiskovanih betonih znaša 0,75%, razen pri celuloznih vlaknih, kjer je znašal 0,33%. Zaradi primerjave krčenja mikroarmiranega betona s krčenjem betona brez mikroarmature smo merili tudi krčenje primerljivega betona enake sestave, ki ni vseboval mikroarmature. Ugotovili smo, da so imela največji vpliv na velikost avtogenega krčenja v zgodnjem obdobju predhodno namočena polipropilenska vlakna. Zmanjšanje krčenja lahko spremlja tudi zmanjšanje trdnosti betona, česar si ne želimo. Poleg krčenja smo zato merili tudi 28-dnevno tlačno trdnost vseh obravnavanih betonov. V splošnem vlakna zmanjšajo sposobnost vgrajevanja kompozita. Spremljali smo vgradljivost kompozita glede na vrsto vlaken. V naših raziskavah so se celulozna vlakna in suha polipropilenska vlakna, ki so se napila vode, izkazala kot večja motilca vgradljivosti.

Abstract

The article presents and describes the phenomenon of shrinkage of fiber-reinforced high-strength concrete at an early age. A significant part of the considered shrinkage takes place in the form of autogenous shrinkage. Different types of fibers affect the early rheological phenomenon with their stiffness, which impedes the process of shrinkage. The influence of fibers on autogenous shrinkage is also reflected in the ability of concrete to absorb water and transmit it to the composite during intense hydration. Within the experimental program, various types of fibres were installed in concrete: short and long steel fibers, dry and pre-soaked polypropylene fibers, pre-soaked basalt fibers, pre-soaked cellulose fibers. The volume content of the fibers contained in the tested concrete is 0.75%, except for cellulose fibers, where it amounted to 0.33%. In order to compare the shrinkage of fiber-reinforced concrete with the shrinkage of concrete without fibers, we also measured the shrinkage of comparable concrete of the same composition, but without fibers. We found that pre-soaked polypropylene fibers had the most significant influence on early autogenous shrinkage. Reduction in shrinkage can also be accompanied by a reduction in the strength of concrete, which we do not want. We measured the 28-day compressive strength of all treated concretes. In general, fibers reduce the workability. We monitored the workability of the composite with regard to the type of fibers. In our research, cellulose fibers and dry polypropylene fibers, which had been watered, proved to be a major impediment to workability.

Ključne besede: beton visoke trdnosti, mikroarmirani beton, avtogeno krčenje
Keywords: high strength concrete, fiber reinforced concrete, autogenous shrinkage

1. UVOD

Vlaknasta mikroarmatura, ki jo dodamo betonu, ovira širjenje razpok, in povečuje duktilnost kompozita, ne more pa nadomestiti statično potrebne armature elementov konstrukcije [1]. Geometrija vlaken mikroarmature vpliva na adhezijski stik med vlakni in matrico in preko tega na učinkovitost dodanih vlaken [2]. Mikroarmatura iz jeklenih ali drugih umetnih vlaken vpliva na duktilnost, širino razpok in na reološke

lastnosti kompozita [3, 4]. N. Banthia in R. Gupta, ki sta raziskovala vpliv geometrije polipropilenskih vlaken na razpokanost betona zaradi plastičnega krčenja ugotavljata, da je mikroarmatura iz polipropilenskih vlaken zelo učinkovita za omejevanje razpokanosti betona zaradi plastičnega krčenja. Trdita, da v splošnem polipropilenska mikroarmatura ugodno vpliva na zmanjšanje širine in števila razpok. Pri tem so tanjša vlakna bolj učinkovita od debelejših, in daljša prav tako bolj učinkovita od krajših [5].

Betoni visoke trdnosti se v gradbeni praksi v zadnjem času čedalje več uporabljajo ne le zaradi visoke trdnosti ampak tudi zaradi večje odpornosti na druge zunanje vplive. Zaradi zagotavljanja visoke trdnosti je pri betonih visoke trdnosti vodovezivno razmerje razmeroma nizko, zato se ustrezna vgradljivost praviloma zagotavlja z dodajanjem superplastifikatorjev.

Ker je v svežem betonu visoke trdnosti proste vode glede na količino cementa tako malo, da v celoti ne zadošča za proces hidratacije, se v kemijskem procesu porabi tudi del vode iz finih por, kar v njih povzroči nastanek podtlakov oziroma nateznih sil, ki delujejo na stene por. Posledica tega je zmanjšanje prostornine relativno podajnega še ne otrdelega betona – fizikalni pojav, ki ga imenujemo *avtogeno krčenje betona*. Pri betonih visoke trdnosti, za razliko od betonov normalne trdnosti, avtogeno krčenje predstavlja znaten del celotnega krčenja betona [6, 7]. Izhlapevanje vode skozi površino betona pa dodatno k avtogenemu krčenju povzroča še *krčenje betona zaradi sušenja*.

V betonu se praviloma krči cementi gel, oziroma cementni kamen, medtem ko se zrna agregata iz večine uporabljenih kamenin praktično ne krčijo oziroma krčenje cementnega gela celo ovirajo. Iz tega razloga je krčenje betona iz agregata, ki je iz kamenine večje trdnosti manjše od krčenja betona iz agregata, ki je iz kamenine manjše trdnosti [7]. Zaradi tega se v cementni pasti in kasneje cementnemu kamnu pojavijo natezne napetosti, ki v mladem betonu hitro dosežejo natezno trdnost. Dodatne notranje napetosti v času hidratacije cementa pa povzroča tudi temperaturni gradient, ki je posledica sproščanja hidratacijske toplote v procesu strjevanja betona. Posledica obeh omenjenih fizikalnih pojavov je nastanek zgodnjih razpok betona v času vezanja cementa.

Bayasi in Zeng, ki sta raziskovala vpliv vlaknaste armature na tlačno trdnost mikroarmiranega betona običajne trdnosti sta ugotovila, da se tlačna trdnost betona v primeru mikroarmiranja s polipropilenskimi vlakni dolžine l = 1,27 cm pri prostorninski vsebnosti vlaken 0,1% poveča za 15%, pri prostorninski vsebnosti vlaken 0,3% pa za 19%, pri vsebnosti vlaken 0,5% pa se trdnost kompozita v primerjavi z betonom brez mikroarmature zmanjša za 2,5% [8].

V okviru predstavljenih raziskav smo študirali vpliv različnih vrst vlaken na zgodnje avtogeno krčenje z vlakni mikroarmiranega betona visoke trdnosti. Elektronsko vodeno merjenje avtogenega krčenja smo izvajali od trenutka zabetoniranja preizkušancev, pri čemer smo za začetek merjenja krčenja privzeli čas, ko je temperatura vzorca začela naraščati in so se pojavile prve opazne deformacije preizkušancev. Laboratorijske raziskave krčenja mikroarmiranega betona visoke trdnosti smo izvajali pri prostorninski vsebnosti vlaken 0,75%, razen pri celuloznih vlaknih, kjer jih je bilo 0,33%.

2 OSNOVNI PRINCIP KRČENJA BETONA V ZGODNJI STAROSTI

Po pričetku vezanja cementa se v betonu, odvisno od pogojev nege, pričnejo prostorninske spremembe v obliki krčenja ali nabrekanja. V primeru, da je med procesom hidratacije omogočen neprekinjen dostop vode v vse pore cementne paste, se pojavi nabrekanje betona. V nasprotnem primeru, ko je gibanje vode v cementno pasto preprečeno, se beton krči.

Krčenje betona sestoji iz kemičnega krčenja, avtogenega krčenja, krčenja zaradi sušenja, plastičnega krčenja, temperaturnega krčenja in krčenja zaradi karbonatizacije. Avtogeno krčenje betona je posledica samoizsuševanja v porah cementnega kamna, ko se porablja voda v procesu hidratacije cementa. Kemično krčenje cementne paste je zmanjšanje volumna cementne paste, ki se pojavi zaradi kemičnega vezanja vode v procesu hidratacije cementa. Pri kemijski reakciji cementa in vode v betonu se sprošča toplota, kar povzroči povišanje temperature betona in posledično deformiranje betona zaradi spremembe temperature.

Med procesom hidratacije se voda porablja za tvorbo hidratacijskih produktov. Z napredovanjem procesa hidratacije se povečuje prostornina por, ki so posledica kemičnega krčenja cementne paste. Po Boylovem zakonu je povečanje prostornine zaprtih por povezano z zmanjševanjem tlaka zraka v porah. Zmanjševanje tlaka posredno vpliva na relativno vlažnost v porah. Ob vzpostavljanju termodinamičnega ravnovesja v porah cementne paste izhlapeva najprej prosta kapilarna voda, nato pa voda iz adsorpcijske ploskve stene pore. Tanjšanje adsorpcijske plasti vode na stenah por povzroča natezne napetosti v adsorpcijski ploskvi. Natezne napetosti v adsorpcijski ploskvi povzročajo znatne deformacije, ki se jim struktura upira s svojo trenutno togostjo. V začetnem obdobju procesa strjevanja, ko je modul elastičnosti cementne paste še razmeroma nizek, lahko omenjene natezne napetosti povzročijo velike zunanje deformacije, ki jih imenujemo avtogeno krčenje.

3 PROGRAM EKSPERIMENTALNIH RAZISKAV

Vpliv vrste vlaken na krčenje mikroarmiranega betona smo raziskovali pri vodovezivnem razmerju sveže betonske mešanice 0,36. Meritve krčenja kompozita smo izvajali na preizkušancih v obliki prizem z dimenzijami 10/10/40 cm, na preizkušancih v obliki kock z robom 15 cm, pa smo informativno ugotavljali 28-dnevno tlačno trdnost betona. Na treh prizmah iz vsake mešanice smo merili celotne specifične

Preglednica 1: Lastnosti uporabljenih jeklenih vlaken

Jeklena vlakna	Dolžina vlaken [mm]	Izmerjeni dimenziji prečnega prereza		Nadomestni premer d_e [mm]	Natezna trdnost vlaken [MPa]
		a [mm]	*b* [mm]		
IRI 50/16	16	0,491	0,502	0,496	797
IRI 50/30	30	0,491	0,502	0,496	797

Preglednica 2: Lastnosti uporabljenih polipropilenskih vlaken

Gostota vlaken [g/cm^3]	Dolžina vlaken [mm]	Nazivne dimenzije vlaken [μm]	Natezna trdnost vlaken [MPa]	Elastični modul vlaken [MPa]
0,91	12	35 × 250-600	340-500	8500-12500

Preglednica 3: Lastnosti uporabljenih bazaltnih vlaken

Gostota vlaken [g/cm^3]	Dolžina vlaken [mm]	Nazivni premer vlaken [μm]	Natezna trdnost vlaken [MPa]	Elastični modul vlaken [MPa]
2,7	12	13	2800-4800	86000-90000

Preglednica 4: Lastnosti uporabljenih celuloznih vlaken

Gostota vlaken [g/cm^3]
1,1

deformacije mikroarmiranega betona visoke trdnosti, na vsaj treh kockah pa 28-dnevno tlačno trdnost. Vsi preizkušanci za merjenje deformacij so bili ves čas hranjeni v klimatski komori pri sobni temperaturi, preizkušanci za določitev tlačne trdnosti pa v vodi.

3.1 Izdelava preizkušancev

Preizkušanci mikroarmiranega betona so bili izdelani iz pranega drobljenega apnenčevega agregata z nazivnim največjim premerom zrn 16 mm z dodatkom kremenčeve mivke. Uporabljena sta bila cement CEM II / A-M 42,5 R in CEM I 52,5 R. Za zagotavljanje primerne vgradljivosti pri relativno nizkem vodovezivnem razmerju, je bil uporabljen superplastifikator naftalenskega tipa, ki je po kemijski sestavi sulfonirani naftalen - formaldehid kondenzat. Preizkušanci so bili mikroarmirani z jeklenimi, s polipropilenskimi, z bazaltnimi ali s celuloznimi vlakni, ki so prikazana na slikah 1 do 4, njihove lastnosti pa so podane v preglednicah 1 do 4.

Preglednica 5: Recepture in lastnosti svežega kompozita preiskovanih preizkušancev

Mešanica	**M1**	**M2**	**M3**	**M4**	**M5**	**M6**	**M7**	**M8**
Fini agregat 0-4 mm [kg/m^3]	1133	1133	1126	1126	1126	1126	1126	1133
Grobi agregat 4-16 mm [kg/m^3]	755	755	750	750	750	750	750	755
Količina veziva [kg/m^3]	400	400	400	400	400	400	400	400
Količina cementa [kg/m^3]	360	360	360	360	360	360	360	360
Vrsta cementa	CEM II	CEM I	CEM II	CEM II	CEM II	CEM II	CEM I	CEM I
Količina mikrosilike [kg/m^3]	40	40	40	40	40	40	40	40
Vrsta vlaken	-	-	IRI50/16	IRI50/30	PP	PP	BV	CV
Način vgradnje vlaken	-	-	suha	suha	suha	vlažna	vlažna	vlažna
Prostorninski delež vlaken [%]	-	-	0,75	0,75	0,75	0,75	0,75	0,33
Vodovezivno razmerje	0,36	0,36	0,36	0,36	0,36	0,36	0,36	0,36
Količina superplastifikatorja [% veziva]	2,05	2,05	2,05	2,05	2,05	2,05	2,05	2,05
Posed [cm]	18	7,5	17	14,5	8,5	1,5	0,5	0
Razlez [cm]	55	33,5	43	46	41	38	39	24
Prostorninska masa [kg/m^3]	2436	2431	2450	2420	2383	2339	2376	2381
$f_{cm,28dni}$ [MPa]	81,40	82,96	86,60	92,10	78,15	78,05	76,58	71,04
Izmerjena deformacija pri času 24 ur po zabetoniranju [‰]	-0,210	-0,293	-0,131	-0,139	-0,168	-0,051	-0,300	-0,197
Avtogena deformacija pri času 24 ur po zabetoniranju [‰]	-0,216	-0,293	-0,144	-0,165	-0,179	-0,064	-0,301	-0,201

Preizkušanci so bili izdelani iz osmih različnih mešanic mikroarmiranega betona visoke trdnosti z vodovezivnim razmerjem 0,36. Pri tem sta bila mešanici M1 in M2 brez vlaken, mešanica M3 je vsebovala kratka jeklena vlakna IRI50/16, M4 dolga jeklena vlakna IRI50/30, M5 suha polipropilenska (PP) vlakna, M6 predhodno navlažena polipropilenska vlakna, M7 predhodno navlažena bazaltna vlakna (BV) in M8 predhodno navlažena celulozna vlakna (CV). Skupna količina veziva je v vseh mešanicah znašala po 400 kg/m^3 kompozita, od tega je bilo 90% cementa (360 kg/m^3) in 10% mikrosilike (40 kg/m^3). Recepture in lastnosti svežih mešanic mikroarmiranega betona so podane v preglednici 5.

3.2 Priprava predhodno navlaženih vlaken

V mešanici z oznako M6 smo uporabili polipropilenska vlakna, v mešanici M7 bazaltna, v mešanici M8 pa celulozna vlakna, ki so bila predhodno 24 ur namočena v vodi. S tehtanjem vlaken in pripravljene količine vode pred namakanjem vlaken in po namakanju vlaken smo ugotovili vsebnost vode v predhodno namočenih vlaknih. Navlažena polipropilenska in celulozna vlakna v cementni pasti služijo kot notranji rezervoar vode [9]. Podatki o vsebnosti vode namočenih vlaken so razvidni iz preglednice 6. Zadržana voda v vlaknih ni upoštevana v vodovezivnem razmerju.

3.3 Izvedba laboratorijskih raziskav

Krčenje preizkušancev smo spremljali neprekinjeno z elektronsko vodenimi meritvami. Avtogeno krčenje betona smo določali na preizkušancih, ki so bili zatesnjeni z nepropustno polietilensko folijo, ki preprečuje sušenje preizkušancev. Računalniško podprte meritve specifičnih deformacij zatesnjenih preizkušancev smo z uporabo elektronskih merilnih uric, izvajali v skladu z japonskim standardom [10] (sliki 5 in 6).

Zaradi zmanjšanja trenja med preizkušancem in podlago oziroma kalupom smo pred vgradnjo betona na dno kalupa vstavili teflonsko folijo (slika 6).

Običajne jeklene kalupe za izdelavo betonskih prizem 10/10/40 cm smo za naše meritve priredili tako, da smo na končnih stranicah jeklenih kalupov izvrtali luknji skozi katere smo namestili bazne palice za merjenje krčenja. Te so bile nameščene tako, da je dolžina merske baze znašala 380 mm (slika 6). Temperaturo betona v sredini vzorca smo merili s pomočjo termo člena. Zajem in obdelava rezultatov meritev specifičnih deformacij betona sta bila avtomatizirana.

4 REZULTATI EKSPERIMENTALNIH RAZISKAV

Rezultati meritev zgodnjega krčenja so v nadaljevanju podani v grafični obliki. Na ustreznih diagramih so podane celotne izmerjene specifične deformacije in ocenjeno avtogeno krčenje.

Slika 1: Uporabljena jeklena vlakna

Slika 2: Uporabljena polipropilenska vlakna

Slika 3: Uporabljena bazaltna vlakna

Slika 4: Uporabljena celulozna vlakna

Preglednica 6: Vsebnost vode v navlaženih vlaknih

Oznaka mešanice in vrsta vlaken	Prostorninski delež vlaken (%)	Masni delež vode v navlaženih vlaknih (%)
M6, polipropilenska	0,75	74
M7, bazaltna	0,75	31
M8, celulozna	0,33	55

Izmerjene časovne spremembe dolžin preizkušancev vsebujejo časovne spremembe dolžin zaradi krčenja betona in časovne spremembe dolžin zaradi časovnih sprememb temperature preizkušancev. Temperature v sredini preizkušancev so bile merjene istočasno z meritvami sprememb dolžin preizkušancev. Časovni potek deformacije krčenja preizkušanca je določen s korekcijo izmerjenih časovnih potekov specifičnih

Slika 5*:* Spremljanje deformiranja betona v zgodnjem obdobju.

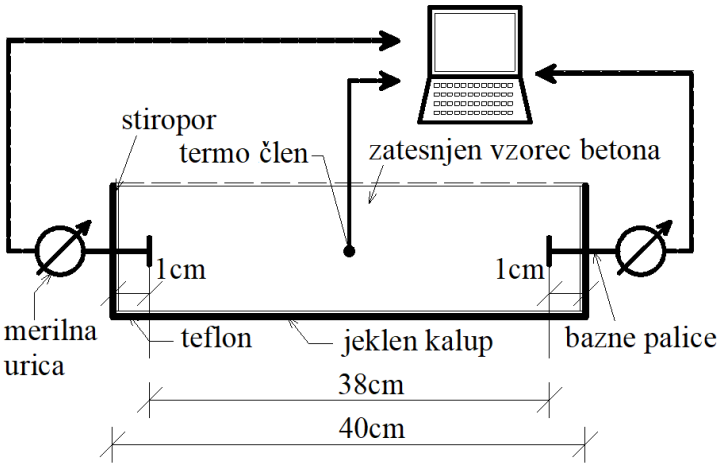

Slika 6: Shematični prikaz instrumentacije preizkušanca.

deformacij na račun temperaturnih raztezkov preizkušancev zaradi časovnih sprememb temperature (enačba 1). Ker se je temperatura preizkušancev spreminjala le v času intenzivnega vezanja cementa, to je v prvih 24-ih urah, pozneje pa je bila temperatura preizkušancev približno enaka temperaturi okolja, je vpliv spreminjanja temperature na dejansko časovno spreminjanje dolžine preizkušancev potrebno upoštevati le v prvih 24-ih urah. Časovno spreminjanje dolžine preizkušancev zaradi spreminjanja temperature v času intenzivnega vezanja cementa, to je v prvih 24-ih urah, je bilo z upoštevanjem temperaturnega razteznostnega koeficienta betona in izmerjenega časovnega spreminjanja temperature ocenjeno analitično. Pri tem je bila za temperaturni razteznostni koeficient svežega betona upoštevana vrednost $\alpha_{T,f}$ = 1,48·10^{-5}, ki je bila določena s posebnimi meritvami [7], za temperaturni razteznostni koeficient otrdelega betona pa vrednost α_T = 1,0·10^{-5}, ki je bila privzeta iz splošne literature. Pri tem je bil beton kot svež upoštevan do časa, ko je začela temperatura preizkušanca naraščati, kar približno predstavlja začetek vezanja cementa. Od 24-e ure dalje, ko se je temperatura preizkušancev ustalila, kar približno pomeni konec intenzivnega vezanja cementa, je bil beton, glede temperaturnega razteznostnega koeficienta, obravnavan kot otrdeli beton. Temperatura preizkušancev je bila v tem času konstantna in ni vplivala na časovno spreminjanje dolžine preizkušancev, zato je krčenje kompozita v tem času enako izmerjeni spremembi dolžine preizkušancev. Za vmesne vrednosti temperaturnega razteznostnega koeficienta v času intenzivnega strjevanja betona do 24-e ure po betoniranju, je bila upoštevana linearna interpolacija med vrednostjo, ki velja za sveži in vrednostjo, ki velja za otrdeli beton. Na sliki 7 so kot primer prikazane srednje vrednosti meritev temperature in celotnih specifičnih deformacij na treh preizkušancih iz mešanice M2 v prvih 24-ih urah po zabetoniranju. Časovni potek deformacij avtogenega krčenja betona (ε_{ca}), ki je določen z upoštevanjem srednjih vrednosti celotnih izmerjenih deformacij (ε_c) na treh vzorcih in računsko določene temperaturne deformacije preizkušancev ($\varepsilon_{(\Delta T)}$) zaradi povišane temperature, je za prvih 24 ur prav tako prikazan na sliki 7 s spodnjo krivuljo.

$$\varepsilon_{ca}=\varepsilon_c+\varepsilon_{(\Delta T)}=\Delta L/L+\alpha_T\cdot\Delta T. \quad (1)$$

Pri tem so:

ΔL *sprememba dolžine preizkušanca na merski bazi*

L *merska baza*

ΔT *sprememba temperature*

4.1 Zgodnje avtogeno krčenje mikroarmiranega betona visoke trdnosti

Na slikah 8, 9 in 10 so prikazani časovni poteki temperature in izmerjenih specifičnih deformacij betona v prvih 24-ih urah, na slikah 11, 12 in 13 pa ob časovnih potekih temperature še ocenjeni časovni poteki deformacij avtogenega krčenja. Pri tem je bilo avtogeno

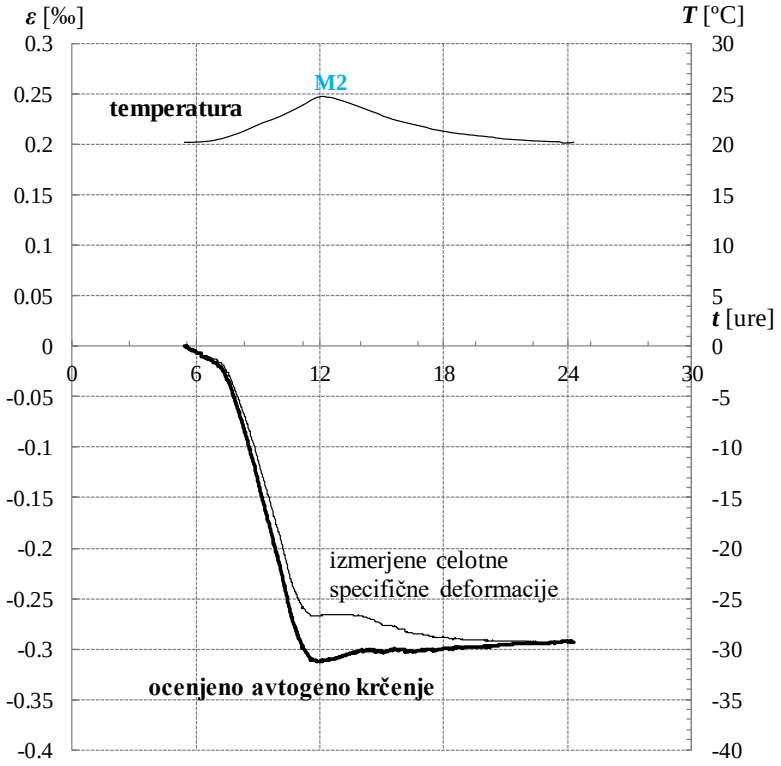

Slika 7*:* Časovni poteki srednjih vrednosti temperature, srednjih vrednosti izmerjenih celotnih specifičnih deformacij in ocenjenega avtogenega krčenja treh zatesnjenih preizkušancev iz mešanice M2 primerjalnega betona visoke trdnosti v prvih 24 urah po zamešanju.

krčenje betona ocenjeno s pomočjo enačbe 1 z upoštevanjem celotnih izmerjenih in ocenjenih temperaturnih deformacij preizkušancev.

Na sliki 8 so prikazane celotne izmerjene deformacije preizkušancev mikroarmiranih s krajšimi jeklenimi vlakni IRI 50/16, daljšimi jeklenimi vlakni IRI 50/30, suhimi polipropilenskimi vlakni in preizkušancev iz primerjalnega betona brez vlaken v prvih 24-ih urah. Sveže betonske mešanice M1, M3, M4, M5 in M6 si imele enako vodovezivno razmerje. Količina agregata v betonskih mešanicah, ki so vsebovala vlakna, je bila zmanjšana za velikost prostornine dodanih vlaken.

Ocenjeno avtogeno krčenje kompozita M3, mikroarmiranega s kratkimi jeklenimi vlakni, je en dan po zabetoniranju, v primerjavi s primerljivim betonom brez vlaken M1, manjše za približno 33%, ocenjeno avtogeno krčenje betona M4, ki vsebuje dolga jeklene vlakna, pa za približno 23% (slika 11).

Slika 9 prikazuje časovno spreminjanje temperature preizkušancev in časovne razvoje izmerjenih celotnih deformacij mikroarmiranega betona visoke trdnosti s suhimi M5 in navlaženimi M6 polipropilenskimi vlakni ter primerjalnega betona brez vlaken M1 v prvih 24-ih urah po zabetoniranju.

Iz prikaza rezultatov ocene avtogenega krčenja (slika 12) je razvidno, da je ocenjeno avtogeno krčenje mikroarmiranega betona s suhimi polipropilenskimi vlakni za približno 17%, ocenjeno avtogeno krčenje kompozita z navlaženimi pa za 70% manjše glede na avtogeno krčenje primerjalnega betona brez vlaken M1.

Na sliki 13 so prikazani poteki ocenjenega avtogenega krčenja preizkušancev iz mikroarmiranega betona visoke trdnosti z vsebnostjo predhodno navlaženih bazaltnih vlaken M7 in z vsebnostjo predhodno navlaženih celuloznih vlakni M8 ter primerjalnega betona brez vlaken M2. Iz prikazanih rezultatov je razvidno, da so celulozna vlakna, glede zgodnjega ocenjenega avtogenega krčenja betona bolj učinkovita kot bazaltna vlakna. Zgodnje ocenjeno avtogeno krčenje preizkušancev iz mešanice M7, ki vsebuje predhodno navlažena bazaltna vlakna, je celo za 3% večje, medtem ko je avtogeno krčenje preizkušancev z vsebnostjo predhodno navlaženih celuloznih vlaken, pri starost kompozita 24 ur, za približno 31% manjše od primerljivega betona brez vlaken.

Z vodo napolnjena celulozna vlakna v mešanici M8 v cementni pasti delujejo kot notranji rezervoar vode. Na ta način je voda po cementni pasti razporejena bolj enakomerno in jo je tudi več kot v primeru enake mešanice brez dodanih navlaženih celuloznih vlaken. Posledica tega so manjše kapilarne sile v svežem mikroarmiranem betonu in s tem manjše ocenjeno avtogeno krčenje v prvih 24-ih urah po zabetoniranju.

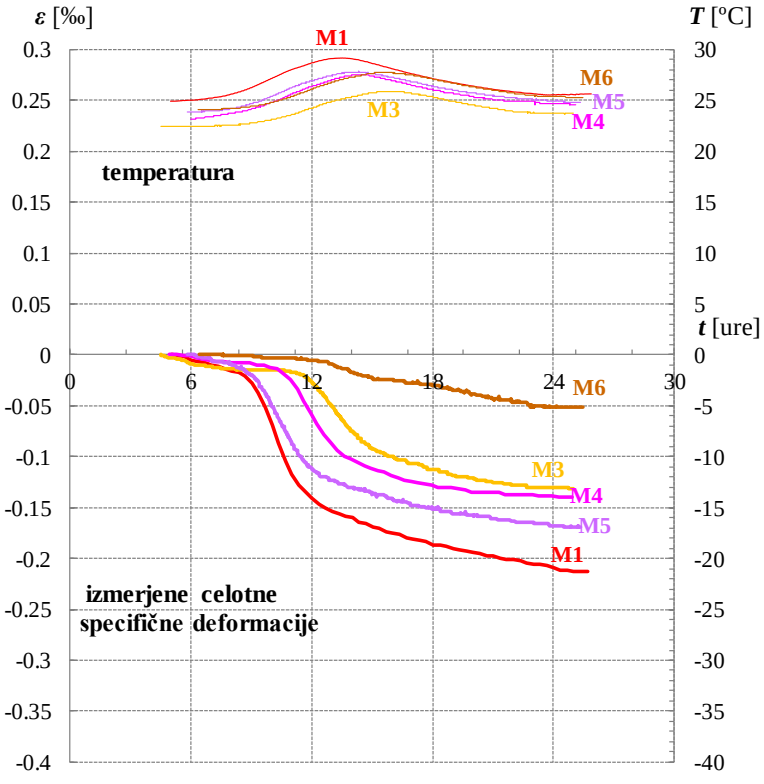

Slika 8: Srednje vrednosti izmerjenih celotnih specifičnih deformacij in temperature preizkušancev iz mikroarmiranega betona visoke trdnosti in primerjalnega betona brez vlaken v prvih 24-ih urah po betoniranju

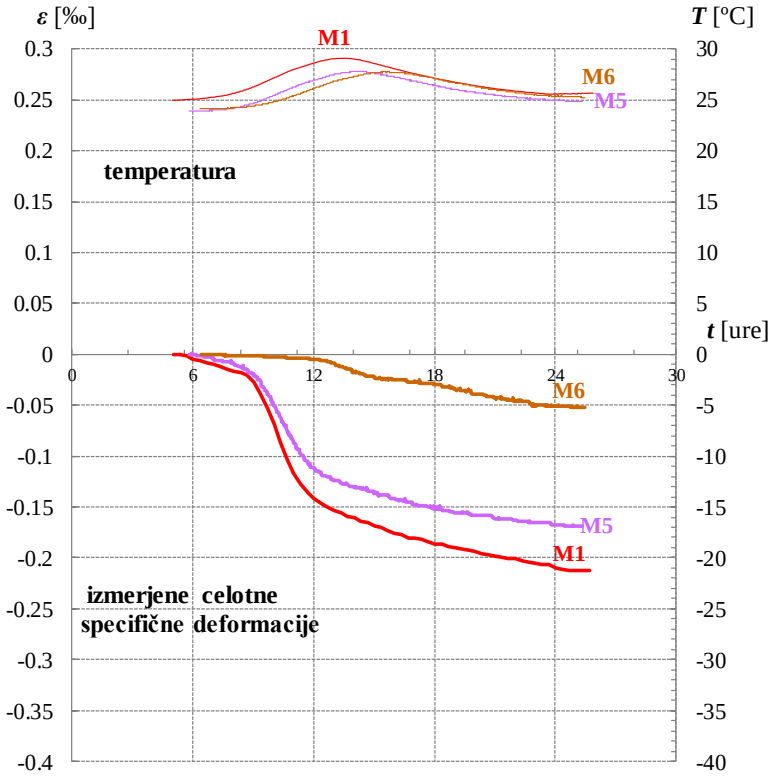

Slika 9*:* Srednje vrednosti izmerjenih celotnih specifičnih deformacij in temperature preizkušancev iz mikroarmiranega betona visoke trdnosti z dodanimi suhimi M5 ali predhodno navlaženimi M6 polipropilenskimi vlakni in primerjalnega betona brez vlaken M1 v prvih 24-ih urah po betoniranju

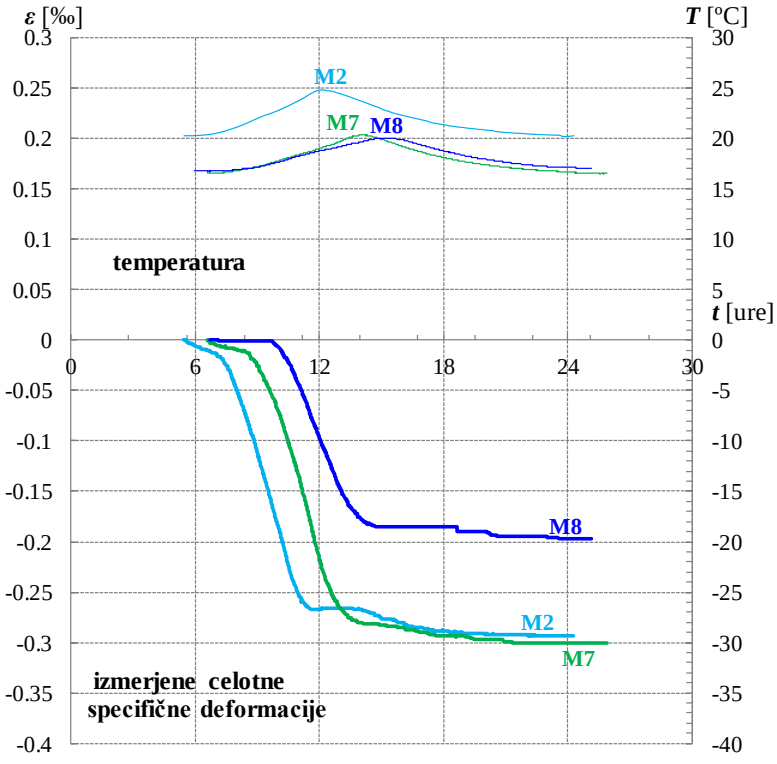

Slika 10*:* Srednje vrednosti izmerjenih celotnih specifičnih deformacij in temperature preizkušancev iz kompozita visoke trdnosti z dodanimi predhodno navlaženimi bazaltnimi vlakni M7 in predhodno navlaženimi celuloznimi vlakni M8 in primerjalnega betona brez vlaken M2 v prvih 24-ih urah po betoniranju

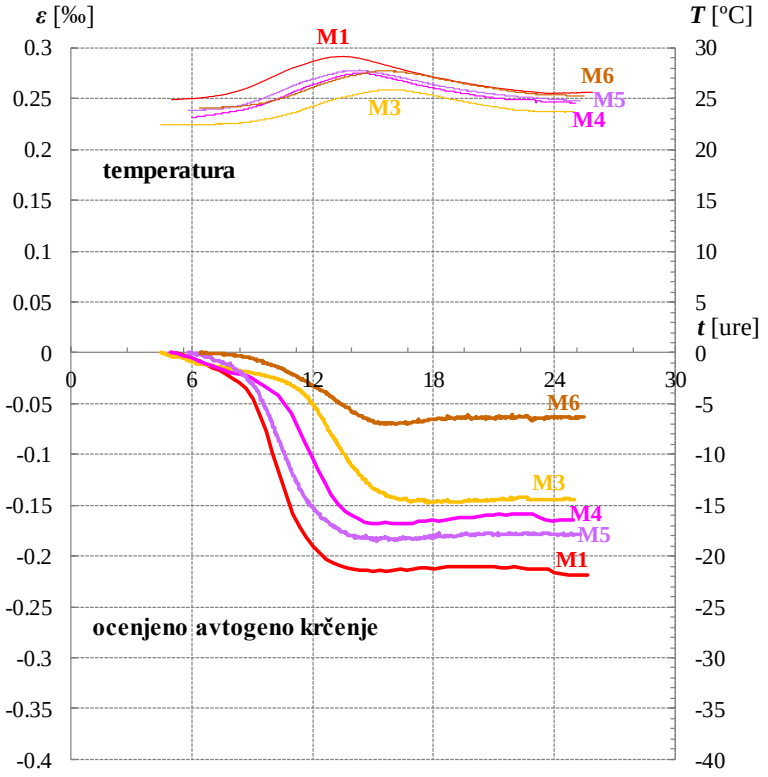

Slika 11*:* Časovni razvoj ocenjenega avtogenega krčenja in temperature preizkušancev iz mikroarmiranega betona visoke trdnosti in primerjalnega betona brez vlaken v prvih 24-ih urah po betoniranju

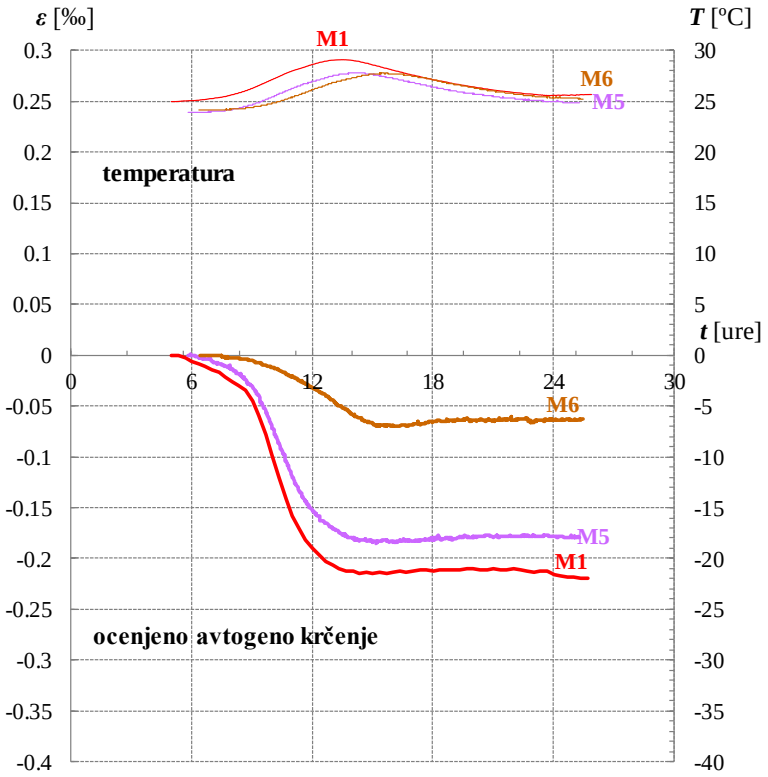

Slika 12*:* Časovni razvoj ocenjenega avtogenega krčenja in temperature preizkušancev iz mikroarmiranega betona visoke trdnosti z dodanimi suhimi M5 ali predhodno navlaženimi M6 polipropilenskimi vlakni in primerjalnega betona brez vlaken M1 v prvih 24-ih urah po betoniranju

4.2 Diskusija dobljenih eksperimentalnih rezultatov

V preiskovanih betonih visoke trdnosti z jeklenimi vlakni se je razvilo do 33% manjše krčenje v primerjavi s krčenjem primerljivega betona brez vlaken. Jeklena vlakna s kljukami na konceh omogočajo dober oprijem z betonom in so, v primerjavi s strjujočim se cementnim gelom, relativno toga. V zgodnjem obdobju znatno vplivajo na krčenje kompozita, ker s svojo sprijemnostjo med vlakni in cementnim gelom ter s svojo togostjo, ovirajo krčenje strjujočega se cementnega gela, ki se krči zaradi kapilarnih sil.

Polipropilenska vlakna so manj toga kot jeklena, zato je tudi vpliv na velikost krčenja manjši.

Pri vmešanju predhodno navlaženih vlaken v mešanico za beton visoke trdnosti se pojavita dva fizikalna učinka, ki ugodno delujeta na zmanjšanje deformacij zaradi avtogenega krčenja betona:

1. oviranje krčenja cementnega gela zaradi *togosti vlaken in sprijemnosti le teh z matrico*, ki je prisotno tudi pri uporabi suhih vlaken,

2. pri uporabi navlaženih vlaken se pojavi še ugoden učinek *dodatne rezerve vode*, ki je nakopičena v vlaknih, ki na kakršenkoli način zadržijo vodo in jo postopoma oddajajo v strjujočo se matrico v času hidratacije [11].

Znatno se učinek fibriliranih polipropilenskih vlaken lahko poveča, če ta pred vgradnjo, za 24 ur, namočimo v vodo. V betonu visoke trdnosti z omenjenimi vlakni se je razvilo le 30% zgodnjega ocenjenega avtogenega krčenja v primerjavi z ocenjenim avtogenim krčenjem primerljivega betona brez vlaken. Voda v predhodno navlaženih polipropilenskih vlaknih se zadržuje delno v poroznih vlaknih in delno v tri-dimenzionalnih porah, ki so med posameznimi vlakni, v snopičih fibriliranih vlaken [12].

Učinek dodatne rezerve vode v kompozitu je opazen tudi v primeru vgradnje predhodno namočenih celuloznih vlaken. Omenjeni kompozit je razvil za približno eno tretjino manjše zgodnje avtogeno krčenje glede na krčenje primerljivega betona brez vlaken.

Bazaltna vlakna imajo majhno togost, po namočenju zadržijo relativno malo vode in je njihova sprijemnost s cementnim gelom nizka. Predvidevamo, da bazaltna vlakna v preiskovanem kompozitu zato niso ublažila zgodnjega avtogenega krčenja le tega.

Iz ocenjenih krivulj časovnega razvoja avtogenega krčenja betona visoke trdnosti z vlakni, ki so prikazane na slikah 11, 12 in 13, je v času med dvanajsto in štiriindvajseto uro opazno rahlo zmanjšanje avtogenega krčenja betona in sicer med časom, ko je v betonu dosežena največja temperatura in časom, ko se temperatura betona izenači s temperaturo okolice. Ta fizikalni pojav je posledica termodinamičnega ravnovesja v porah cementnega kamna. Ko začne temperatura v betonu padati, se beton krči, s čimer se zmanjša tudi prostornina zaprtih por v cementnem kamnu. Zaradi zmanjšanja prostornine zaprte pore se po zakonih termodinamike poveča relativna vlažnost v pori,

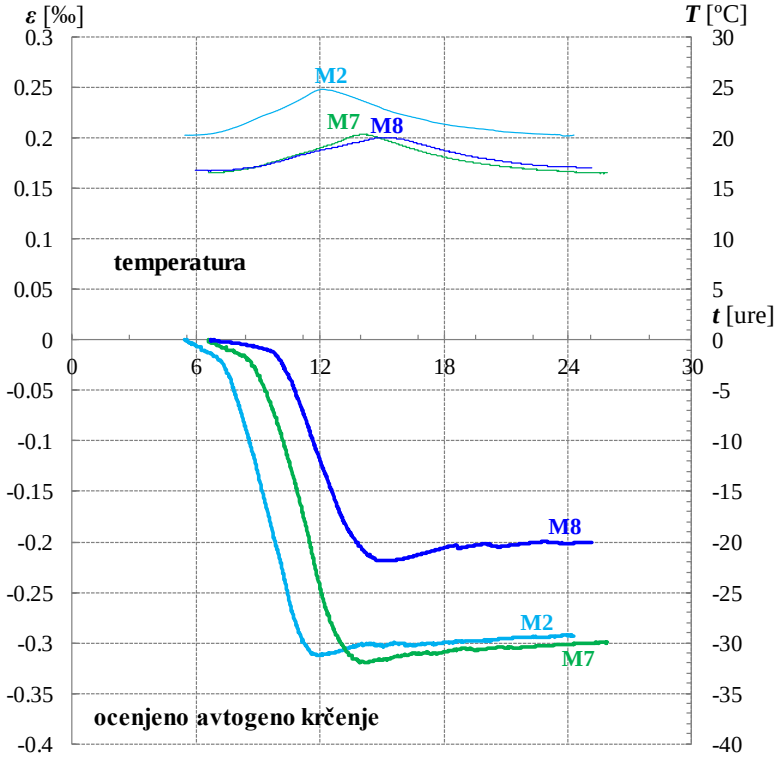

Slika 13*:* Časovni razvoj ocenjenega avtogenega krčenja in temperature preizkušancev iz kompozita visoke trdnosti z dodanimi predhodno navlaženimi bazaltnimi vlakni M7 in predhodno navlaženimi celuloznimi vlakni M8 in primerjalnega betona brez vlaken M2 v prvih 24-ih urah po betoniranju

kar zmanjša natezne sile, ki delujejo na stene pore to pa povzroči zmanjšanje avtogenega krčenja betona. Zaradi padca temperature zraka v zaprti pori, ob vzpostavitvi termodinamičnega ravnovesja, naraste relativna vlažnost zraka, kar povzroči še dodatno zmanjšanje avtogenega krčenja kompozita [7].

5 ZAKLJUČKI

Na podlagi rezultatov opravljenih eksperimentalnih raziskav zgodnjega avtogenega krčenja z jeklenimi, polipropilenskimi, bazaltnimi ali celuloznimi vlakni ojačenega betona visoke trdnosti in analize dobljenih rezultatov podajamo naslednje ugotovitve:

- Zmanjšanje zgodnjega avtogenega krčenja betonov visoke trdnosti z vlakni je močno odvisno od vrste uporabljenih vlaken.
- Vlakna v kompozitu vplivajo na velikost krčenja s svojo togostjo in/ali s sposobnostjo zadržanja vode med mešanjem in oddajanja le te v kompozit med procesom hidratacije.
- Glede oviranja krčenja betona v prvem dnevu po zabetoniranju so se, izmed vseh uporabljenih vlaken, izkazala kot najbolj učinkovita predhodno navlažena polipropilenska vlakna. Predvidevamo, da je manjše krčenje kompozita z vsebnostjo predhodno navlaženih polipropilenskih vlaken v primerjavi z betonom brez vlaken, posledica dveh vplivov in sicer togosti vlaken in sprijemnosti le-teh z matrico ter dodatne rezerve vode, ki je ujeta v vlaknih.
- Predhodno navlaženim polipropilenskim vlaknom glede ugodnega vpliva na velikost zgodnjega avtogenega krčenja kompozitov po vrstnem redu sledijo krajša jeklena vlakna, dolžine l=16mm, predhodno navlažena celulozna vlakna, daljša jeklena vlakna, dolžine l=30mm, suha polipropilenska vlakna in predhodno navlažena bazaltna vlakna.
- Pri prostorninskem deležu vlaken 0,75%, je vgradljivost kompozita, ne glede na vrsto uporabljenih vlaken, opazno zmanjšana.

LITERATURA

1. *Pfyl, T., Marti, P., Versuche an Stahlfaserverstärkten Stahlbetonelementen, ETH Zürich, 2001.*
2. *Institution of Civil Engineers, The technology of SFRC for practical applications, UK, Part 1, May 1974, pp 143-159.*
3. *Balaguru, P. N., Shah, S. P., Fiber-Reinforced Cement Composites, McGraw-Hill, Inc., New York, 1992.*
4. *Bentur, A., Mindess, S., Fiber Reinforced Cementitious Composites, Taylor and Francis, London and New York, 2007.*
5. *N. Banthia, R. Gupta, Influence of polypropylene fiber geometry on plastic shrinkage cracking in concrete, Cement and Concrete Research, Vol. 36 No.7, 2006, pp 1263-1267.*
6. *Barr, B., EL-Baden, A., Shrinkage of normal and high strength fibre reinforced concrete, Proceedings of the Institution of Civil Engineers, Structures & Buildings 156, 2003, 15-25.*
7. *Saje, D., Tlačna trdnost in krčenje betonov visoke trdnosti, Doktorska disertacija, 2001.*
8. *Bayasi, Z., Zeng, J., Properties of polypropylene fiber reinforced concrete, ACI Material Journal. Vol. 90(6), 1993, pp 605-610.*
9. *Saje, D., Bandelj, B., Lopatič, J., Saje, F., Notranja nega betona, v: Lopatič, J. (ur.), Saje, F. (ur.), Markelj, V. (ur.). Zbornik 30. zborovanja gradbenih konstruktorjev, 2008. Ljubljana: Slovensko društvo gradbenih konstruktorjev. 2008, str. 245-252.*
10. *JIS A 1129-1., Methods of test for length change of mortar and concrete, JIS Standards, Tokyo, 2001.*
11. *Saje, D., Reduction of the early autogenous shrinkage of high strength concrete. Advances in Materials Science and Engineering, 2015, str. 1-8, http://www.hindawi.com/journals/amse/2015/310641/.*
12. *Saje, D., Bandelj, B., Šušteršič, J., Lopatič, J., Saje, F., Shrinkage of polypropylene fibre reinforced high performance concrete. Journal of materials in civil engineering, ISSN 0899-1561, 2011, vol. 23, iss. 7, str. 941-952.*

Možnost uporabe mikroarmiranega betona za izdelavo zabojnika za NSRAO

Possibility of using fibre reinforced concrete for the production of the LILW disposal container

Jakob Šušteršič, Rok Ercegovič,

IRMA Inštitut za raziskavo materialov in aplikacije, Ljubljana

Franc Sinur, Boštjan Duhovnik

IBE Ljubljana

Aljoša Šajna

ZAG Ljubljana

Teja Török Resnik

Pomgrad Murska Sobota

Povzetek

Zabojnik za odlaganje z nizko in srednje radioaktivnimi odpadki (NSRAO) je bil razvit z uporabo samo-zgoščevalnega betona (SCC), ki zagotavlja dolgotrajne mehanske lastnosti in izjemno nizko prepustnost za tekočine. V članku so predstavljeni rezultati dodatnih raziskav, ki dopolnjujejo oceno obnašanja SCC med uporabo. Glavni poudarek je na predstavitvi in razpravi o rezultatih MA-SCC-JV (mikroarmiranega samo-zgoščevalnega betona z jeklenimi vlakni) v svežem in strjenem stanju. Iz teh rezultatov je razvidno, da obstaja možnost nadaljnjega izboljšanja lastnosti SCC in s tem zabojnika.

Abstract

The disposal container with low and intermediate level radioactive waste (LILW) was developed using self-consolidating concrete (SCC), which provides long term mechanical properties and extremely low permeability for liquids. In the paper, some results of additional investigations are presented, which complement the assessment of the behavior of SCC during use. The main focus is the presentation and discussion of the results of SFR-SCC (steel fiber reinforced - self-consolidating concrete) tests in fresh and harden state. From these results it can be seen that there is a possibility of further improving the properties of the SCC and thus the container.

Ključne besede: mikroarmirani samo-zgoščevalni beton z jeklenimi vlakni, samo-zgoščevalni beton, odlagalni zabojnik za NSRAO, posed-razlez, krčenje, cepile trdnosti
Keywords: steel fiber reinforced self-consolidating concrete, self-consolidating concrete, disposal container with LILW, slump-flow, shrinkage, split strengths

1. UVOD

SCC je bil razvit v okviru razvojnega projekta za izdelavo kontejnerja za odlaganje nizko in srednje radioaktivnih odpadkov (NSRAO). Uporablja se za izdelavo armiranobetonskih sten, dna in pokrova zabojnika. Poleg SCC sta bila razvita še naslednja dva kompozita:

1. polnilna malta za zapolnitev prostora med vstavljenimi sodi z NSRAO in notranjo površino zabojnika ter
2. tesnilna malta za zapiranje praznega prostora med malto za polnjenje in notranjo površino pokrova in za tesnjenje stika med pokrovom in zgornjo površino sten.

V okviru projekta so bile določene zahteve za lastnosti osnovnih materialov za pripravo kompozitov in za lastnosti vseh treh kompozitov (SCC, polnilne in tesnilne malte). Te zahteve so določene v Programu testiranja zabojnikov, meritev in preskusov [1]. Podane so tudi v članku Sinurja in Duhovnika [2]. Za pridobitev Slovenskega tehničnega soglasja (STS) je bilo potrebno razviti kompozite z lastnostmi, ki izpolnjujejo vse zahteve. Rezultati preskusov iz poročila Rezultati testiranja, meritev in preskusov zabojnikov [3] so pokazali, da so izpolnjene vse zahteve. Zabojniki s takimi kompoziti so bili izdelani[4] in testirani v preskuševališču v proizvodnem obratu Pomgrad v Lipovcih [5]

V tem članku so podane le kratke informacije o zabojniku in rezultatih preiskav SCC. V nadaljevanju so predstavljeni rezultati preiskav nekaterih ključnih značilnosti MA-SCC-JV, na podlagi katerih bi lahko ocenili možnost uporabe MA-SCC-JV za izdelavo zabojnika za odlaganje NSRAO.

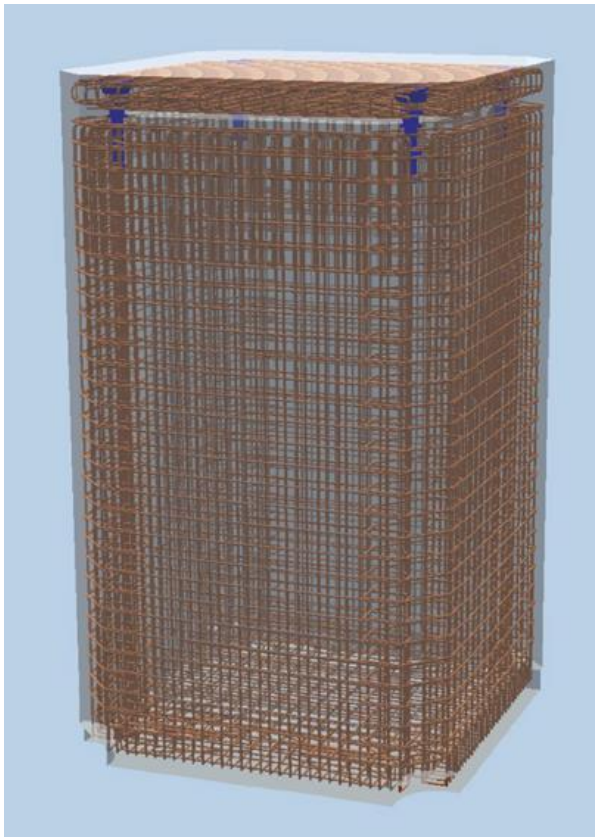

Slika 1. 3D pogled zabojnika z armaturo [2].

2. KRATKA INFORMACIJA O ODLAGALNEM ZABOJNIKU IN LASTNOSTIH SCC

V razvojnem projektu zabojnika za odlaganje z oznako N2d je sodelovala velika ekipa strokovnjakov IBE (odlagališče in projektant zabojnika), Pomgrad (proizvajalec prototipov zabojnika), ZAG in IRMA (sodelujoča inštituta v projektu).

2.1. Odlagalni zabojnik

Betonski zabojnik, kot eden najpomembnejših elementov inženirskega dela večstopenjskega sistema za preprečevanje prehoda radioaktivnih snovi iz odlagališča v okolje deluje kot: (a) biološki ščit v času pred odložitvijo, (b) mehanska zaščita NSRAO med skladiščenjem in odlaganjem, (c) osnovni element varnosti med izvajanjem transporta in internega transporta (premeščanja) NSRAO v zabojniku, (d) osnovni gabaritni kriterij v procesu priprave odpadkov na odlaganje in (e) osrednji predmet ravnanja z NSRAO na območju odlagalnega silosa.

Najpomembnejša in najbolj specifična zahteva za zabojnik je poleg odpornosti in stabilnosti proti vsem predvidenih obremenitev v fazi polnjenja in transporta pred končno odložitvijo tudi trajnost v pričakovani življenjski dobi 300 let.

Glede na znane okoljske razmere, katerim bodo zabojniki izpostavljeni po odlaganju v silosu, bodo zabojniki izpostavljeni karbonatizaciji v prvi fazi (v obdobju 2020 - 2061), po polnjenju in zapiranju silosa ter opustitvi. črpanje vode od leta 2062 dalje, bo silos z zabojniki izpostavljen podzemni vodi.

Zabojniki, pripravljeni za odlaganje, bodo prepeljani na odlagališče v skladu z določbami zahtev za prevoz nevarnega blaga po cesti (ADR) [6]. Določbe ADR [6] so bile uvedene v nacionalno zakonodajo z Zakonom o prevozu nevarnega blaga (ZPNB) [7]. Ta natančno določa, da je treba zabojnike za prevoz nevarnega blaga preskusiti z „drop testom“.

Skupno bo odloženih 950 zabojnikov tipa N2d z največjo dovoljeno maso 40 t. Zabojniki se odlagajo v silos s pomočjo portalnega dvigala in posebnih ročajev. Prazna mesta med zabojniki in zabojniki ter steno silosa se zapolnijo z betonom

2.1.1 Geometrijske značilnosti zabojnika N2d

Osnovna geometrija zabojnika je bila določena na osnovi vgradnje 4 TTC sodov. Zabojnik N2d je nadgradnja zabojnika N2b, ki se bistveno razlikuje le pri zasnovi pokrova in sidranja pokrova v armiranobetonski zabojnik.

Specifične rešitve zabojnika so podane v nadaljevanju in so rezultat razvoja zabojnika s pridobitvijo Slovenskega tehničnega soglasja (STS): (1) Zunanje mere (širina = 1,95 m, dolžina = 1,95 m, višina = 3,30 m), (2) debelina spodnje plošče = 23 cm, (3) debelina stene na vrhu = 20 cm, (4) debelina stene na dnu = 23 cm, (5) debelina pokrova = 20 cm, (6) masa prazne

Preglednica 1. Povprečni rezultati preskusov lastnosti svežega SCC**.**

Lastnost (merjena po standardu)	Povprečna vrednost
Posed – razlez (SIST EN 12350-8:2010)	680/710 mm
Gostota (SIST EN 12350-6:2009)	2393 kg/m^3
Vsebnost zraka (SIST EN 12350-7:2009, Poglavje 5)	2,0 %
w/c razmerje (SIST 1026:2016, Dodatek NC)	0,37

Preglednica 2. Povprečni rezultati preskusov lastnosti strjenega SCC.

Lastnost (merjena po standardu)	Povprečna vrednost
Tlačna trdnost pri 28 dneh (SIST EN 12390-3:2009)	86,0 MPa
Prodor vode pri 28 dneh (SIST EN 12390-8:2009)	3,0 mm
Krčenje do 182 dni (DIN 4227-Part 1)	0,374 mm/m
Odpornost proti zmrzovanju/tajanju/do 200 ciklov (SIST 1026:2016, Dodatek ND)	101,0 %
Modul elastičnosti pri 28 dneh (DIN 1048)	42500 MPa
Totalna poroznost (EN 1936: 2006)	10,85 %
Vsebnost kloridov (SIST EN 206: 2013, Poglavje 5.2.8)	0,070 %

posode s pokrovom = 14,92 t, (7) največja dovoljena masa polne posode = 40 t.

2.2 Nekatere lastnosti SCC

Da bi dosegli popolno polnjenje gosto armiranih elementov zabojnika (stene, dno in pokrov) (slika 1) [2], je bila v okviru razvojnega projekta razvita sestava SCC. SCC se je v elemente vgrajeval z neprekinjenim vlivanjem skozi cev [4]. Pri pripravi sestave SCC so upoštevana pravila za SCC, ki so določena v SIST EN 206: 2013.

V laboratoriju smo pripravili veliko število mešanic SCC, pri čemer smo spreminjali količine in razmerja posameznih komponent tako, da smo dobili mešanico, ki je bila primerna za izbrano metodo vgrajevanja. Povprečni rezultati meritev svežega in strjenega SCC so podani v preglednicah 1 in 2. Rezultati so v mejah zahtevanih vrednosti [2, 3].

2.2.1. Priraščanje tlačne trdnosti SCC s časom

Priraščanje tlačne trdnosti SCC, polnilne in tesnilne malte glede na čas je razvidno iz slike 2.

Priraščanje tlačne trdnosti pri zgodnejši starosti SCC in polnilna malta do 28 dni, je veliko bolj intenzivno kot v primeru starosti nad 28 dni. Podobno priraščanje modula elastičnosti SCC je bilo ugotovljeno v daljšem časovnem obdobju.

2.2.2. Merjenje avtogenega krčenja SCC.

Avtogeno krčenje je večje pri betonu visoke trdnosti ali betonu z nižjim razmerjem v/c [8]. Avtogeno krčenje betona, imenovano tudi hidratacijsko krčenje, je posledica samo-sušenja v porah cementnega kamna, ko se vode v porah porabi v procesu hidratacije cementa. Tako se avtogeno krčenje pojavi takoj, ko se začne postopek hidratacije cementa v betonu. Glede na vrsto betonske mešanice se postopek krčenja začne približno 2 do 24 ur po mešanju. Ker se v tem času že vzpostavi nega in je beton vgrajen v opažih, se izhlapevanje vode bistveno prepreči. V tem času pride do deformacij betona zaradi avtogenega krčenja in temperaturnih deformacij betona. Po končani negi se beton deformira - krči se zaradi izhlapevanja vode s površine betonskega elementa.

Meritve avtogenega krčenja so bile izvedene v skladu z japonskim standardom JIS A 1129 v laboratoriju Fakultete za gradbeništvo in geodezijo v Ljubljani. Na sliki 3 tanka črta prikazuje potek celotnega izmerjenega zgodnjega krčenja SCC. To je povprečna vrednost rezultatov meritev na treh prizmah z dimenzijami 10 × 10 × 40 cm. Razvoj temperature SCC kot funkcije časa je podan z rdečo črto (zgornji diagram). Potek ocenjene avtogene deformacije SCC je predstavljen z debelo linijo, ki se določi z odštetjem temperaturne deformacije betona od celotnega izmerjenega krčenja. Rezultati kažejo relativno majhno avtogeno krčenje SCC. Izmerjeno je tudi manjše krčenje SCC zaradi sušenja. Povprečno krčenje SCC pri starosti 182 dni je 0,374 mm / m.

V enem od prejšnjih raziskovalnih projektov [9] so bili opravljeni laboratorijski preskusi krčenja mikroarmiranega visoko zmogljivega betona z vsebnostjo 0,25 vol.%, 0,50 vol.% in 0,75 vol.% naslednjih vlaken: daljša (l = 32 mm, d = 0,5 mm) ali krajša (l = 16 mm, d = 0,5 mm) jeklena ali polipropilenska (l = 12 mm).

Na podlagi razprav o rezultatih izvedene eksperimentalne raziskave o krčenju visokozmogljivega betona, ki vsebuje polipropilenska ali krajša/daljša jeklena vlakna, je mogoče podati naslednje zaključke: (1) Skupno krčenje mikroarmiranega betona je bilo pri vseh preiskanih vsebnostih in vrstah uporabljenih vlaken manjše kot pri primerljivem betonu brez vlaken. Ob koncu merilnega obdobja je bilo celotno krčenje preiskovanega mikroarmiranega betona glede na vsebnost in vrsto uporabljenih vlaken približno 17% do 29% manjše kot pri primerljivem betonu brez vlaken. Razlike v skupnem krčenju mikroarmiranega betona z različnimi vsebnostmi in različnimi vrsta vlaken, so bile relativno majhne. 2) Za zmanjšanje zgodnjega avtogenega krčenja betona je uporaba jeklenih vlaken učinkovitejša kot uporaba suhih polipropilenskih vlaken. Pri uporabi jeklenih vlaken z vsebnostjo 0,25 vol.% ali 0,50 vol.% so daljša vlakna učinkovitejša, medtem ko so v primeru vsebnosti 0,75 vol.% krajša vlakna učinkovitejša. (3) Za zmanjšanje skupnega avtogenega krčenja pri vsebnosti vlaken 0,25 vol.% so najbolj učinkovita daljša jeklena vlakna, medtem ko so polipropilenska vlakna najmanj učinkovita. Pri vsebnosti vlaken 0,50 vol.% in 0,75 vol.% pa je relativno majhna razlika v učinkovitosti jeklenih in polipropilenskih vlaken pri zmanjšanju celotnega avtogenega krčenja. (4) Krčenje betona zaradi sušenja je pri vseh preiskanih vsebnostih in vrstah uporabljenih vlaken bistveno manjše od ustreznega krčenja zaradi sušenja primerljivega navadnega betona brez vlaken.

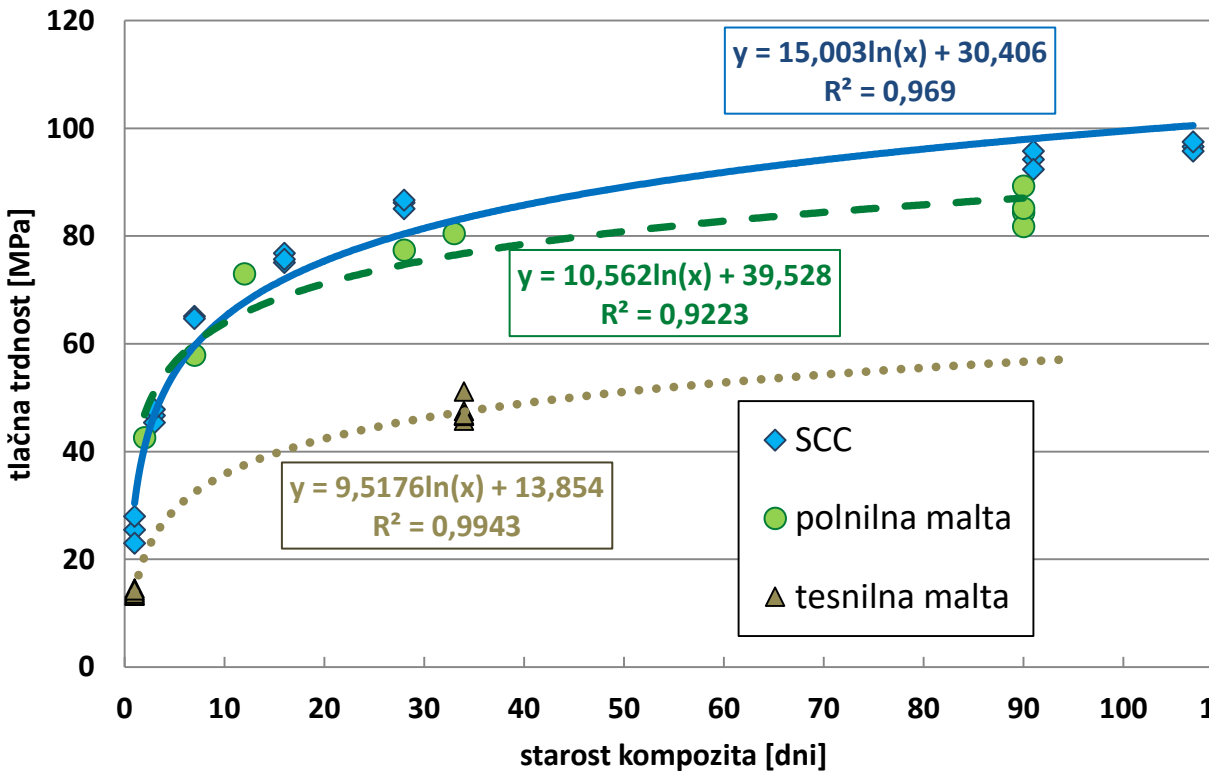

Slika 2. Tlačna trdnost SCC, polnilne in tesnilne malte v odvisnosti od starosti kompozita.

3. SFR-SCC

V nadaljevanju laboratorijskih preiskav so se pripravili in raziskali MA-SCC-JV (mikroarmirani samo-zgoščevalni betoni z jeklenimi vlakni). Dodane so bile različne količine (0,25, 0,5, 0,75 in 1 vol.%) jeklenih vlaken s sidri, enake dolžine 16 mm in različne debeline (premeri presekov) 0,50 , 0,40 in 0,35 mm. Tako so znašali faktorji oblike (razmerje med dolžino in premerom vlakna) l/d = 32, 40 in 46.

V tem članku so podane samo informacije in nekateri rezultati raziskav MA-SCC-JV. Cilj je bil ugotoviti možni potencial za nadaljnje izboljšanje obnašanja odlagalnega zabojnika med uporabo, zlasti z zagotavljanjem njegove dolge življenjske dobe.

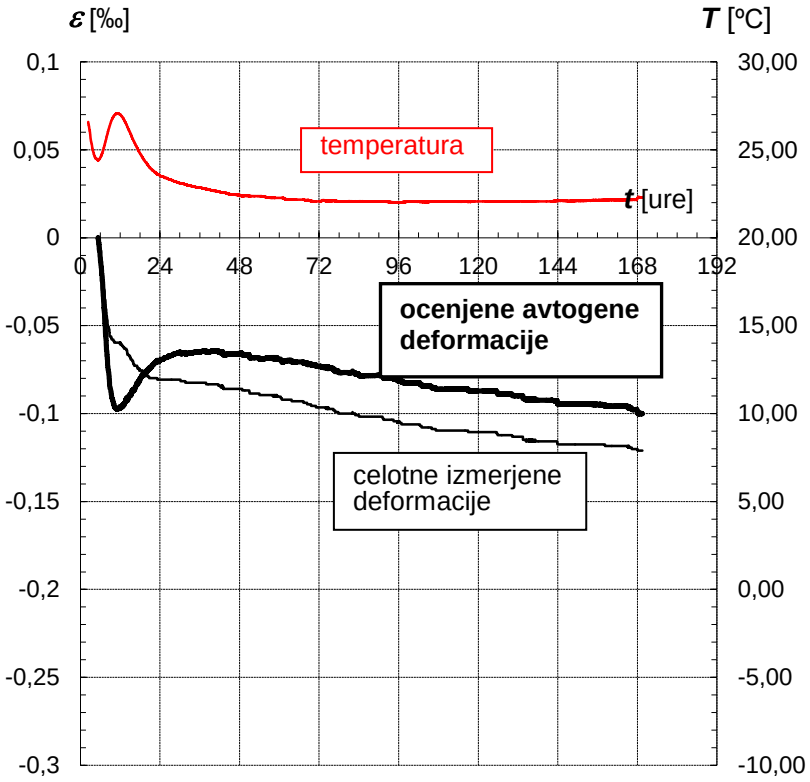

Slika 3. Rezultati merjenja avtogenega krčenja SCC do 7 dni po mešanju.

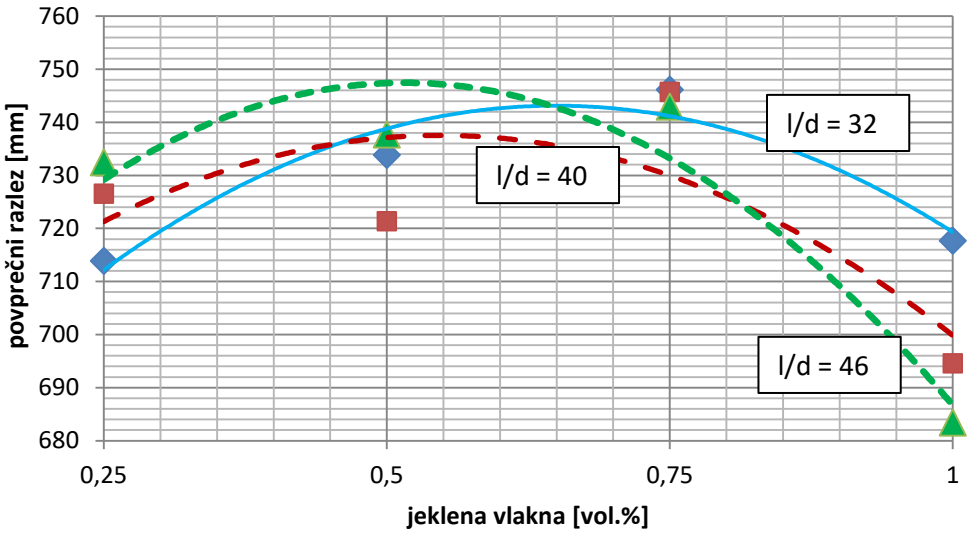

Slika 4. Povprečni razlez svežega MA-SCC-JV v odvisnosti od vsebnosti vlaken njihovega faktorja oblike.

3.1 Preiskave svežega MA-SCC-JV

Izvedeni so bili isti preskusi svežega MA-SCC-JV kot za svež SCC. Preiskovalo se je, kako količina vlaken in njihovi faktorji oblike vplivajo na obdelovalnost in vgradljivost MA-SCC-JV. V tem članku so podani le rezultati preskusa poseda/razlez. Meril se je povprečni razlez svežega MA-SCC-JV po standardu SIST EN 12350-8. Dobljeni rezultati so prikazani na sliki 4, v odvisnosti od količine dodanih vlaken in njihovega faktorja oblike (l/d = 32, 40 in 46).

Rezultati kažejo, da vlakna v količini do 0,75 vol.% ne vplivajo na obdelovalnost in vgradljivost svežega MA-SCC-JV. Nekateri rezultati kažejo, da prisotnost vlaken celo izboljša obdelovalnost, kot da bi vlakna povečala notranjo "drsenje" sveže MA-SCC-JV mase in ne ovirajo njene obdelovalnosti - pretočne sposobnosti, kot se dogaja pri večji količini daljših vlaken. Obdelovalnost svežega MA-SCC-VL se rahlo zmanjša, če se doda 1 vol.% vlaken. Zmanjšanje obdelovalnosti je večje, če se uporabljajo vlakna z večjim faktorjem oblike.

3.2. Preiskave strjenega MA-SCC-JV

Glavni namen dodajanja vlaken betonu je povečanje njegove duktilnosti, žilavosti in odpornosti proti širjenju razpok. Izvaja se več vrst preskusov. Ta članek bo podal le nekaj rezultatov preskusa cepitve s klinom (WST).

WST je preskusna metoda za izvajanje stabilnih preskusov mehanike loma na betonskih in betonu podobnih materialih. Predlagali so jo Brühwiler in Wittman [10] ter Linsbauer in Tschegg [11]. Metodo, ki sta jo predlagala zadnja avtorja [11], se je uporabila v teh in v prejšnjih [12-14] raziskavah, da bi dobili diagrame obtežba - CMOD. Ekvivalentne trdnosti do izbrane širine razpok (CW = 0,1, 0,2, 0,3 in 0,4 mm) se izračunajo z enačbo, pri kateri se uporabljajo parametri, ki izhajajo iz diagrama obtežba - CMOD.

Preskusi po metodi WST so bili izvedeni na kockah z dolžino roba 150 mm in z začetno globino zareza 50 mm, pri starosti 28 dni. Princip preskusne metode je prikazan na sliki 5 [15].

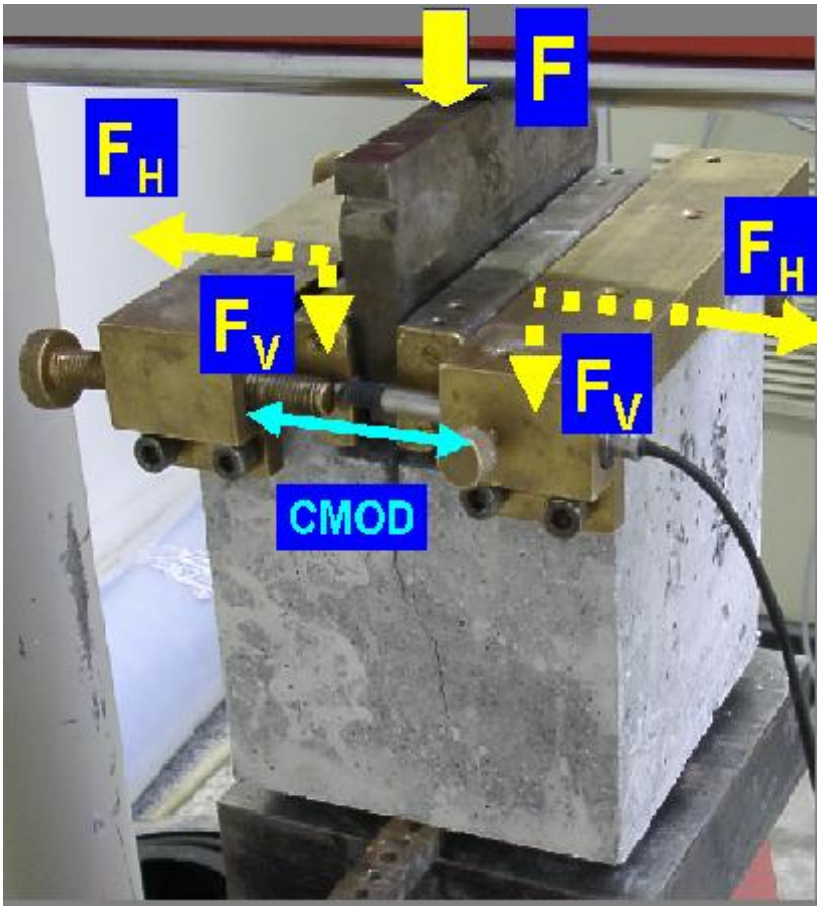

Slika 5. Princip WST metode [15].

Preglednica 3. Povprečni rezultati trdnosti SCC in MA-SCC-JV dobljeni z WST

	f_{FC} (MPa)	f_{ct} (MPa)	$f_{0,1}$ (MPa)	$f_{0,2}$ (MPa)	$f_{0,3}$ (MPa)	$f_{0,4}$ (MPa)
SCC	2,8	3,2	2,7	2,2	1,8	1,5
MA-SCC-JV z 1 vol.% vlaken z l/d = 30	4,9	5,7	4,5	4,9	4,9	4,8
MA-SCC-JV z 1 vol.% vlaken z l/d = 40	5,2	6,1	5,0	5,2	5,4	5,5

Karakteristična diagrama obtežba - CMOD za SCC brez vlaken in MA-SCC-JV z 1 vol.% jeklenih vlaken z l/d = 30 sta podana na sliki 6.

Obstaja zelo velika razlika med površinami pod diagrami, ki predstavljajo količino absorbirane energije SCC in MA-SCC-JV med preskusom. Iz teh diagramov se izračunajo naslednje trdnosti: končna trdnost f_{ct}, trdnost pri prvi razpoki f_{FC} in ekvivalentne trdnosti do izbrane širine razpoke (CW = 0,1, 0,2, 0,3 in 0,4 mm). Za SCC, MA-SCC-JV z 1 vol.% jeklenih vlaken z l/d = 30 in 40 so podane povprečne vrednosti teh trdnosti v preglednici 3.

Povprečne končne trdnosti f_{ct} so prikazane na sliki 7, v odvisnosti od faktorja oblike l/d (faktor oblike l/d = 0 ima SCC brez vlaken).

Povprečna trdnost pri prvi razpoki f_{FC} in ekvivalentne trdnosti do izbrane širine razpoke f_{CW} so podane na sliki 8, v odvisnosti od širine razpoke (CW = 0, 0,1, 0,2, 0,3 in 0,4 mm). Trdnost pri prvi razpoki f_{FC} se določi v trenutku, ko nastane razpoka in je njena širina 0.

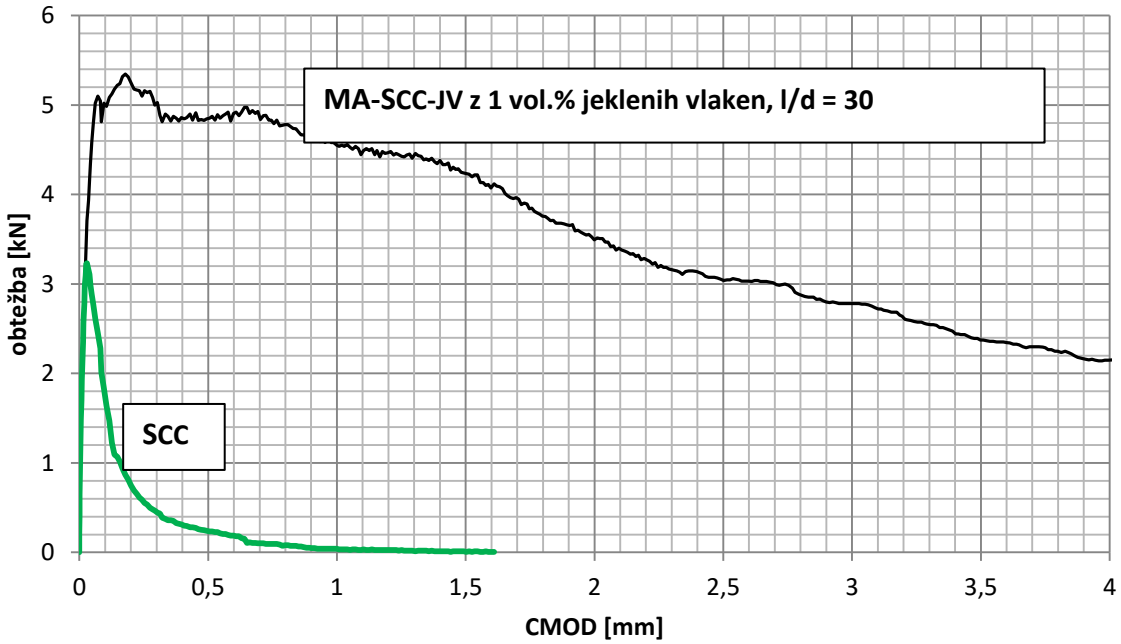

Slika 6. Karakteristična diagrama obtežba – CMOD za SCC brez vlaken in MA-SCC-JV z 1 vol.% jeklenih vlaken z l/d = 30.

Iz povprečnih rezultatov trdnosti (preglednica 3, sliki 7 in 8) je razvidno, da so te pri MA-SCC-JV precej višje kot pri SCC. Vlakna pomembno vplivajo na obnašanje betona po nastanku prve razpoke. Pri preskušanju SCC brez vlaken so se s povečevanjem širine razpoke zmanjševale ekvivalentne trdnosti – prišlo je do »mehčalnega« odziva (slika 8). Po drugi strani pa je pri preskušanju MA-SCC-JV prišlo »strjevalnega« odziva, ekvivalentne trdnosti so se povečevale s povečevanjem širine razpoke (slika 8). To še posebej velja, kadar so uporabljena vlakna z večjim faktorjem oblike (l/d = 40).

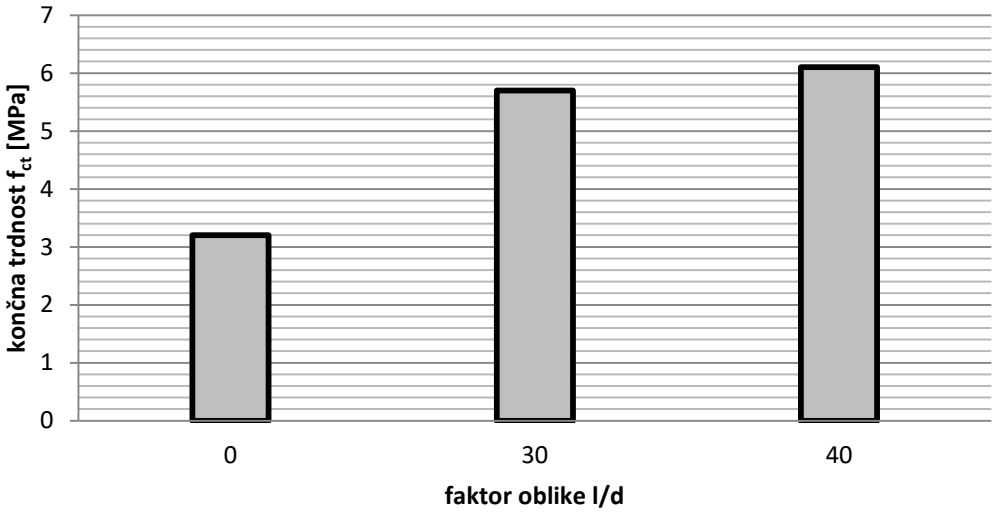

Slika 7. Povprečne končne trdnosti f_{ct} v odvisnosti od faktorja oblike l/d.

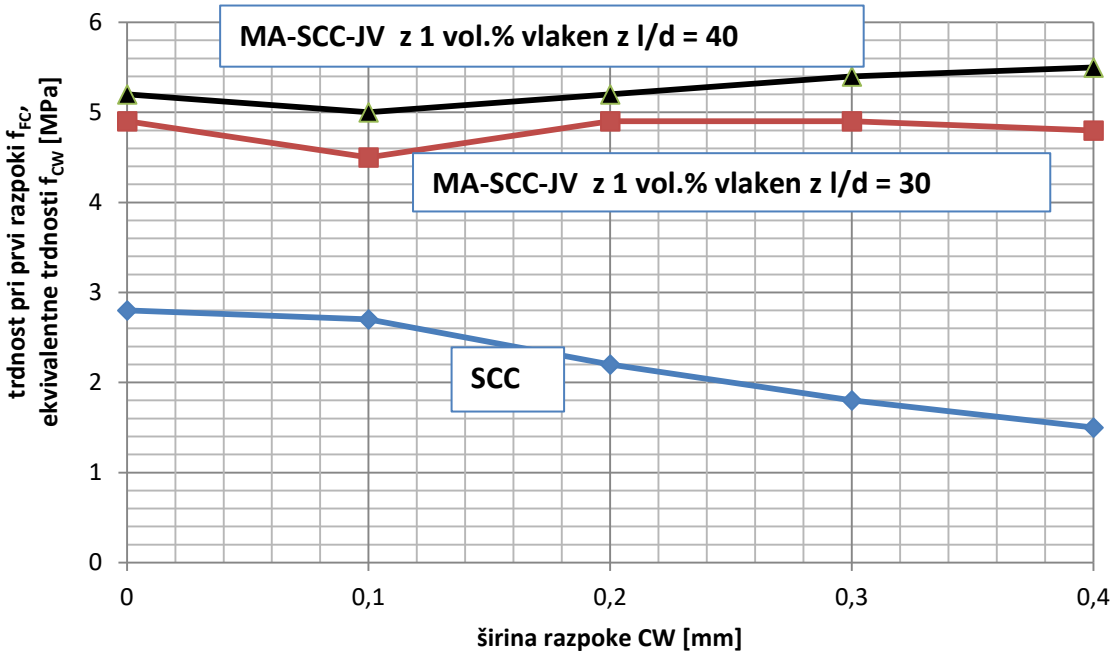

Slika 8. Povprečna trdnost pri prvi razpoki f_{FC} in ekvivalentne trdnosti do izbrane širine razpoke f_{CW} v odvisnosti od širine razpoke (CW = 0, 0,1, 0,2, 0,3 in 0,4 mm).

3 ZAKLJUČEK

SCC, katerega sestava je bila razvita v okviru razvojnega projekta zabojnika za odlaganje NSRAO, kaže lastnosti (v svežem stanju), ki zagotavljajo dobro obdelovalnost in zgoščenost v stenah, dnu in pokrovu zabojnika, kljub veliki količini armaturnih palic. Podobno obnašanje je bilo ugotovljeno v svežem MA-SCC-JV, kljub dodanim vlaknom. Nekateri rezultati kažejo, da prisotnost vlaken v količini do 0,75 vol.% celo izboljšajo obdelovalnost, kot če bi vlakna povečevala notranjo "drsenje" sveže mase MA-SCC-JV in ne ovirajo njegove obdelovalnosti - pretočnosti.

Dobljeni rezultati meritev avtogenega krčenja in krčenja zaradi sušenja SCC kažejo, da ni tveganja za razpokanost, seveda, pod pogojem, da se izvede dobra nega vgrajenega SCC. Rezultati predhodnih eksperimentalnih raziskav o krčenju visoko zmogljivega mikroarmiranega betona pa kažejo, da je celotno krčenje mikroarmiranega betona manjše od primerljivega betona brez vlaken. Za zmanjšanje zgodnjega avtogenega krčenja visoko zmogljivega mikroarmiranega betona je učinkovitejša uporaba kratkih jeklenih vlaken (dolžine 16 mm) z vsebnostjo 0,75 vol.% kot uporaba daljših vlaken (dolžine 32 mm).

Ena od bistvenih ugotovitev raziskav je, da je bil dobljen »strjevalni« odziv MA-SCC-JV z 1 vol.% vlaken, medtem ko je bil dosežen »mehčalni« odziv, ko se je preiskoval SCC brez vlaken. To še posebej velja, kadar se uporabljajo vlakna z večjim faktorjem oblike.

Na podlagi dosedanjih rezultatov raziskav lahko sklepamo, da obstaja možnost povečanja odpornosti SCC proti širjenju razpok z dodajanjem določene količine jeklenih vlaken, brez poslabšanja obdelovalnosti in vgradljivosti SCC, ki bi se uporabljal za izdelavo zabojnika za odlaganje NSRAO.

LITERATURA

1. *S Duhovnik, B., Kavnik, T., Šušteršič, J., Šajna. A. (2017) Program testiranja zabojnikov, meritve in preskusi, potrebni za certificiranje zabojnika, Št. NRVB-POM_Program, Murska Sobota, Pomgrad.*
2. *Sinur, F. & Duhovnik, B. (2018) Odlagalni zabojnik za nizko- in srednjeradioaktivne odpadke. Zbornik 25. Slo. kolok. o betonih (str. 53-60). Ljubljana, IRMA.*
3. *Török Resnik, T, Šušteršič, J., Šajna, A., Kavnik, T., Sinur, F. (2017) Rezultati testiranj zabojnikov, meritve in preskusi, potrebni za certificiranje zabojnika, Št. NRVB-POM_Rezultati, Murska Sobota, Pomgrad.*
4. *Török Resnik, T., Kavnik, T. (2018) Odlagalni zabojnik za odlaganje nizko in srednje radioaktivnih odpadkov (NSRAO): Izdelava prototipov zabojnikov in testiranje padcev zabojnikov, Zbornik 25. Slo. kolok. o betonih (str. 61-68). Ljubljana, IRMA.*
5. *Bohinc,U., Robič, S., Šajna, A. (2018) Preskus padca AB zabojnika za odlagališče NSRAO in vrednotenje poškodb, Zbornik 25. Slo. kolok. o betonih (str. 79-87). Ljubljana, IRMA.*
6. *European Agreement concerning the International Carriage of Dangerous Goods by Road (ADR); http://www.unece.org/trans/danger/publi/adr/adr2017/17contentse0.htlm.*
7. *Zakon o prevozu nevarnega blaga (ZPNB), Ur.l. UPB1 33/06, 41/09, 97/10.*
8. *Saje, D. (2005) Krčenje betona visokih trdnosti v prvih dneh po vgraditvi, Zbornik 12. Slo. kolok. o betonih (str. 41-48). Ljubljana, IRMA.*
9. *Saje, D., Bandelj, B., Šušteršič, J., Lopatič, J., Saje F. ((2012) Autogenous and Drying Shrinkage of Fibre Reinforced High-Performance Concrete. Journal of advanced concrete technology, Feb. 2012, Vol. 10, No. 2, str. 59-73*
10. *Brühwiler E., Wittman F.H. (1988) The Wedge Splitting Test, a New Method of Performing Stable Fracture Mechanics Tests. Fracture and Damage of Concrete and Rock. Pergamon Press. 1988. Ed. H.P. Rossmanith. (str. 117 – 125).*
11. *Linsbauer H., Tschegg, E.K. (1986) 'Die Bestimmung der Bruchenegie an Würfelproben' (Fracture Energy Determination of Concrete with Cube-Shaped Specimens). Zement und Beton, 31 1, (str. 38 – 40).*
12. *Šušteršič J., Kolenc M., Zajc A., Riček F., Zajc P.M. (1999) High-Performance Fibre Reinforced Concrete for Mine Roadway Support Panels. Proceedings, Second CANMET/ACI International Conference Gramado, RS, Brazil,. SP-186. (str. 101 – 112).*
13. *Šušteršič, J., Ukrainczyk, V., Zajc, A., Šajna, A. (2001) Evaluation of Crack Opening Resistance of SFRC. Concrete Under Severe Conditions. Vol. 2.*

Vancouver.. Eds. N. Banthia, K. Sakai, O.E. Gjørv. (str. 1594 – 1601).

14. *Šušteršič J., Zajc A., Leskovar I., Dobnikar V. (2003) Improvement in the crack opening resistance of FRC with low content of short fibres. Ed.: Dhir, Ravindra K. Role of concrete in sustainable development : proceedings of the International Symposium dedicated to professor Surendra Shah, Northwestern University, USA held on 3-4 September 2003 at the University of Dundee, Scotland, UK. London: ″Thomas Telford″, str. 167-174.*
15. *Tschegg, E.K. 'New Equipments for Fracture Tests on Concrete'; Materialprüfung 33 (1991) 11 - 12, München, 1991, str. 338 - 342.*

Ocena trajnosti prednapetih železniških pragov iz mikroarmiranega betona

Estimation of the durability of prestressed railway sleepers from fiber reinforced concrete

Andrej Zajc, Jakob Šušteršič in David Polanec

IRMA Inštitut za raziskavo materialov in aplikacije, Ljubljana

Povzetek

V članku se obravnava problematika trajnosti prednapetih železniških pragov iz mikroarmiranega betona (PŽP-MAB). Na kratko je opisan razvoj teh pragov do poskusne proizvodnje in vgradnje v poskusno polje, ki je v uporabi že 23 let. Z občasnimi pregledi se spremlja obnašanje PŽP-MAB med uporabo. Ugotavlja se, da do sedaj ni bilo opaziti razpok, še posebno na mestih nastopa največjih nateznih napetosti. Na nekaj PŽP-MAB pa so bile ugotovljene poškodbe na spodnjem delu zaradi abrazijskih in udarnih obremenitev, do te mere, da so morali biti odstranjeni s proge. Za ta problem obstaja rešitev, ki bi se morala upoštevati pri proizvodnji PŽP-MAB, v kolikor bi bila vzpostavljena ta proizvodnja.

Abstract

The paper deals with the problem of the durability of prestressed railway sleepers from fiber reinforced concrete (PRS-FRC). The development of these spleepers is briefly described up to experimental production and installation into the test field, which has been in use for 23 years. Periodic reviews monitor the behavior of the PRS-FRC during use. It is noted that until now no cracks have been observed, especially in the places where the greatest tensile stresses occur. On some PRS-FRC, damage to the lower part was detected due to abrasion and impact loads, to the extent that they had to be removed from the line. There is a solution for this problem, which should be taken into account in the production of the PRS-FRC, insofar as this production would be established.

Ključne besede: prednapeti betonski železniški prag, mikroarmirani beton, jeklena vlakna, razpoke, odpornost proti abraziji, odpornost proti udaru
Keywords: prestressed concrete railway sleeper, fiber reinforced concrete, steel fibers, cracks, abrasion resistance, impact resistance

1. UVOD

Razvoj novega betonskega železniškega praga v sodelovanju s Salonit Anhovo je potekal v okviru razvojno-raziskovalnega projekta, ki ga je financiralo Ministrstva za znanost in tehnologijo [1 - 4]. Potreba po razvoju visokozmogljivega betonskega praga so nakazale meritve in raziskave, ki so se izvajale na progovnih odsekih v Sloveniji, kjer so bili betonski železniški pragovi vgrajeni že nekaj let in niso vzdržali eksploatacijskih obremenitev. Razpoke so se zelo pogosto pojavile na srednjem delu praga, zgoraj, kot je razvidno iz slike 1 [5].

Rezultati preskusov novo razvitega prednapetega železniškega praga iz mikroarmiranega betona (PŽP-MAB) so pokazali, da ima bistveno izboljšane mehanske lastnosti v primerjavi s prednapetimi betonskimi pragovi, ki so se uporabljali pri nas in drugih državah.

Poleg številnih preiskav karakteristik uporabljenih materialov so bile izvršene tudi preiskave samega praga. Diagram v sliki 2 prikazuje obnašanje praga pri tri točkovni upogibni preiskavi, kot je bila predvidena s takratnim veljavnim pravilnikom.

V trenutku pojava prve razpoke so preskušani PŽP-MAB prenesli koncentrirano obtežbo okoli 80 kN (po takrat veljavnem pravilniku je bila minimalna zahtevana koncentrirana obtežba v sredini pri pojavu prve razpoke 38 kN) pri deformaciji praga približno 3 mm.

Ker so mehanske lastnosti praga direktno povezane s sestavo betona, iz katerega je izdelan, je možno prirejati mehanske lastnosti PŽP-MAB potrebam. To pomeni, da bi se lahko za potrebe železnice izdelovalo več vrst pragov v odvisnosti od zahtev na progah, v katere bi železnica pragove vgradila.

2.0 MAB – SESTAVA IN NEKATERE LASTNOSTI V STRJENEM STANJU

2.1 Sestava MAB

Za izdelavo prototipnih pragov se je uporabljala sestava MAB, ki je bila določena v okviru obsežnih laboratorijskih preiskav, njena dokončna sestava pa se je določila med poskusno proizvodnjo, pri kateri so posamezni parametri variirali med naslednjimi vrednostmi:

(a)

(b)

Slika 1(a), (b): Tipične razpoke na prednapetih betonskih pragih [5]

Preglednica 1: Povprečne vrednosti rezultatov preskusov lastnosti 90 dni starega MAB in betona brez vlaken

lastnost		MAB	beton brez vlaken
tlačna trdnost	(MPa)	95,0	84,0
tlačna trdnost pri starosti 1 dan	(MPa)	44,5	39,6
upogibna natezna trdnost	(MPa)	8,7	7,5
udarna žilavost po Charpy-jevi metodi	(kJ/m^2)	18,4	10,9
odpornost proti obrusu po Böhmejevi metodi	($cm^3/50cm^2$)	11,9	14,3

- cement = 300 – 340 kg/m^3,
- $(v/c)_{ef}$ = 0,35 – 0,38,
- jeklena vlakna (z dolžino 32 mm in premerom 0,5 mm) = 0,50 – 0,63 vol.%,
- mineralni dodatek = 8,5 – 10,0 mas.% na vsebnost cementa,
- kemijski dodatek = 2,0 – 3,0 mas.% na vsebnost cementa,
- poroznost = 2,0 – 3,0 vol.%.

Uporabljal se je eruptivni agregat z D_{max} = 16 mm.

2.2 Primerjava med nekaterimi lastnostmi strjenega MAB in betonom brez vlaken

Vpliv dodanih vlaken na mehanske lastnosti strjenega MAB je razviden iz preglednice 1, kjer so podane povprečne vrednosti rezultatov preskusov lastnosti 90 dni starega MAB in betona brez vlaken.

2.3 Odpornost proti utrujanju

Prizme dimenzij 10×10×40 cm so bile v več fazah preiskovane po naslednjem vrstnem redu: statični in dinamični modul elastičnosti, upogibne karakteristike pri statični obremenitvi z risanjem delovnega diagrama obtežba – upogib, iz katerega je bila, poleg drugih parametrov, določena obtežba pri prvi razpoki F_b.

Nato so sledile preiskave odpornosti proti utrujanju z naslednjimi parametri: $F_{max} = 0,7 – 0,9 \times F_b$, $F_{min} = 0,1\ F_b$, število ciklov N = 10.000, hitrost nanašanja obtežbe je znašala 1 cikel v sekundi.

Po utrujanju so se isti preskušanci preiskovali glede na statični in dinamični modul elastičnosti ter upogibne karakteristike, kot pred utrujanjem. Pri statičnem obremenjevanju prizme na upogib in pri utrujanju je

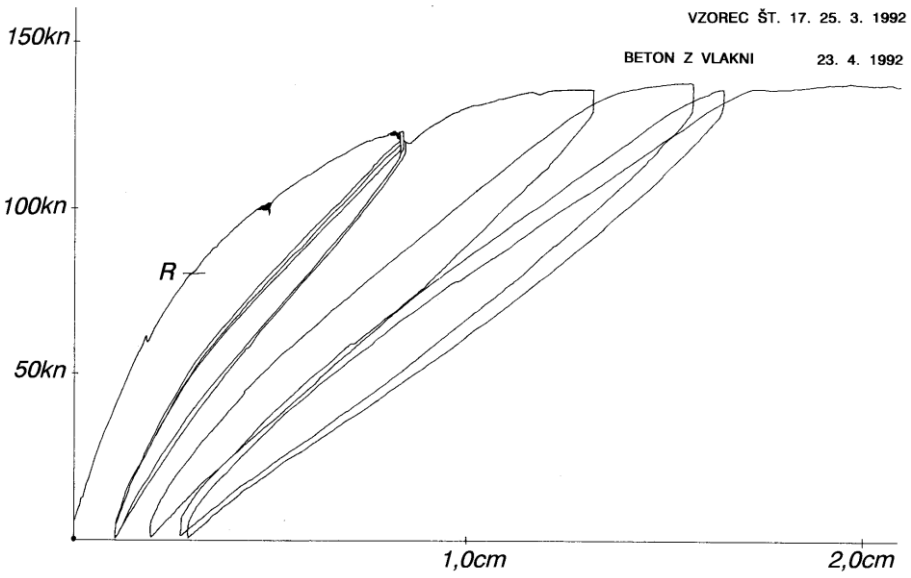

Slika 2: Značilni diagram obtežba – upogib, dobljen s preskusom PŽP-MAB.

delovala točkovna obtežba na sredini medsebojne razdalje podpor l = 30 cm.

Iz rezultatov je razvodno, da sta se po utrujanju statični in dinamični modul zmanjšala, pri večini preskušancev pa se je absorbirana energija po prvi razpoki povečala (slika 3). V trenutku nastanka prve razpoke se aktivirajo v betonu vgrajena vlakna, kar privede do povečanja žilavosti in odpornosti MAB proti utrujanju.

3.0 STATIČNA ZASNOVA PŽP-MAB

Upoštevajoč možnosti in omejitve, ki jih nudita MAB in oblika praga je bila statična zasnova definirana na naslednji način:

1. kakovostne značilnosti MAB omogočajo uporabo le štirih vrvi za prednapenjanje;
2. sledeč obliki praga, vrvi za prednapenjanje potekajo prostorsko poligonalno, razen v srednji tretjini praga, kjer so med seboj vzporedne in zagotavljajo enak pozitivni in negativni moment v trenutku nastanka prve razpoke;
3. poligonalni potek vrvi v predelih praga pod tirnicama zagotavlja poleg vzdolžne tudi prečno tlačno napetost zaradi prednapenjanja in s tem zmanjšuje vpliv prečnih deformacij, kar je tudi sicer značilnost MAB (efekt velikega števila drobnih stremen);
4. doseganje visokih začetnih tlačnih trdnosti MAB omogoča, ob upoštevanju manjših prečnih deformacij MAB, uporabo večjih sil prednapenjanja, kar v kritičnem srednjem prerezu zagotavlja višjo začetno tlačno napetost in s tem večjo deformacijo v trenutku nastanka prve razpoke.

4.0 VGRADNJA PŽP-MAB V POSKUSNO POLJE

Zaradi poligonalnega poteka kablov in oblike naležne ploskve je bil razvit tudi nov stroj za proizvodnjo takih pragov, ki omogoča istočasno vibriranje betona, prednapenjanje vrvi in oblikovanje naležne ploskve. Delovanje stroja je bilo preskušeno pri polindustrijski proizvodnji 1000 kosov pragov. V nadaljevanju projekta je sledila vgraditev pragov izdelanih v okviru polindustrijske proizvodnje v železniško progo in vzpostavljeno je bilo opazovanje z vstavljenimi merskimi celicami v nekatere pragove.

V sklopu remonta desnega tira na odseku Borovnica – Verd, na železniški progi Ljubljana – Sežana so bili v letu 1996 poskusno vgrajeni PŽP-MAB in sicer v Km 587+363/837, v krivini z R = 500 m. Preko pragov, ki so vgrajeni na medsebojni razdalji 60 cm, so položene tirnice oblike UIC 60 s Pandrol pritrditvijo (slika 4).

Gramozna greda je bila v celoti odstranjena ter nadomeščena z novo iz tolčenca. Pod gramozno gredo je vgrajena tamponska plast debeline 50 cm. Maksimalna hitrost vlakov na obravnavanem odseku znaša 80 km/h, kategorija proge pa je D3 (225 kN osnega pritiska ter 7,2 kN/m).

5.0 PROGRAM MARITEV VGRAJENIH PŽP-MAB V POSKUSNO POLJE

Z namenom opazovanja obnašanja poskusnih PŽP-MAB v železniški progi so bili v 4 pragove med poskusno proizvodnjo vgrajeni merilni lističi za meritev deformacij. Po 90 dneh starosti so bile izvedene umeritvene preiskave, ki bi pri meritvah v eksploataciji omogočile definiranje dejansko nastopajočih obremenitev v pragih skozi daljše obdobje uporabe.

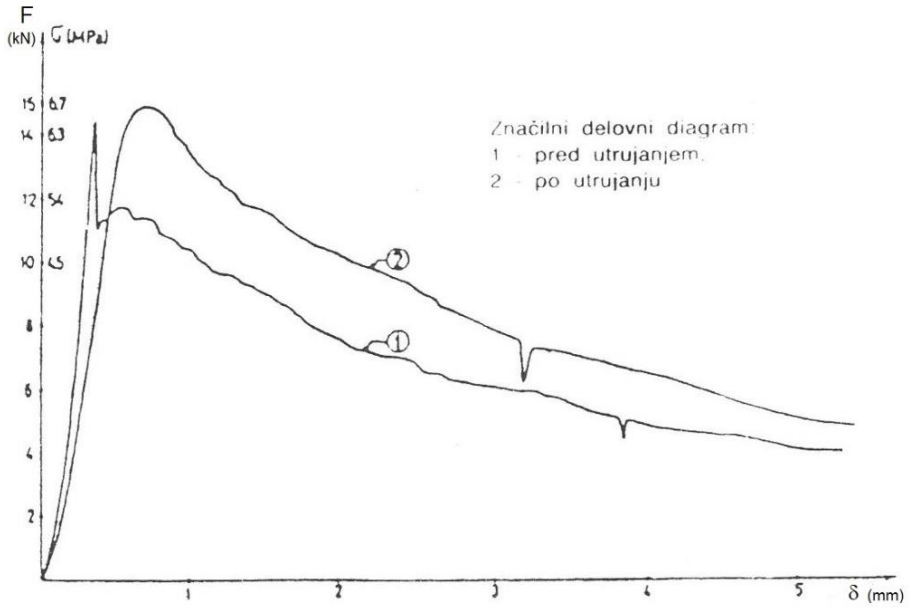

Slika 3: Značilna delovna diagrama obtežba – upogib (F – δ), dobljena pri tri točkovnem upogibnem preskusu, pred utrujanjem (1) in po utrujanju (2).

Nadalje je program opazovanja predvideval, da bi se lahko s temi meritvami ovrednotili vplivi obrabljanja gramozne grede med dvema podbijanjima ter efekti zmanjšanja obremenitev, ki naj bi se pokazali po izvedbi podbijanja. Poleg tega bi bile merljive tudi maksimalne obremenitve, ki lahko nastopijo v eksploataciji ter njihova povprečna pogostost v odvisnosti od časovnega zamika med dvema vzdrževalnima cikloma.

Zaradi navedenega bi morale meritve potekati daljši čas, predvidoma najmanj 6 mesecev. Trajanje opazovanja pa je v osnovi odvisno od: (1) kakovosti dobljenih rezultatov, (2) stanja merilnih lističev, ki so vgrajeni v pragih in (3) stanja električnih vodov, preko katerih se meritve izvajajo.

Pri vsem tem pa je in bo obstajal osnovni pogoj – zagotovljena morajo biti zadostna sredstva za izvedbo meritev in vrednotenje dobljenih rezultatov. Za izvedbo

Slika 4: Pritrjene trnice oblike UIC 60 na PŽP-MAB s Pandrol pritrditvijo.

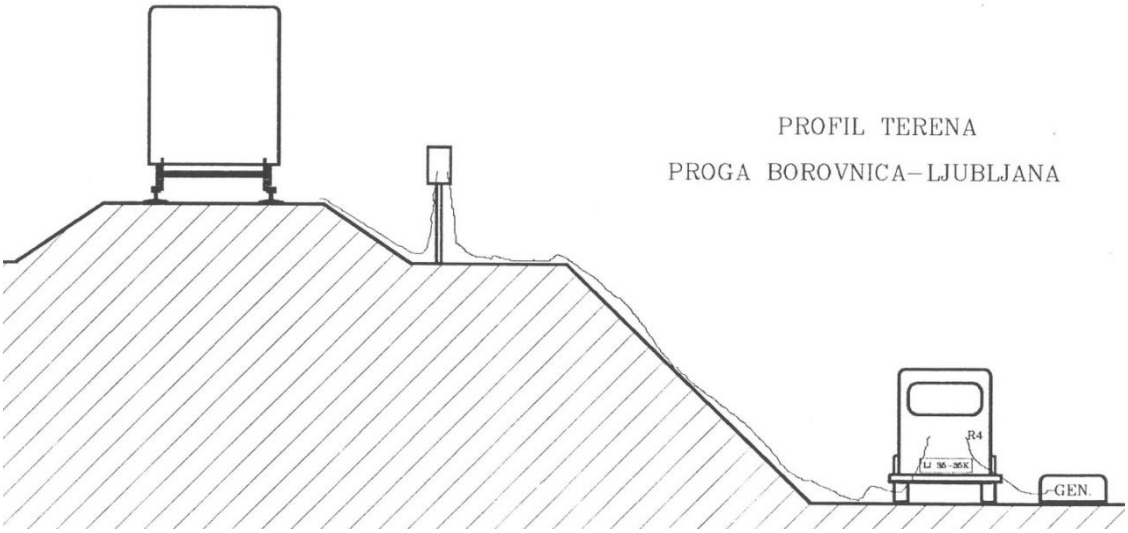

Slika 5: Shema principa meritev dinamičnih deformacij PŽP-MAB [6].

predmetnih meritev so bila pridobljena sredstva, ki so omogočala izvedbo le uvodnih meritev.

6.0 MERJENJE DINAMIČNIH DEFORMACIJ PŽP-MAB

Meritve je zasnoval in izvedel Laboratorij za tehnično fiziko Fakultete za strojništvo Ljubljana. Uvodne meritve deformacij med prehodom vlaka so se izvedle na enem od štirih PŽP-MAB, ki so imeli vgrajene merilne lističe. Rezultati meritev so podani v poročilu [6], v obliki diagramov. Shematičen prikaz izvajanja meritev je razviden iz slike 5.

V slikah 6 do 8 so podani diagrami, ki prikazujejo specifične deformacije (ε) v odvisnosti od časa (t) med prehodom različnih vrst kompozicij vlakov (dveh tovornih – A v sliki 6 in B v sliki 7 ter enega potniškega v sliki 8). V vsaki od teh slik je podana skica praga z označenimi mesti merilnih lističev: (poz. 1) na

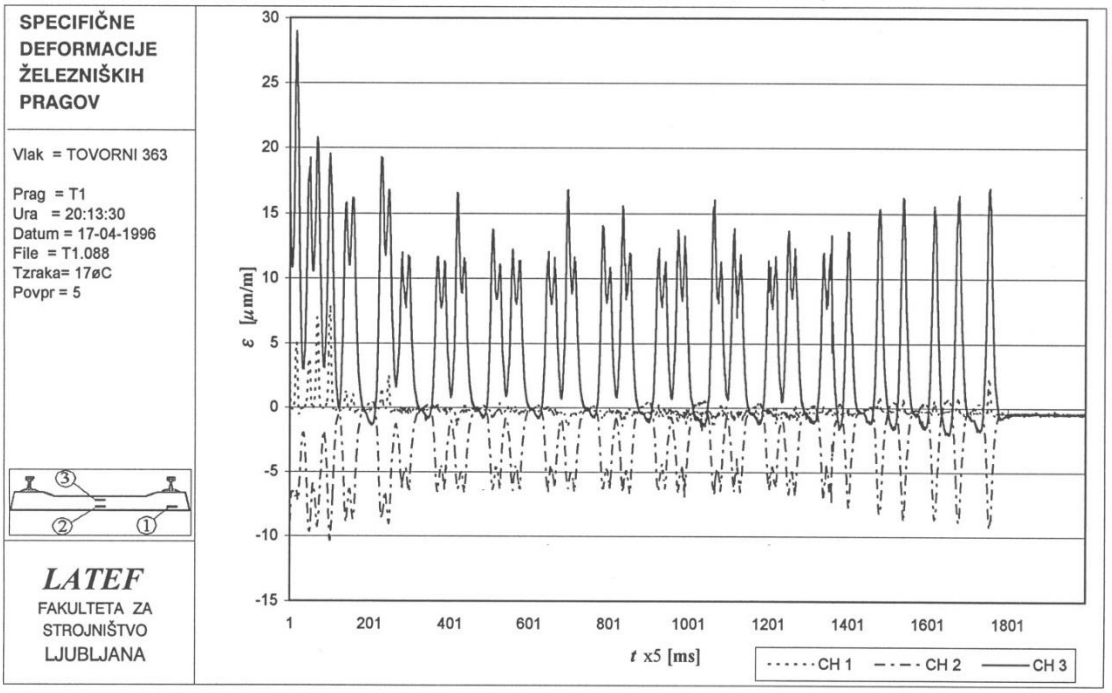

Slika 6: Specifične deformacije PŽP-MAB pri prehodu tovornega vlaka A [6].

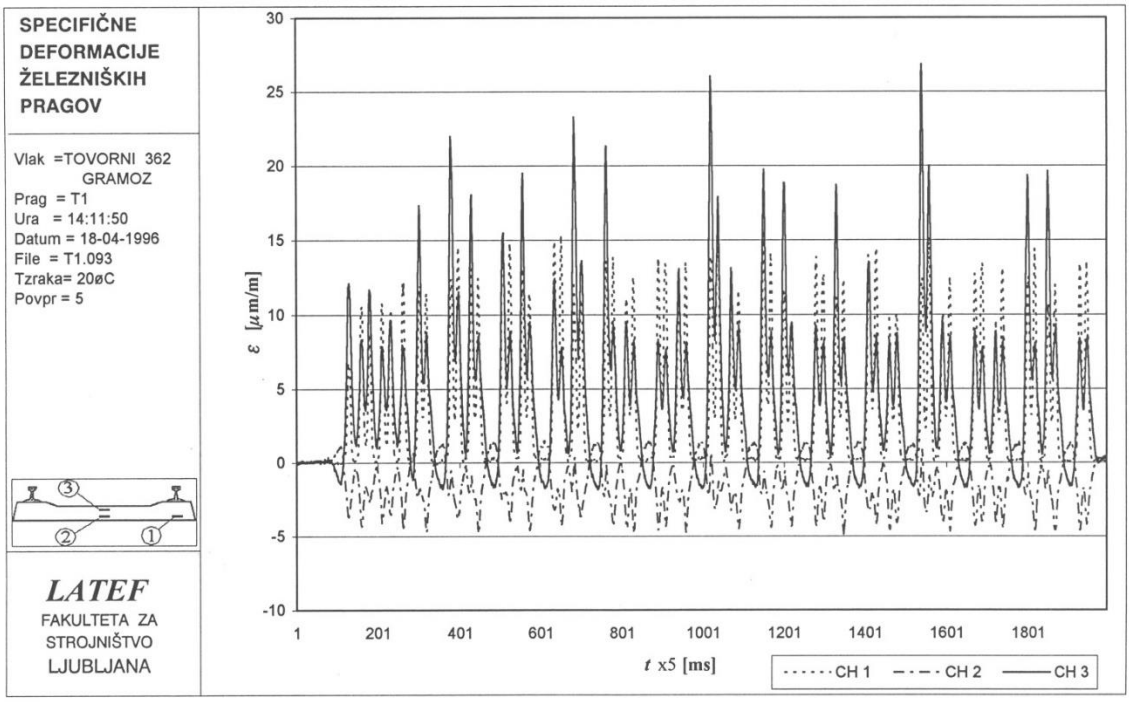

Slika 7: Specifične deformacije PŽP-MAB pri prehodu tovornega vlaka B [6].

spodnjem delu praga, pod tirnico, (poz. 2) na spodnjem deli praga, na sredini in (poz. 3) na zgornjem delu praga, na sredini.

Kot je razvidno iz vseh treh slik (6 do 8), so največje specifične deformacije dobljene v natezni coni, na zgornjem delu praga, na sredini (poz. 3). V odvisnosti od vrste vlaka in mase lokomotive ter vagonov so prav tako lahko velike natezne specifične deformacije na spodnjem delu praga, pod tirnico (poz. 1). Relativno majhne pa so specifične deformacije v tlačni coni, na spodnjem delu praga, na sredini (poz. 2). Dobljene specifične deformacije so bile pričakovane. Kot je bilo že podano v programu meritev, bi se dosti več informacij dobilo z dolgotrajnimi meritvami, najmanj 6 mesecev, na osnovi katerih bi se dalo sklepati o obnašanju vgrajenih PŽP-MAB med uporabo.

7.0 VIZUALNA OPAZOVANJA OBNAŠANJA VGRAJENIH PŽP-MAB

Vizualna opazovanja obnašanja vgrajenih PŽP-MAB potekajo ves čas od vgradnje pa do danes, to je v obdobju njihove uporabe 23 let.

Po treh letih uporabe vgrajenih PŽP-MAB so Slovenske železnice, Sekcija za vzdrževanje prog Postojna pripravile poročilo o stanju desnega tira Borovnica –

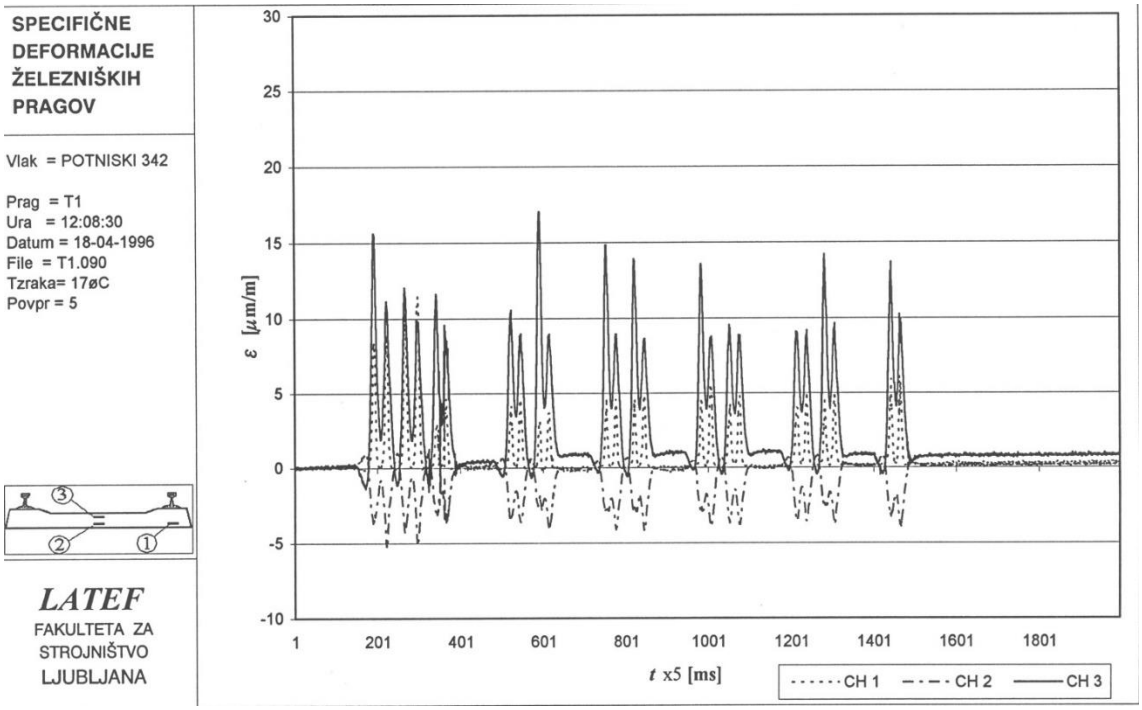

Slika 8: Specifične deformacije PŽP-MAB pri prehodu potniškega vlaka [6].

Slika 9: Grajeni PŽP-MAB po 9 letni uporabi. Posneto v smeri Postojna, v obratni smeri vožnje vlakov

Verd na odseku z PŽP-MAB [7]. V tem poročilu je podano naslednje mnenje: »Pri dosedanjem spremljanju stanja tira z merilnim vozom ter vizualnimi pregledi ugotavljamo, da je stanje tira na obravnavanem odseku z mikroarmiranimi betonskimi pragi dobro, tako v pogledu stabilnosti kakor tudi v pogledu smerne in višinske ureditve tira. V medtirju, t.j. na notranji strani krivine, je opaziti bel gramoz od brušenja zaradi vibracij pri prevozu vlakov. Pri vizualnih pregledih vgrajenih mikroarmiranih betonskih pragov nismo opazili kakršnikoli nepravilnosti ali poškodb oz. razpok.«

Po 9 letni uporabi je bil izvršen detajlni pregled s strani IRMA. Pri tem pregledu pav tako niso bile na PŽP-MAB ugotovljene nobene poškodbe in razpoke (slika 9).

V letošnjem letu, to je po 23 letni uporabi je IRMA izvedel ponovni detajlni pregled vgrajenih PŽP-MAB (slika 10).

Pri pregledu posameznih vgrajenih PŽP-MAB prav tako ni bilo opaziti poškodb. Posebna pozornost je bila posvečena pregledu zgornjega dela pragov, na sredini, kjer bi se lahko pojavile razpoke. Ta predpostavka izhaja iz rezultatov meritev PŽP-MAB (slike 6 – 8) in ugotovljenih razpok na enih od prvih vgrajenih prednapetih betonskih pragih pri nas (slika 1(a), (b)).

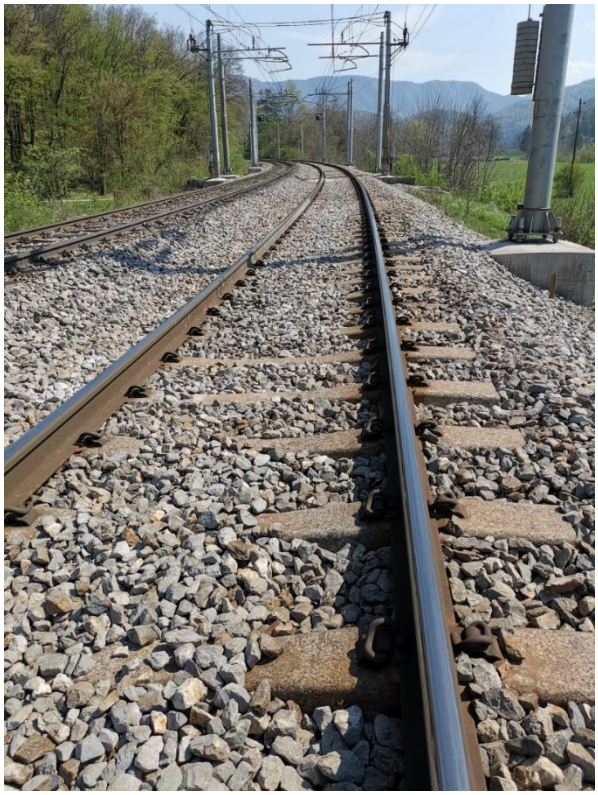

Slika 10: Vgrajeni PŽP-MAB po 23 letni uporabi. Posneto v smeri Postojna, v obratni smeri vožnje vlakov.

Slika 11: Vgrajeni PŽP-MAB po 23 letni uporabi brez razpok na zgornjem delu, na sredini.

Takih razpok na PŽP-MAB po 23 letni uporabi ni bilo opaziti (slika 11).

Na površini pragov je bilo opaziti jeklena vlakna, ki rjavijo (slika 11). Korozijski produkti tankega vlakna (0,5 mm) pa niso taki, da bi razdirali betonsko matrico (slika 12).

Že predhodne raziskave [8] so pokazale, da jeklena vlakna samo na površini ali blizu površine elementov iz MAB rjavijo in povzročajo površinsko barvanje z rjavo barvo zaradi nastajanja rje, ki ne vpliva na trdnost in žilavost MAB, vendar vliva na videz površine elementa.

Pri nadaljnjem pregledu je bilo na nekaj mestih opaziti zamenjavo PŽP-MAB z lesenimi pragovi (slika 13).

Na odstranjenih PŽP-MAB je razvidno, da je prišlo na spodnjem delu do abrazijskih in mehanskih poškodb (slika 14). Na nekaterih seže poškodba do kabla (slika 15). Iz te fotografije je možno tudi videti, da je v betonu prisotnih zelo malo število jeklenih vlaken, kar je opaziti tudi na spodnjih delih vseh ostalih odstranjenih PŽP-MAB.

To pomeni, da so se vlakna pri vgrajevanju (med vibriranjem) neenakomerno razporedila po celotni masi svežega betona. Vlakna so med vibriranjem tonila v svežem betonu tako, da je na zgornjem delu opaženega praga (spodnjem delu vgrajenega praga) (slika 16) prisotna relativno najmanjša količina vlaken.

Zaradi manjše količine vlaken na spodnjem delu PŽP-MAB se je zmanjšala odpornost MAB proti obrusu po Böhmejevi metodi. Iz preglednice 1 je razvidno, da dodana predvidena količina vlaken povečuje odpornost MAB proti obrusu, oziroma količina obrušenega MAB je manjša od količine obrušenega betona brez vlaken. Z zmanjševanjem količine vlaken se odpornost MAB proti obrusu zmanjšuje.

Iz preglednice 1 je prav tako razvidno, da je udarna žilavost MAB s predvideno količino vlaken precej večja v primerjavi z betonom brez vlaken. Z zmanjševanjem količine vlaken se tudi zmanjšuje udarna žilavost MAB, zaradi česar prihaja med podbijanjem do dodatnih poškodb spodnjega dela PŽP-MAB.

Slika 12: Jekleno vlakno z dolžino 30 mm in premerom 0,5 mm na površini praga.

Slika 13: Zamenjava na spodnjem delu abrazijsko in mehansko poškodovanih PŽP-MAB z lesenimi pragovi.

8.0 MOŽNOSTI NADALJNJEGA RAZVOJA IN UPORABE PŽP-MAB

V kolikor bi obstajala možnost vgradnje PŽP-MAB v določene progovne odseke v Sloveniji, bi bilo potrebno pri pripravi novih PŽP-MAB upoštevati in popraviti pomanjkljivost, ki se je pokazale pri poskusni proizvodnji, to je enakomerna porazdelitev vlaken po celotnem volumnu praga. Na ta način se bo izboljšala, ne samo odpornost proti obrabi in proti udarnim obremenitvam spodnjega dela PŽP-MAB, ampak tudi učinkovitost dodanih jeklenih vlaken. Pri tem bo potrebno upoštevati ugotovitve raziskav, kjer je v

Slika 14: Na spodnjem delu abrazijsko in mehansko poškodovani PŽP-MAB..

Slika 15: Poškodbe spodnjega dela PŽP-MAB do kabla.

zaključkih podana ugotovitev, da se na osnovi dobljenih rezultatov laboratorijskih preiskav in matematičnega modela sklepa, da učinkovitost dodanih jeklenih vlaken v MAB ni odvisna samo od njihovih dimenzij in količin, ampak tudi od kakovosti cementne paste, pri čemer ima pomemben vpliv tudi njena poroznost [9].

Še vedno pa ostaja globalno vprašanje o smiselnosti uporabe betonskih železniških pragov, vgrajenih na gredo iz apnenčevega agregata, kar je slučaj na trasah slovenskih železnic. Betonski pragovi bi se morali vgrajevati na gredo iz eruptivnega agregata, ki pa je v Sloveniji na razpolago v zelo omejenih količinah. Zato obstaja in bo obstajala samo ena možnost, da se betonski pragovi še veno vgrajujejo na gredo iz apnenčevega agregata. Pri tem pa je potrebno, da se na spodnjo (naležno) površino praga pritrdi plast gume. Ta guma mora biti sposobna dušiti vibracije, ki nastopijo med prehodom vlaka preko teh pragov. Na ta način bi se zmanjšala intenzivnost drobljenja apnenčevih zrn, ne samo zgornjega, ampak tudi spodnjega ustroja grede. Obstaja pa tudi možnost, da se spodnji del praga, v določeni debelini izdela iz betonskega kompozita z granulirano gumo. Številni rezultati preskusa dušenja vibracij kompozitov z granulirano gumo in z različnimi modificiranimi sestavami [10, 11] izkazujejo, da bi se lahko ti kompoziti uporabljali za zgoraj opisan namen.

9.0 ZAKLJUČEK

Na osnovi občasnih pregledov vgrajenih PŽP-MAB v poskusno polje se lahko zaključi, da v obdobju 23 letne uporabe ni prišlo do nastanka razpok, predvsem na mestih največjih nateznih napetosti, to je na sredini praga, zgoraj. Zaradi neenakomerne porazdelitve jeklenih vlaken po volumnu praga je prišlo na nekaterih PŽP-MAB do poškodb na spodnjem delu tako, da so morali biti odstranjeni s proge. Poškodbe so nastale zaradi abrazijskih in udarnih obremenitev. V zadnjih 20. letih so pridobljena nova znanja, na osnovi katerih obstaja možnost rešitve tega problema. Ostaja pa še vedno osnovni problem uporabe betonskih železniških pragov, vgrajenih na gredo iz apnenčevega agregata. Ta problem bi se dal delno rešit z izdelavo sloja spodnje, naležne površine praga z določeno debelino iz materiala, ki ima sposobnost absorbiranja vibracij.

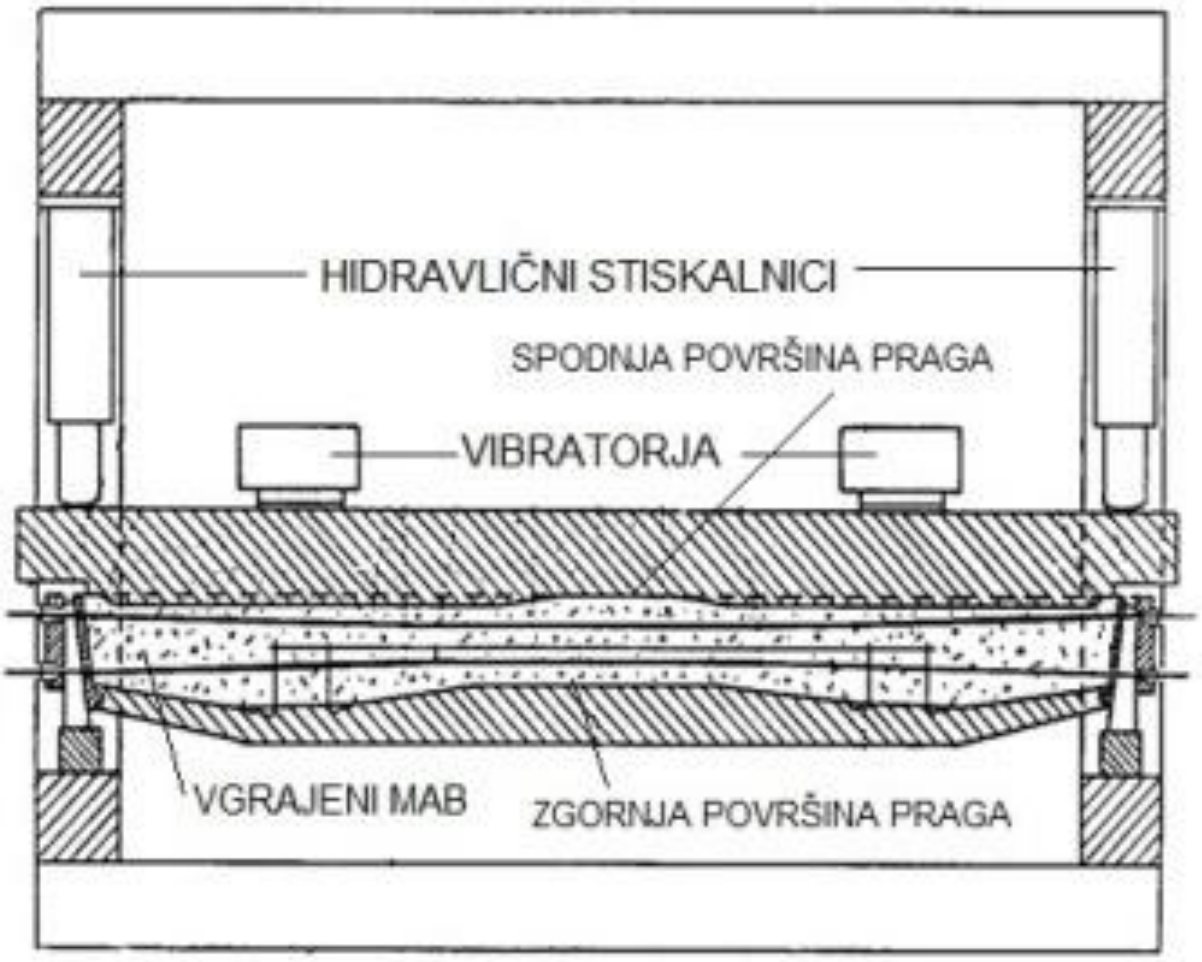

Slika 16: Princip izdelave PŽP-MAB.

LITERATURA

1. *Zajc A. et al Razvoj mikroarmiranega betonskega železniškega praga. RR projekt, Ministrstvo za znanost in tehnologijo – 42-0820-93. IRMA. 1993.*
2. *Korla J., Zajc A., Šušteršič J. Prenapeti betonski prag iz mikroarmiranega betona. Zbornik gradiv in referatov. Slovenski kolokvij o betonih. Mikroarmirane malte in betoni. Ljubljana 1994. IRMA . str. 31 – 36.*
3. *Šušteršič J. Vorgespannte Eisenbahnschwellen aus Stahlfaserbeton. Zem. Beton (Vienna), vol. 37. 1995.*
4. *Šušteršič J. Vorgespannte Eisenbahnschwellen aus Stahlfaserbeton. Bau im Spiegel. jesen 1996. str. 9.*
5. *Leskovar I., Zajc A. Poročilo o preiskavah materialno – tehničnega stanja prednapetih železniških pragov na progi Borovnica – Preserje. Opr. št. 585-90/5013-Če. ZRMK, Inštitut za materiale. 29.05.1990.*
6. *Susič E., Mužič P, Grabec I. Poročilo o merjenju dinamičnih deformacij železniških pragov. Univerza v Ljubljani, Fakulteta za strojništvo, Laboratorij za tehniško fiziko. Ljubljana, april 1996.*
7. *Baša I. Poročilo o stanju desnega tira Borovnica – Verd na odseku z mikroarmiranimi betonskimi pragi. Slovenske železnice, Sekcija za vdrževanje prog Postojna. Štev. 935/99-I-ing.AK. 12. avgust 1999.*
8. *Šušteršič J., Zajc A., Leskovar I., Ercegovič, R. Study of corrosion resistance of steel fibres in SFRC. V: OH, B. H. (ur.). Concrete under severe conditions: environment and loading : proceedings of the Fourth International Conference on Concrete under Severe Conditions, CONSEC '04, Seoul, Korea, June 27-30, 2004. Volume 2. Seoul: Seoul National University, Korea Concrete Institute. 2004.*
9. *Šušteršič J., Korla J., Zajc, A. Učinkovitost jeklenih vlaken v mikroarmiranih betonih in brizganih betonih. Zbornik referatov, 10. mednarodni simpozij o gradnji predorov in podzemnih prostorov, 16-18 november 2011, Ljubljana: Naravoslovnotehniška fakulteta, 2011, str. 205-211.*
10. *Šušteršič J. Sposobnost dušenja vibracij betonov z granulirano gumo. Doseganje posebnih lastnosti betonov z uporabo odpadnih materialov : zbornik gradiv in referatov. Ljubljana: IRMA, Inštitut za raziskavo materialov in aplikacije. 2012, str. 31-40.*
11. *Šušteršič J. Ability of mechanical vibration damping of fiber reinforced polymer and latex-modified concrete with granulated rubber. Proceedings of the 1st Kosova seminar on polymers in concrete, 29-30 May 2013. Prishtina: University of Pristina "Hasan Prishtina". 2013, str. 103-115.*